

## 10. Electroweak Model and Constraints on New Physics

Revised April 2024 by J. Erler (KPH, JGU Mainz) and A. Freitas (Pittsburgh U.).

10.1	Introduction	1
10.2	Renormalization and radiative corrections	3
10.2.1	The Fermi constant	3
10.2.2	The electromagnetic coupling	4
10.2.3	Quark masses	5
10.2.4	The weak mixing angle	7
10.2.5	Radiative corrections	9
10.3	Low energy electroweak observables	10
10.3.1	Neutrino scattering	10
10.3.2	Parity violating lepton scattering	13
10.3.3	Atomic parity violation	14
10.4	Precision flavor physics	16
10.4.1	The $\tau$ lifetime	16
10.4.2	The muon anomalous magnetic moment	18
10.5	Physics of the massive electroweak bosons	19
10.5.1	The $Z$ boson mass	20
10.5.2	Electroweak physics off the $Z$ pole	21
10.5.3	$Z$ pole physics	23
10.5.4	$W$ and $Z$ decays	27
10.6	Global fit results	28
10.7	Constraints on new physics	33
10.8	Alternative scenarios	39

### 10.1 Introduction

The standard model of the electroweak interactions (SM) [1–4] is based on the gauge group  $SU(2) \times U(1)$ , with gauge bosons  $W_\mu^i$ ,  $i = 1, 2, 3$ , and  $B_\mu$  for the  $SU(2)$  and  $U(1)$  factors, respectively, and the corresponding gauge coupling constants  $g$  and  $g'$ . The left-handed fermion fields of the  $i^{\text{th}}$  fermion family transform as doublets  $\Psi_i = \begin{pmatrix} \nu_i \\ \ell_i^- \end{pmatrix}$  and  $\begin{pmatrix} u_i \\ d_i' \end{pmatrix}$  under  $SU(2)$ , where  $d_i' \equiv \sum_j V_{ij} d_j$ , and  $V$  is the Cabibbo-Kobayashi-Maskawa mixing [5, 6] matrix. The right-handed fields are  $SU(2)$  singlets. From Higgs and electroweak precision data it is known that there are precisely three sequential fermion families. Constraints on  $V$  and tests of universality are discussed in Ref. [7] and in Section 12 on the “CKM Quark-Mixing Matrix” in this *Review*. The extension of the formalism to allow an analogous leptonic mixing matrix is discussed in Section 14 on “Neutrino Masses, Mixing, and Oscillations” in this *Review*.

A complex scalar Higgs doublet,  $\phi$ , is added to the model for mass generation through spontaneous symmetry breaking with potential<sup>1</sup> given by,

$$V(\phi) = \mu^2 \phi^\dagger \phi + \frac{\lambda^2}{2} (\phi^\dagger \phi)^2, \quad \phi \equiv \begin{pmatrix} \phi^+ \\ \phi^0 \end{pmatrix}. \quad (10.1)$$

<sup>1</sup>There is no generally accepted convention to write the quartic term. Our numerical coefficient simplifies Eq. (10.5a) below and the squared coupling preserves the relation between the number of external legs and the power counting of couplings at a given loop order. This structure also naturally emerges from physics beyond the SM, such as Supersymmetry.

## 10. Electroweak Model and Constraints on New Physics

For  $\mu^2$  negative,  $\phi$  develops a vacuum expectation value,  $v/\sqrt{2} = |\mu|/\lambda$ , where  $v = 246.22$  GeV, breaking part of the electroweak (EW) gauge symmetry, after which only one neutral Higgs scalar,  $H$ , remains in the physical particle spectrum. In non-minimal models there are additional charged and neutral scalar Higgs particles. Higgs boson physics is reviewed in Section 11 on the “Status of Higgs Boson Physics” in this *Review*.

After symmetry breaking the Lagrangian for the fermion fields,  $\psi_i$ , is

$$\begin{aligned}\mathcal{L}_F = & \sum_i \bar{\psi}_i \left( i \not{\partial} - m_i - \frac{m_i H}{v} \right) \psi_i - \frac{g}{2\sqrt{2}} \sum_i \bar{\Psi}_i \gamma^\mu (1 - \gamma^5) (T^+ W_\mu^+ + T^- W_\mu^-) \Psi_i \\ & - e \sum_i Q_i \bar{\psi}_i \gamma^\mu \psi_i A_\mu - \frac{g}{2 \cos \theta_W} \sum_i \bar{\psi}_i \gamma^\mu (g_V^i - g_A^i \gamma^5) \psi_i Z_\mu .\end{aligned}\quad (10.2)$$

Here  $\theta_W \equiv \tan^{-1}(g'/g)$  is the weak mixing angle and  $e = g \sin \theta_W$  is the positron electric charge. Furthermore,

$$A_\mu \equiv B_\mu \cos \theta_W + W_\mu^3 \sin \theta_W , \quad (10.3a)$$

$$W_\mu^\pm \equiv \frac{W_\mu^1 \mp i W_\mu^2}{\sqrt{2}} , \quad (10.3b)$$

$$Z_\mu \equiv -B_\mu \sin \theta_W + W_\mu^3 \cos \theta_W , \quad (10.3c)$$

are the photon field ( $\gamma$ ) and the charged ( $W^\pm$ ) and neutral ( $Z$ ) weak boson fields, respectively.

The Yukawa coupling of  $H$  to  $\psi_i$  in the first term in  $\mathcal{L}_F$ , which is flavor diagonal in the minimal model, is  $g m_i / 2 M_W$ . From the bosonic interaction Lagrangian,

$$\mathcal{L}_{HV} = \frac{1}{2} (v + H)^2 \left[ \frac{g^2}{2} W_\mu^+ W^{\mu-} + \frac{g^2 + g'^2}{4} Z_\mu Z^\mu \right] - V \left( \frac{v + H}{\sqrt{2}} \right) , \quad (10.4)$$

one obtains the EW boson masses (at tree level, *i.e.*, to lowest order in perturbation theory)

$$M_H = \lambda v , \quad (10.5a)$$

$$M_W = \frac{gv}{2} = \frac{ev}{2 \sin \theta_W} , \quad (10.5b)$$

$$M_Z = \sqrt{g^2 + g'^2} \frac{v}{2} = \frac{ev}{2 \sin \theta_W \cos \theta_W} , \quad (10.5c)$$

$$M_\gamma = 0 . \quad (10.5d)$$

The second term in  $\mathcal{L}_F$  represents the charged-current weak interaction [8–10], where  $T^+$  and  $T^-$  are the weak isospin raising and lowering operators. For example, the coupling of a  $W$  to an electron and a neutrino is

$$- \frac{e}{2\sqrt{2} \sin \theta_W} \left[ W_\mu^- \bar{e} \gamma^\mu (1 - \gamma^5) \nu + W_\mu^+ \bar{\nu} \gamma^\mu (1 - \gamma^5) e \right] . \quad (10.6)$$

For momenta small compared to  $M_W$ , this term gives rise to the effective four-fermion interaction with the Fermi constant given by  $G_F/\sqrt{2} = 1/2v^2 = g^2/8M_W^2$ . CP violation is incorporated into the EW model by a single observable phase in  $V_{ij}$ .

The third term in  $\mathcal{L}_F$  describes electromagnetic interactions (QED) [11, 12], and the last is the weak neutral-current interaction [9, 10, 13]. The vector and axial-vector couplings are

$$g_V^i \equiv t_{3L}(i) - 2Q_i \sin^2 \theta_W , \quad (10.7a)$$

$$g_A^i \equiv t_{3L}(i) , \quad (10.7b)$$

where  $t_{3L}(i)$  is the weak isospin of fermion  $i$  (+1/2 for  $u_i$  and  $\nu_i$ ; -1/2 for  $d_i$  and  $e_i$ ) and  $Q_i$  is the charge of  $\psi_i$  in units of  $e$ .

The first term in Eq. (10.2) also gives rise to fermion masses, and in the presence of right-handed neutrinos to Dirac neutrino masses. The possibility of Majorana masses is discussed in Section 14 on “Neutrino Mass, Mixing, and Oscillations” in this *Review*.

## 10.2 Renormalization and radiative corrections

In addition to the Higgs boson mass,  $M_H$ , the fermion masses and mixings, and the strong coupling constant,  $\alpha_s$ , the SM has three parameters. The set with the smallest experimental errors contains the  $Z$  mass<sup>2</sup>, the Fermi constant, and the fine structure constant. The latter two will be discussed in more detail in the next two subsections. (The numerical values quoted in Sections 10.2–10.4 correspond to the main fit result in Table 10.7.)

### 10.2.1 The Fermi constant

The Fermi constant,

$$G_F = 1.1663788(6) \times 10^{-5} \text{ GeV}^{-2} , \quad (10.8)$$

is derived from the  $\mu$  lifetime formula<sup>3</sup>,

$$\frac{\hbar}{\tau_\mu} = \frac{G_F^2 m_\mu^5}{192\pi^3} F(\rho) \left[ 1 + H_1(\rho) \frac{\hat{\alpha}(m_\mu)}{\pi} + H_2(\rho) \frac{\hat{\alpha}^2(m_\mu)}{\pi^2} + H_3 \frac{\hat{\alpha}^3(m_\mu)}{\pi^3} \right] , \quad (10.9)$$

where  $\rho = m_e^2/m_\mu^2$ , and where

$$F(\rho) = 1 - 8\rho + 8\rho^3 - \rho^4 - 12\rho^2 \ln \rho = 0.99981295 , \quad (10.10a)$$

$$H_1(\rho) = \frac{25}{8} - \frac{\pi^2}{2} - \left( 9 + 4\pi^2 + 12 \ln \rho \right) \rho + 16\pi^2 \rho^{3/2} + \mathcal{O}(\rho^2) = -1.80793 , \quad (10.10b)$$

$$\begin{aligned} H_2(\rho) &= \frac{156815}{5184} - \frac{518}{81}\pi^2 - \frac{895}{36}\zeta(3) + \frac{67}{720}\pi^4 + \frac{53}{6}\pi^2 \ln 2 \\ &\quad - (0.042 \pm 0.002)_{\text{had}} - \frac{5}{4}\pi^2 \sqrt{\rho} + \mathcal{O}(\rho) = 6.64 , \end{aligned} \quad (10.10c)$$

$$\hat{\alpha}(m_\mu)^{-1} = \alpha^{-1} + \frac{1}{3\pi} \ln \rho + \mathcal{O}(\alpha) = 135.901 . \quad (10.10d)$$

$H_1$  and  $H_2$  capture the QED corrections within the Fermi model. The results for  $\rho = 0$  have been obtained in Refs. [16] and [17, 18] for  $H_1$  and  $H_2$ , respectively, where the term in parentheses is from the hadronic vacuum polarization [17]. The mass corrections to  $H_1$  have been known for some time [19], while those to  $H_2$  are more recent [20]. Notice the term linear in  $m_e$  in  $H_2$  whose

<sup>2</sup>We emphasize that in the fits described in Sec. 10.6 and Sec. 10.7 the values of the SM parameters are affected by all observables that depend on them. This is of no practical consequence for  $\alpha$  and  $G_F$ , however, since they are very precisely known. Also note that other choices for the three SM input parameters (see *e.g.* Ref. [14]) will lead to equivalent fit results within theoretical uncertainties.

<sup>3</sup>In the spirit of the Fermi theory, we incorporated the small propagator correction,  $3/5 m_\mu^2/M_W^2$ , into  $\Delta r$  (see below). This is also the convention adopted by the MuLan collaboration [15]. While this breaks with historical consistency, the numerical difference was negligible in the past.

appearance was unforeseen and can be traced to the use of the muon pole mass in the prefactor [20]. The coefficient  $H_3 = -15.3 \pm 2.3$  has been estimated in Refs. [21–23]. The remaining uncertainty in  $G_F$  is mostly experimental and has been reduced by an order of magnitude by the MuLan collaboration [15] at the PSI.

### 10.2.2 The electromagnetic coupling

The fine structure constant,  $\alpha$ , can be extracted from the anomalous magnetic moment of the electron,  $a_e = (1159652180.59 \pm 0.13) \times 10^{-12}$  [24]. Application of QED corrections up to five loop order [25–27] allows to extract the value  $\alpha^{-1} = 137.035999166(15)$ . (Here the number in parentheses denotes the uncertainty in the last digits shown.) Another approach combines measurements of the Rydberg constant and atomic masses with interferometry of atomic recoil kinematics. Applied to  $^{87}\text{Rb}$  [28] and  $^{133}\text{Cs}$  [29], this method implies the results  $\alpha^{-1} = 137.035999206(11)$  and  $\alpha^{-1} = 137.035999046(27)$ , respectively, which differ by  $5.5\sigma$  from each other, and when combined would give  $\alpha^{-1} = 137.035999183(10)$ . Finally, combining the anomalous magnetic moment and atomic interferometry methods, which unlike in the past are now in agreement, leads to the world average,

$$\alpha^{-1} = 137.035999178(8). \quad (10.11)$$

This combination differs from the value in Section 1 (“Physical Constants”) in this *Review*, which does not use the latest experimental inputs.

In most EW renormalization schemes it is convenient to define a running  $\alpha$  dependent on the energy scale of the process, with  $\alpha^{-1} \approx 137.036$  appropriate at very low energy, *i.e.* close to the Thomson limit. The OPAL [30] and L3 [31] collaborations at LEP could also observe the running directly in small and large angle Bhabha scattering, respectively. For scales above a few hundred MeV the low energy hadronic contribution to vacuum polarization introduces a theoretical uncertainty in  $\alpha$ . In the modified minimal subtraction ( $\overline{\text{MS}}$ ) scheme<sup>4</sup> [32] (used for this *Review*), and with  $\alpha_s(M_Z) = 0.1187 \pm 0.0017$  we have  $\hat{\alpha}^{(4)}(m_\tau)^{-1} = 133.450 \pm 0.006$  and  $\hat{\alpha}^{(5)}(M_Z)^{-1} = 127.930 \pm 0.008$ . The latter corresponds to a quark sector contribution (without the top) to the conventional (on-shell) QED coupling,

$$\alpha(M_Z) = \frac{\alpha}{1 - \Delta\alpha(M_Z)}, \quad (10.12)$$

of  $\Delta\alpha_{\text{had}}^{(5)}(M_Z) = 0.02783 \pm 0.00006$ . These values are updated with respect to Ref. [33] with the uncertainty reduced (partly due to a more precise charm quark mass). Various evaluations of  $\Delta\alpha_{\text{had}}^{(5)}(M_Z)$  are summarized in Table 10.1, where the relation<sup>5</sup> between the  $\overline{\text{MS}}$  and on-shell definitions (obtained using Refs. [37, 38]) is given by,

$$\begin{aligned} \Delta\hat{\alpha}(M_Z) - \Delta\alpha(M_Z) &= \frac{\alpha}{\pi} \left[ \frac{100}{27} - \frac{1}{6} - \frac{7}{4} \ln \frac{M_Z^2}{M_W^2} + \frac{\alpha_s(M_Z)}{\pi} \left( \frac{605}{108} - \frac{44}{9} \zeta(3) \right) \right. \\ &\quad + \frac{\alpha_s^2}{\pi^2} \left( \frac{976481}{23328} - \frac{253}{36} \zeta(2) - \frac{781}{18} \zeta(3) + \frac{275}{27} \zeta(5) \right) \\ &\quad + \frac{\alpha_s^3}{\pi^3} \left( \frac{1483517111}{3359232} - \frac{22781}{144} \zeta(2) - \frac{3972649}{7776} \zeta(3) - \frac{31}{81} \zeta(2)^2 + \frac{521255}{7776} \zeta(5) \right. \\ &\quad \left. \left. - \frac{7315}{324} \zeta(7) + \frac{5819}{54} \zeta(2) \zeta(3) + \frac{14675}{162} \zeta(3)^2 \right) \right] = 0.007122(2)(5), \end{aligned} \quad (10.13)$$

<sup>4</sup>In this Section we denote quantities defined in the  $\overline{\text{MS}}$  scheme by a caret; the exception is the strong coupling constant,  $\alpha_s$ , which will always correspond to the  $\overline{\text{MS}}$  definition and where the caret will be dropped. Furthermore,  $\alpha^{(n)}$  and  $\alpha_s^{(n)}$  denote the running couplings with  $n$  quark flavors.

<sup>5</sup>In practice,  $\alpha(M_Z)$  is directly evaluated in the  $\overline{\text{MS}}$  scheme using the FORTRAN package GAPP [34], including the QED contributions of both leptons and quarks. The leptonic three-loop [35] and four-loop [36] contributions in the on-shell scheme have also been obtained.

and where the first entry of the lowest order term is from fermions and the other two are from  $W^\pm$  loops, which are usually excluded from the on-shell definition. Fermion mass effects and corrections of  $\mathcal{O}(\alpha^2)$  contributing to Eq. (10.13) are small, partly cancel each other and are not included here. The first error in Eq. (10.13) is parametric (from  $\alpha_s$ ) and the second is from the truncation of the perturbative expansion. The most recent results of  $\Delta\alpha_{\text{had}}^{(5)}(M_Z)$  [39–42] typically assume the validity of perturbative QCD (PQCD) at scales of  $\sim 2$  GeV and above and are in good agreement with each other. In regions where PQCD is not trusted, one can use  $e^+e^- \rightarrow \text{hadrons}$  cross-section data (for a list of references see, *e.g.*, Ref. [41]) and isospin rotated information derived from  $\tau$  decay spectral functions [43], where the latter derive from OPAL [44], CLEO [45], ALEPH [46], and Belle [47]. Very recently new results appeared from the CMD-3 experiment [48] at the  $e^+e^-$  collider VEPP-2000. There is noticeable spread in the results, with lattice QCD [49] and CMD-3 (KLOE) suggesting stronger (weaker) running. While VEPP-2000 and VEPP-4M scanned center-of-mass (CM) energies up to 2 GeV and between about 3 and 4 GeV, respectively, the BaBar collaboration studied multi-hadron events radiatively returned from the  $\Upsilon(4S)$ , reconstructing the radiated photon and normalizing to  $\mu^\pm\gamma$  final states.

We include all of this information by using as actual input (fit constraint) instead of  $\Delta\alpha_{\text{had}}^{(5)}(M_Z)$  the low energy contribution by the three light quarks,

$$\Delta\alpha_{\text{had}}^{(3)}(2.0 \text{ GeV}) = (60.30 \pm 0.43) \times 10^{-4}, \quad (10.14)$$

which we obtained relying on the analysis in Ref. [41], with  $\tau$  decay data and the latest CMD-3 results added following Ref. [50]. Its correlation (86% [51]) with  $a_\mu$  discussed in Sec. 10.4.2, is included in the fits. The non-linear  $\alpha_s$  dependence of  $\hat{\alpha}(M_Z)$  and the resulting correlation with the input variable  $\alpha_s$  are fully taken into account by calculating the perturbative and heavy quark contributions to  $\hat{\alpha}(M_Z)$  in each call of the fits according to Ref. [33]. Part of the uncertainty ( $\pm 0.37 \times 10^{-4}$ ) in  $\Delta\alpha_{\text{had}}^{(5)}(M_Z)$  is from the combination of  $e^+e^-$  annihilation data,  $\tau$  decays into two-pion final states, and constraints from lattice QCD (LQCD), but un-calculated higher order perturbative QCD corrections ( $\pm 0.21 \times 10^{-4}$ ) and the  $\overline{\text{MS}}$  quark mass values (see below) also contribute.

### 10.2.3 Quark masses

Further free parameters entering into Eq. (10.2) are the quark and lepton masses, where  $m_i$  is the mass of the  $i^{\text{th}}$  fermion  $\psi_i$ . For the light quarks, as described in Section 60 on “Quark Masses” in this *Review*,  $\hat{m}_u = 2.16_{-0.26}^{+0.49}$  MeV,  $\hat{m}_d = 4.67_{-0.17}^{+0.48}$  MeV, and  $\hat{m}_s = 93.4_{-3.4}^{+8.6}$  MeV. These are running  $\overline{\text{MS}}$  masses evaluated at the scale  $\mu = 2$  GeV. For the charm mass we use the constraint [58],

$$\hat{m}_c(\hat{m}_c) = 1274 \pm 8 + 2616 [\alpha_s(M_Z) - 0.1182] \text{ MeV}, \quad (10.15)$$

which is based on QCD sum rules [59, 60], and recalculate  $\hat{m}_c$  in each call of our fits to account for its  $\alpha_s$  dependence. Similarly, for the bottom quark mass we use [61],

$$\hat{m}_b(\hat{m}_b) = 4180 \pm 8 - 108 [\alpha_s(M_Z) - 0.1182] \text{ MeV}, \quad (10.16)$$

with a theoretical correlation of about 60% arising from the PQCD truncation uncertainty which is similar for  $\hat{m}_c(\hat{m}_c)$  and  $\hat{m}_b(\hat{m}_b)$ . To improve the precisions in  $\hat{m}_c(\hat{m}_c)$  and  $\hat{m}_b(\hat{m}_b)$  in the future it would help to remeasure the threshold regions of the heavy quarks, as well as the electronic decay widths of the narrow  $c\bar{c}$  and  $b\bar{b}$  resonances. It would also be important to obtain data on the  $R$ -ratio in  $e^+e^-$  annihilation for center-of-mass energies  $\gtrsim 11.2$  GeV, as in this region QCD perturbation theory cannot be sufficiently relied upon for  $b$  quarks [61].

**Table 10.1:** Evaluations of the on-shell  $\Delta\alpha_{\text{had}}^{(5)}(M_Z)$  by different groups (for a more complete list of evaluations see the 2012 edition of this *Review*). For better comparison we adjusted central values and errors to correspond to a common and fixed value of  $\alpha_s(M_Z) = 0.120$ , except for Ref. [49], for which  $\alpha_s$  is not an explicit input. References quoting results without the top quark decoupled are converted to the five flavor definition. Ref. [52] uses  $\Lambda_{\text{QCD}} = 380 \pm 60$  MeV; for the conversion we assumed  $\alpha_s(M_Z) = 0.118 \pm 0.003$ .

Reference	Result	Comment
Krasnikov, Rodenberg [53]	$0.02737 \pm 0.00039$	PQCD for $\sqrt{s} > 2.3$ GeV
Kühn & Steinhauser [54]	$0.02778 \pm 0.00016$	full $\mathcal{O}(\alpha_s^2)$ for $\sqrt{s} > 1.8$ GeV
Groote <i>et al.</i> [52]	$0.02787 \pm 0.00032$	use of QCD sum rules
Martin <i>et al.</i> [55]	$0.02741 \pm 0.00019$	incl. new BES data
de Troconiz, Yndurain [56]	$0.02754 \pm 0.00010$	PQCD for $s > 2$ GeV <sup>2</sup>
Burkhardt, Pietrzyk [57]	$0.02750 \pm 0.00033$	PQCD for $\sqrt{s} > 12$ GeV
Erler, Ferro-Hernández [39]	$0.02761 \pm 0.00010$	conv. from $\overline{\text{MS}}$ scheme
Jegerlehner [40]	$0.02755 \pm 0.00013$	Euclidean split technique
Davier <i>et al.</i> [41]	$0.02760 \pm 0.00010$	PQCD for $\sqrt{s} = 1.8\text{--}3.7$ & $> 5$ GeV
Keshavarzi <i>et al.</i> [42]	$0.02761 \pm 0.00011$	PQCD for $\sqrt{s} > 11.2$ GeV
Cè <i>et al.</i> [49]	$0.02773 \pm 0.00015$	LQCD for Euclidian $Q^2 < 5$ GeV <sup>2</sup>

The top quark “pole” mass (the quotation marks are a reminder that the experiments do not strictly measure the pole mass and that quarks do not form asymptotic states) has been kinematically reconstructed by the Tevatron collaborations, CDF and DØ, in leptonic, hadronic, and mixed channels with the result [62],

$$m_t = 174.30 \pm 0.35_{\text{stat.}} \pm 0.54_{\text{syst.}} \text{ GeV} \text{ (Tevatron).} \quad (10.17)$$

Likewise, using data from CM energies  $\sqrt{s} = 7$  and  $8$  TeV (Run 1), ATLAS and CMS (including alternative technique measurements) at the LHC obtained [63],

$$m_t = 172.52 \pm 0.14_{\text{stat.}} \pm 0.30_{\text{syst.}} \text{ GeV} \text{ (LHC Run 1).} \quad (10.18)$$

In addition, there are results derived from  $\sqrt{s} = 13$  TeV data (Run 2). The CMS collaboration obtained  $m_t = 171.77 \pm 0.04_{\text{stat.}} \pm 0.37_{\text{syst.}} \text{ GeV}$  [64] in the lepton + jets channel,  $m_t = 172.33 \pm 0.14_{\text{stat.}} \pm 0.69_{\text{syst.}} \text{ GeV}$  [65] in the di-lepton channel,  $m_t = 172.34 \pm 0.20_{\text{mostly stat.}} \pm 0.70_{\text{syst.}} \text{ GeV}$  [66] in the all-jets channel, and  $m_t = 172.13 \pm 0.32_{\text{stat.}} \pm 0.70_{\text{syst.}} \text{ GeV}$  [67] in  $t$ -channel single top events (leptonic decays). ATLAS quotes  $m_t = 174.41 \pm 0.39_{\text{stat.}} \pm 0.71_{\text{syst.}} \text{ GeV}$  [68] from the lepton + jets channel and  $m_t = 172.21 \pm 0.20_{\text{stat.}} \pm 0.78_{\text{syst.}} \text{ GeV}$  [69] from the di-lepton channel. Assuming that the correlation matrix for individual channels of the Run 1 combination [63] is approximately applicable also at Run 2 (and that the same applies to the effective 9% correlation between ATLAS and CMS which can also be extracted from Ref. [63]), we arrive at the result,

$$m_t = 172.13 \pm 0.06_{\text{stat.}} \pm 0.30_{\text{syst.}} \text{ GeV} \text{ (LHC Run 2).} \quad (10.19)$$

To combine the two LHC runs, we use the largest correlation coefficient (0.51) between 7 TeV and 8 TeV results from the same experiment and channel in Ref. [63], and obtain,

$$m_t = 172.30 \pm 0.07_{\text{stat.}} \pm 0.27_{\text{syst.}} \text{ GeV} \text{ (LHC).} \quad (10.20)$$

**Table 10.2:** Notations used to indicate the various  $\sin^2 \theta_W$  schemes discussed in the text. Numerical values and the uncertainties induced by the imperfectly known SM parameters and unknown higher orders [83] are also given for illustration.

Scheme	Notation	Value	Uncertainty
On-shell	$s_W^2$	0.22348	$\pm 0.00010$
$\overline{\text{MS}}$	$\hat{s}_Z^2$	0.23129	$\pm 0.00004$
$\overline{\text{MS}}$ (ND)	$\hat{s}_{\text{ND}}^2$	0.23147	$\pm 0.00004$
$\overline{\text{MS}}$	$\hat{s}_0^2$	0.23873	$\pm 0.00005$
Effective angle	$\hat{s}_\ell^2$	0.23161	$\pm 0.00004$

This treatment is highly conservative in view of the fact that for their lepton + jets channels novel leptonic invariant mass and profile likelihood approaches were used by ATLAS and CMS, respectively, implying reduced correlations with the more traditional analyzes at Run 1. Note that the statistical uncertainty of the combination (0.07 GeV) is larger than that of the CMS lepton+jets measurement at 13 TeV (0.04 GeV) [64] because the latter has a relatively large systematic uncertainty and thus gets a small weight in the average. See Ref. [70] for a detailed discussion.

The Tevatron and LHC average values, (10.17) with (10.20), differ by  $2.8\sigma$ . In the inter-collider combination we treat them as uncorrelated, yielding

$$m_t = 172.61 \pm 0.25_{\text{exp.}} \text{ GeV} + \Delta m_{\text{MC}}, \quad (10.21)$$

where  $\Delta m_{\text{MC}}$  is defined to account for any difference between the top pole mass,  $m_t$ , and the mass parameter implemented in the Monte Carlo event generators employed by the experimental groups.  $\Delta m_{\text{MC}}$  is expected to be of order  $\alpha_s(Q_0)Q_0$  with a low scale  $Q_0 \sim \mathcal{O}(1 \text{ GeV})$  [71], but its value is unknown in hadron collider environments so that we will treat it as an uncertainty instead<sup>6</sup>, and choose for definiteness  $Q_0 = \Gamma_t = 1.42 \text{ GeV}$  to arrive at  $\Delta m_{\text{MC}} = 0 \pm 0.52 \text{ GeV}$ . We further assume that an uncertainty [74] of  $\pm 0.32 \text{ GeV}$  in the relation [75] between  $m_t$  and the  $\overline{\text{MS}}$  definition,  $\hat{m}_t(\hat{m}_t)$ , entering electroweak radiative correction libraries, including the renormalon ambiguity [76], is already included in  $\Delta m_{\text{MC}}$ , as  $m_t$  merely serves as an intermediate bookkeeping device in Ref. [71]. A promising future direction to arrive at a competitive independent constraint on  $m_t$  is to analyze differential top quark pair production cross-sections at next-to-next-to-leading order (NNLO) [77, 78] as  $m_t$  extraction based on them are easier to interpret, and experimentally they have become much more precise recently [79–82]. The combination in Eq. (10.21) differs slightly from the average,  $m_t = 172.57 \pm 0.29_{\text{exp.}} \text{ GeV}$ , which appears in the Top Quark Listings in this *Review*, and which is based exclusively on published results and assumes vanishing correlations. For more details and references, see Section 61 on the “Top Quark” and the Quarks Listings in this *Review*.

#### 10.2.4 The weak mixing angle

The observables  $\sin^2 \theta_W$  and  $M_W$  can be calculated from  $M_Z$ ,  $\hat{\alpha}(M_Z)$ , and  $G_F$ , when values for  $m_t$  and  $M_H$  are given, or conversely,  $M_H$  can be constrained by  $\sin^2 \theta_W$  and  $M_W$ . The value of  $\sin^2 \theta_W$  is extracted from neutral-current processes (see Sec. 10.3) and  $Z$  pole observables (see Sec. 10.5.4) and depends on the renormalization prescription. There are a number of popular schemes [9] leading to values which differ by small factors depending on  $m_t$  and  $M_H$ . The notation for these schemes is shown in Table 10.2.

<sup>6</sup>However, see Ref. [72, 73] for proposed procedures to calibrate the Monte-Carlo mass parameter at hadron colliders.

- (i) The on-shell scheme [84] promotes the tree-level formula  $\sin^2 \theta_W = 1 - M_W^2/M_Z^2$  to a definition of the renormalized  $\sin^2 \theta_W$  to all orders in perturbation theory, *i.e.*,

$$\sin^2 \theta_W \rightarrow s_W^2 \equiv 1 - \frac{M_W^2}{M_Z^2} , \quad (10.22a)$$

$$M_W = \frac{A_0}{s_W(1 - \Delta r)^{1/2}} , \quad M_Z = \frac{M_W}{c_W} , \quad (10.22b)$$

where  $c_W \equiv \cos \theta_W$ ,  $A_0 = (\pi \alpha / \sqrt{2} G_F)^{1/2} = 37.28038(1)$  GeV, and  $\Delta r$  includes the radiative corrections relating  $\alpha$ ,  $\alpha(M_Z)$ ,  $G_F$ ,  $M_W$ , and  $M_Z$ . One finds  $\Delta r \sim \Delta r_0 - \rho_t \tan^{-2} \theta_W$ , where  $\Delta r_0 = 1 - \alpha/\hat{\alpha}(M_Z) = 0.06646(6)$  is due to the running of  $\alpha$ , and

$$\rho_t = \frac{3G_F m_t^2}{8\sqrt{2}\pi^2} = 0.00934 \times \frac{m_t^2}{(172.61 \text{ GeV})^2} , \quad (10.23)$$

represents the dominant (quadratic)  $m_t$  dependence. There are additional contributions to  $\Delta r$  from bosonic loops, including those which depend logarithmically on  $M_H$  and higher-order corrections<sup>7</sup>. One has  $\Delta r = 0.03685 \mp 0.00020 \pm 0.00006$ , where the first uncertainty is from  $m_t$  (the  $\mp$  sign indicates that increasing  $m_t$  has the effect of decreasing  $\Delta r$ ) and the second is from  $\alpha(M_Z)$ . Thus the value of  $s_W^2$  extracted from  $M_Z$  includes an uncertainty ( $\mp 0.00007$ ) from the currently allowed range of  $m_t$ . This scheme is simple conceptually. However, the relatively large ( $\sim 3\%$ ) correction from  $\rho_t$  causes large spurious contributions in higher orders.  $s_W^2$  depends not only on the gauge couplings but also on the spontaneous-symmetry breaking, and it is awkward in the presence of any extension of the SM which perturbs the value of  $M_Z$  (or  $M_W$ ). Other definitions are motivated by the tree-level coupling constant definition  $\theta_W = \tan^{-1}(g'/g)$ :

- (ii) In particular, the  $\overline{\text{MS}}$  scheme introduces the quantity,

$$\sin^2 \hat{\theta}_W(\mu) \equiv \frac{\hat{g}'^2(\mu)}{\hat{g}^2(\mu) + \hat{g}'^2(\mu)} , \quad (10.24)$$

where the couplings  $\hat{g}$  and  $\hat{g}'$  are defined by modified minimal subtraction and the scale  $\mu$  is conveniently chosen to be  $M_Z$  for many EW processes. The value of  $\hat{s}_Z^2 \equiv \sin^2 \hat{\theta}_W(M_Z)$  extracted from  $M_Z$  is less sensitive than  $s_W^2$  to  $m_t$  (by a factor of  $\tan^2 \theta_W$ ), and is less sensitive to most types of new physics. It is also very useful for comparing with the predictions of grand unification. There are actually several variant definitions of  $\sin^2 \hat{\theta}_W(M_Z)$ , differing according to whether or how finite  $\alpha \ln(m_t/M_Z)$  terms are decoupled (subtracted from the couplings). One cannot entirely decouple the  $\alpha \ln(m_t/M_Z)$  terms from all EW quantities because  $m_t \gg m_b$  breaks SU(2) symmetry. The scheme that will be adopted here decouples the  $\alpha \ln(m_t/M_Z)$  terms from the  $\gamma$ - $Z$  mixing [32, 85], essentially eliminating any  $\ln(m_t/M_Z)$  dependence in the formulae for asymmetries at the  $Z$  pole when written in terms of  $\hat{s}_Z^2$ . (A similar definition is used for  $\hat{\alpha}$ .) The on-shell and  $\overline{\text{MS}}$  definitions are related by

$$\hat{s}_Z^2 = c(m_t, M_H) s_W^2 = (1.0349 \pm 0.0003) s_W^2 . \quad (10.25)$$

The quadratic  $m_t$  dependence is given by  $c \sim 1 + \rho_t / \tan^2 \theta_W$ . The expressions for  $M_W$  and  $M_Z$  in the  $\overline{\text{MS}}$  scheme are

$$M_W = \frac{A_0}{\hat{s}_Z(1 - \Delta \hat{r}_W)^{1/2}} , \quad M_Z = \frac{M_W}{\hat{\rho}^{1/2} \hat{c}_Z} , \quad (10.26)$$

---

<sup>7</sup>All explicit numbers quoted here and below include the two- and three-loop corrections described near the end of Sec. 10.2.

and one predicts  $\Delta\hat{r}_W = 0.06937 \pm 0.00006$ .  $\Delta\hat{r}_W$  has no quadratic  $m_t$  dependence, because shifts in  $M_W$  are absorbed into the observed  $G_F$ , so that the error in  $\Delta\hat{r}_W$  is almost entirely due to  $\Delta r_0 = 1 - \alpha/\hat{\alpha}(M_Z)$ . The quadratic  $m_t$  dependence has been shifted into  $\hat{\rho} \sim 1 + \rho_t$ , where including bosonic loops,  $\hat{\rho} = 1.01016 \pm 0.00009$ .

- (iii) A variant  $\overline{\text{MS}}$  quantity  $\hat{s}_Z^2$  (used in the 1992 edition of this *Review*) does not decouple the  $\alpha \ln(m_t/M_Z)$  terms [86]. It is related to  $\hat{s}_Z^2$  by

$$\hat{s}_Z^2 = \frac{\hat{s}_{\text{ND}}^2}{1 + \frac{\alpha}{\pi} d}, \quad d = \frac{1}{3} \left( \frac{1}{\hat{s}^2} - \frac{8}{3} \right) \left[ \left( 1 + \frac{\alpha_s}{\pi} \right) \ln \frac{m_t}{M_Z} - \frac{15\alpha_s}{8\pi} \right]. \quad (10.27)$$

Thus,  $\hat{s}_Z^2 - \hat{s}_{\text{ND}}^2 = -0.0002$ .

- (iv) Some of the low-energy experiments discussed in the next section are sensitive to the weak mixing angle at almost vanishing momentum transfer [39, 87–89]. Thus, Table 10.2 also includes  $\hat{s}_0^2 \equiv \sin^2 \hat{\theta}_W(0)$ .
- (v) Yet another definition, the effective angle [90, 91],  $\bar{s}_f^2 \equiv \sin \theta_{\text{eff}}^f$ , for the  $Z$  vector coupling to fermion  $f$ , is based on  $Z$  pole observables and described in Sec. 10.5.

### 10.2.5 Radiative corrections

Experiments are at such level of precision [83] that complete one-loop, dominant two-loop, and partial three and four-loop radiative corrections must be applied. For neutral-current and  $Z$  pole processes, these corrections are conveniently divided into two classes:

1. QED diagrams involving the emission of real photons or the exchange of virtual photons in loops, but not including vacuum polarization diagrams. These graphs often yield finite and gauge-invariant contributions to observable processes. However, they are dependent on energies, experimental cuts, *etc.*, and must be calculated individually for each experiment.
2. EW corrections, including  $\gamma\gamma$ ,  $\gamma Z$ ,  $ZZ$ , and  $WW$  vacuum polarization diagrams, as well as vertex corrections, box graphs, *etc.*, involving virtual  $W$  and  $Z$  bosons. One-loop corrections [92] are included for all processes, and many two-loop corrections are also important. In particular, two-loop corrections involving the top quark modify  $\rho_t$  in  $\hat{\rho}$ ,  $\Delta r$ , and elsewhere by

$$\rho_t \rightarrow \rho_t \left[ 1 + R(M_H, m_t) \frac{\rho_t}{3} \right]. \quad (10.28)$$

$R(M_H, m_t)$  can be described as an expansion in  $M_Z^2/m_t^2$ , for which the leading  $m_t^4/M_Z^4$  [93, 94] and next-to-leading  $m_t^2/M_Z^2$  [95, 96] terms are known. The complete two-loop calculation of  $\Delta r$  (without further approximation) has been performed in Refs. [97–101]. More recently, Ref. [102] obtained the  $\overline{\text{MS}}$  quantities  $\Delta\hat{r}_W$  and  $\hat{\rho}$  to two-loop accuracy, confirming the prediction of  $M_W$  in the on-shell scheme from Refs. [99, 103] within about 4 MeV. Similarly, the EW two-loop corrections for the relation between  $\bar{s}_{\ell,b}^2$  and  $s_W^2$  are known [104–109], as well as for the partial decay and total decay widths and the effective couplings of the  $Z$  boson [110–113]. For  $\bar{s}_{s,c}$  only two-loop corrections from diagrams with closed fermion loops are available [114], but given the experimental precision this is more than adequate.

The mixed QCD-EW contributions to gauge boson self-energies of order  $\alpha\alpha_s m_t^2$  [115, 116],  $\alpha\alpha_s^2 m_t^2$  [117, 118], and  $\alpha\alpha_s^3 m_t^2$  [119–121] increase the predicted value of  $m_t$  by 6%. This is, however, almost entirely an artifact of using the pole mass definition for  $m_t$ . The equivalent corrections when using the  $\overline{\text{MS}}$  definition  $\hat{m}_t(\hat{m}_t)$  increase  $m_t$  by less than 0.5%. The sub-leading  $\alpha\alpha_s$  corrections [122–125] are also included. Further three-loop corrections of order  $\alpha\alpha_s^2$  [126, 127],  $\alpha^3 m_t^6$ ,  $\alpha^2 \alpha_s m_t^4$  [128, 129],  $\alpha_f^3$  and  $\alpha_f^2 \alpha_s$  [130, 131] are rather small (here  $\alpha_f$

denotes electroweak corrections with a closed fermion loop). The same is true for  $\alpha^3 M_H^4$  [132] corrections unless  $M_H$  approaches 1 TeV. The theoretical uncertainty from unknown higher-order corrections [83] is estimated to amount to 4 MeV for the prediction of  $M_W$  [103] and  $4.5 \times 10^{-5}$  for  $\bar{s}_\ell^2$  [114].

Throughout this *Review* we utilize EW radiative corrections from the program GAPP [34], which works entirely in the  $\overline{\text{MS}}$  scheme, and which is independent of the ZFITTER [133] and GRIFFIN [134] packages.

### 10.3 Low energy electroweak observables

In the following we discuss EW precision observables obtained at low momentum transfers [135], *i.e.*,  $Q^2 \ll M_Z^2$ . It is convenient to write the four-fermion interactions relevant to  $\nu$ -hadron,  $\nu$ - $e$ , as well as parity violating  $e$ -hadron and  $e$ - $e$  neutral-current processes, in a form that is valid in an arbitrary gauge theory (assuming massless left-handed neutrinos). One has<sup>8</sup>,

$$-\mathcal{L}^{\nu e} = \frac{G_F}{\sqrt{2}} \bar{\nu} \gamma_\mu (1 - \gamma^5) \nu \bar{e} \gamma^\mu (g_{LV}^{\nu e} - g_{LA}^{\nu e} \gamma^5) e , \quad (10.29a)$$

$$-\mathcal{L}^{\nu h} = \frac{G_F}{\sqrt{2}} \bar{\nu} \gamma_\mu (1 - \gamma^5) \nu \sum_q \left[ g_{LL}^{\nu q} \bar{q} \gamma^\mu (1 - \gamma^5) q + g_{LR}^{\nu q} \bar{q} \gamma^\mu (1 + \gamma^5) q \right] , \quad (10.29b)$$

$$-\mathcal{L}^{ee} = -\frac{G_F}{\sqrt{2}} g_{AV}^{ee} \bar{e} \gamma_\mu \gamma^5 e \bar{e} \gamma^\mu e , \quad (10.29c)$$

$$-\mathcal{L}^{eh} = -\frac{G_F}{\sqrt{2}} \sum_q \left[ g_{AV}^{eq} \bar{e} \gamma_\mu \gamma^5 e \bar{q} \gamma^\mu q + g_{VA}^{eq} \bar{e} \gamma_\mu e \bar{q} \gamma^\mu \gamma^5 q \right] , \quad (10.29d)$$

where one must include the charged-current contribution for  $\nu_e$ - $e$  and  $\bar{\nu}_e$ - $e$  and the parity conserving QED contribution for electron scattering. The SM tree level expressions for the four-Fermi couplings are given in Table 10.3. Note that they differ from the respective products of the gauge couplings in (10.7) in the radiative corrections and in the presence of possible physics beyond the SM.

#### 10.3.1 Neutrino scattering

The cross-section in the laboratory system for  $\nu_\mu e \rightarrow \nu_\mu e$  or  $\bar{\nu}_\mu e \rightarrow \bar{\nu}_\mu e$  elastic scattering [9, 136] is (in this subsection we drop the redundant index  $L$  in the effective neutrino couplings),

$$\frac{d\sigma_{\nu, \bar{\nu}}}{dy} = \frac{G_F^2 m_e E_\nu}{2\pi} \left[ (g_V^{\nu e} \pm g_A^{\nu e})^2 + (g_V^{\nu e} \mp g_A^{\nu e})^2 (1-y)^2 - (g_V^{\nu e 2} - g_A^{\nu e 2}) \frac{y m_e}{E_\nu} \right] , \quad (10.30)$$

where the upper (lower) sign refers to  $\nu_\mu (\bar{\nu}_\mu)$ , and  $y \equiv T_e/E_\nu$  (which runs from 0 to  $(1+m_e/2E_\nu)^{-1}$ ) is the ratio of the kinetic energy of the recoil electron to the incident  $\nu$  or  $\bar{\nu}$  energy. For  $E_\nu \gg m_e$  this yields a total cross-section

$$\sigma = \frac{G_F^2 m_e E_\nu}{2\pi} \left[ (g_V^{\nu e} \pm g_A^{\nu e})^2 + \frac{1}{3} (g_V^{\nu e} \mp g_A^{\nu e})^2 \right] . \quad (10.31)$$

The most accurate measurements of  $\sin^2 \theta_W$  from  $\nu$ -lepton scattering (see Sec. 10.6) are from the ratio  $R \equiv \sigma_{\nu_\mu e}/\sigma_{\bar{\nu}_\mu e}$ , in which many of the systematic uncertainties cancel. The results are  $\sin^2 \theta_W = 0.211 \pm 0.037$  [137],  $\sin^2 \theta_W = 0.195 \pm 0.022$  [138], and  $\sin^2 \theta_W = 0.2324 \pm 0.0083$  [139], where radiative corrections (other than  $m_t$  effects) are small compared to the precision of present

<sup>8</sup>We use here slightly different definitions (and to avoid confusion also a different notation) for the coefficients of these four-Fermi operators than we did in previous editions of this *Review*. The new couplings [13] are defined in the static limit,  $Q^2 \rightarrow 0$ , with specific radiative corrections included, while others (more experiment specific ones) are assumed to be removed by the experimentalist. They are convenient in that their determinations from very different types of processes can be straightforwardly combined.

**Table 10.3:** SM tree level expressions for the neutral-current parameters for  $\nu$ -hadron,  $\nu$ - $e$ , and  $e^-$  scattering processes. To obtain the SM values in the last column, the tree level expressions have to be multiplied by the low-energy neutral-current  $\rho$  parameter,  $\rho_{\text{NC}} = 1.00060$ , and further vertex and box corrections need to be added as detailed in Ref. [13]. The dominant  $m_t$  dependence is again given by  $\rho_{\text{NC}} \sim 1 + \rho_t$ .

Quantity	SM tree level	SM value
$g_{LV}^{\nu_\mu e}$	$-\frac{1}{2} + 2 \hat{s}_0^2$	-0.0395
$g_{LA}^{\nu_\mu e}$	$-\frac{1}{2}$	-0.5063
$g_{LL}^{\nu_\mu u}$	$\frac{1}{2} - \frac{2}{3} \hat{s}_0^2$	0.3457
$g_{LL}^{\nu_\mu d}$	$-\frac{1}{2} + \frac{1}{3} \hat{s}_0^2$	-0.4288
$g_{LR}^{\nu_\mu u}$	$-\frac{2}{3} \hat{s}_0^2$	-0.1553
$g_{LR}^{\nu_\mu d}$	$\frac{1}{3} \hat{s}_0^2$	0.0777
$g_{AV}^{ee}$	$\frac{1}{2} - 2 \hat{s}_0^2$	0.0224
$g_{AV}^{eu}$	$-\frac{1}{2} + \frac{4}{3} \hat{s}_0^2$	-0.1886
$g_{AV}^{ed}$	$\frac{1}{2} - \frac{2}{3} \hat{s}_0^2$	0.3418
$g_{VA}^{eu}$	$-\frac{1}{2} + 2 \hat{s}_0^2$	-0.0349
$g_{VA}^{ed}$	$\frac{1}{2} - 2 \hat{s}_0^2$	0.0246

experiments and have negligible effect. As shown in Fig. 10.1, one can determine  $g_{V,A}^{\nu e}$  from the experimental data as well. The cross-sections for  $\nu_e$ - $e$  and  $\bar{\nu}_e$ - $e$  may be obtained from Eq. (10.30) by replacing  $g_{V,A}^{\nu e}$  by  $g_{V,A}^{\nu e} + 1$ , where the 1 is due to the charged-current contribution.

A precise determination of the on-shell  $s_W^2$ , which depends only very weakly on  $m_t$  and  $M_H$ , is obtained from deep inelastic scattering (DIS) of neutrinos [136, 143] from (approximately) isoscalar targets. The ratio  $R_\nu \equiv \sigma_{\nu N}^{\text{NC}} / \sigma_{\nu N}^{\text{CC}}$  of neutral-to-charged-current cross-sections has been measured to 1% accuracy by CDHS [144] and CHARM [145] at CERN. CCFR [146] at Fermilab has obtained an even more precise result, so it is important to obtain theoretical expressions for  $R_\nu$  and  $R_{\bar{\nu}} \equiv \sigma_{\bar{\nu} N}^{\text{NC}} / \sigma_{\bar{\nu} N}^{\text{CC}}$  to comparable accuracy. Fortunately, many of the uncertainties from the strong interactions and neutrino spectra cancel in the ratio. A large theoretical uncertainty is associated with the  $c$ -threshold, which mainly affects  $\sigma^{\text{CC}}$ . Using the slow rescaling prescription [147, 148] the central value of  $\sin^2 \theta_W$  from CCFR varies as  $0.0111(m_c/\text{GeV} - 1.31)$ , where  $m_c$  is the effective mass which is numerically close to the  $\overline{\text{MS}}$  mass  $\hat{m}_c(\hat{m}_c)$ , but their exact relation is unknown at higher orders. For  $m_c = 1.31 \pm 0.24$  GeV, which was determined from  $\nu$ -induced di-muon production [149], this contributes  $\pm 0.003$  to the total error of  $\Delta \sin^2 \theta_W = \pm 0.004$  (the experimental uncertainty was also  $\pm 0.003$ ). This uncertainty largely cancels, however, in the Paschos-Wolfenstein ratio [150],

$$R^- = \frac{\sigma_{\nu N}^{\text{NC}} - \sigma_{\bar{\nu} N}^{\text{NC}}}{\sigma_{\nu N}^{\text{CC}} - \sigma_{\bar{\nu} N}^{\text{CC}}} . \quad (10.32)$$

It was measured by Fermilab's NuTeV collaboration [151] for the first time, and required a high-intensity and high-energy anti-neutrino beam.

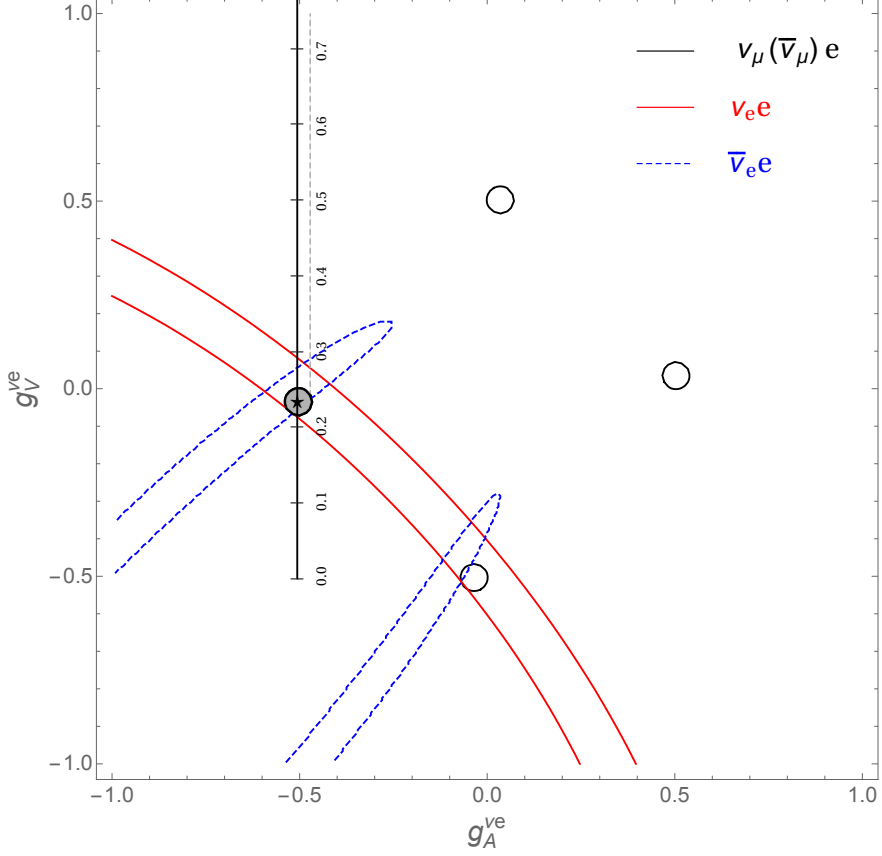


**Figure 10.1:** Allowed contours in  $g_A^{\nu e}$  vs.  $g_V^{\nu e}$  from neutrino-electron scattering and the SM prediction as a function of  $\hat{s}_Z^2$ . (The SM best fit value,  $\hat{s}_Z^2 = 0.23129$ , is also indicated.) The  $\nu_e$ - $e$  [140, 141] and  $\bar{\nu}_e$ - $e$  [142] constraints are at  $1\sigma$ , while each of the four equivalent  $\nu_\mu(\bar{\nu}_\mu)$ - $e$  [137–139] solutions ( $g_{V,A} \rightarrow -g_{V,A}$  and  $g_{V,A} \rightarrow g_{A,V}$ ) are at the 90% CL. The global best fit region (shaded) almost exactly coincides with the corresponding  $\nu_\mu(\bar{\nu}_\mu)$ - $e$  region. The solution near  $g_A = 0$  and  $g_V = -0.5$  is eliminated by  $e^+e^- \rightarrow \ell^+\ell^-$  data under the weak additional assumption that the neutral current is dominated by the exchange of a single  $Z$  boson.

A simple zero<sup>th</sup>-order approximation is,

$$R_\nu = g_L^2 + g_R^2 r , \quad R_{\bar{\nu}} = g_L^2 + \frac{g_R^2}{r} , \quad (10.33a)$$

$$R^- = g_L^2 - g_R^2 , \quad r \equiv \frac{\sigma_{\bar{\nu}N}^{CC}}{\sigma_{\nu N}^{CC}} , \quad (10.33b)$$

where  $r$  is the ratio of  $\bar{\nu}$  to  $\nu$  charged-current cross-sections which can be measured directly<sup>9</sup>, and

$$g_L^2 \equiv (g_{LL}^{\nu u})^2 + (g_{LL}^{\nu d})^2 \approx \frac{1}{2} - \sin^2 \theta_W + \frac{5}{9} \sin^4 \theta_W , \quad (10.34a)$$

$$g_R^2 \equiv (g_{LR}^{\nu u})^2 + (g_{LR}^{\nu d})^2 \approx \frac{5}{9} \sin^4 \theta_W . \quad (10.34b)$$

<sup>9</sup>In the simple parton model, ignoring hadron energy cuts,  $r \approx (1 + 3\epsilon)/(3 + \epsilon)$ , where  $\epsilon \sim 0.125$  is the ratio of the fraction of the nucleon's momentum carried by anti-quarks to that carried by quarks.

In practice, Eq. (10.33b) must be corrected for quark mixing, quark sea effects,  $c$  quark threshold effects, non-isoscalarity,  $W$ - $Z$  propagator differences, the finite muon mass, QED and EW radiative corrections. Details of the neutrino spectra, experimental cuts,  $x$  and  $Q^2$  dependence of structure functions, and longitudinal structure functions, enter only at the level of these corrections and therefore lead to very small uncertainties. CCFR quotes  $s_W^2 = 0.2236 \pm 0.0041$  for the reference values  $(m_t, M_H) = (175, 150)$  GeV with very little sensitivity to  $(m_t, M_H)$ .

The NuTeV collaboration found  $s_W^2 = 0.2277 \pm 0.0016$  (for the same reference values), which was  $3.0\sigma$  higher than the SM prediction [151]. However, since then several groups have raised concerns about the interpretation of the NuTeV result, which could affect the extracted  $g_{L,R}^2$  (and thus  $s_W^2$ ) including their uncertainties and correlation. These include the assumption of symmetric strange and anti-strange sea quark distributions, the electron neutrino contamination from  $K_{e3}$  decays, isospin symmetry violation in the parton distribution functions and from QED splitting effects, nuclear shadowing effects, and a more complete treatment of EW and QCD radiative corrections. A more detailed discussion and a list of references can be found in the 2016 edition of this *Review*. The precise impact of these effects would need to be evaluated carefully by the collaboration, but in the absence of such an effort we do not include the  $\nu$ DIS constraints in our default set of fits.

Recently, the COHERENT collaboration was the first to observe the coherent elastic neutrino nucleus scattering (CE $\nu$ NS) process [152] on a target consisting mostly of  $^{133}\text{Cs}$  and  $^{127}\text{I}$ , and at the opposite end of the kinematic scale where the momentum transfer is significantly smaller than the inverse of the nuclear radius. Subsequently, COHERENT [153] observed CE $\nu$ NS using a liquid  $^{40}\text{Ar}$  detector, as well. The coherence enhances the process roughly proportional to the square of the number of neutrons in the nuclei, but the process is difficult to observe as the experimental signature is a mere keV scale nuclear recoil.

### 10.3.2 Parity violating lepton scattering

Reviews on weak polarized electron scattering may be found in Refs. [9, 154]. The SLAC polarized electron-deuteron DIS (eDIS) experiment [155] measured the parity violating right-left asymmetry,

$$A_{RL} \equiv \frac{\sigma_R - \sigma_L}{\sigma_R + \sigma_L}, \quad (10.35)$$

where  $\sigma_{R,L}$  is the cross-section for the deep-inelastic scattering of a right- or left-handed electron,  $e_{R,L}N \rightarrow eX$ . In the quark parton model,

$$\frac{A_{RL}}{Q^2} = a_1 + a_2 \frac{1 - (1 - y)^2}{1 + (1 - y)^2}, \quad (10.36)$$

where  $Q^2 > 0$  is the momentum transfer and  $y$  is the fractional energy transfer from the electron to the hadrons. For the deuteron or other isoscalar targets, one has, neglecting the  $s$  quark and anti-quarks,

$$a_1 = \frac{3G_F}{5\sqrt{2}\pi\alpha} \left( g_{AV}^{eu} - \frac{1}{2}g_{AV}^{ed} \right) \approx \frac{3G_F}{5\sqrt{2}\pi\alpha} \left( -\frac{3}{4} + \frac{5}{3}\hat{s}_0^2 \right), \quad (10.37a)$$

$$a_2 = \frac{3G_F}{5\sqrt{2}\pi\alpha} \left( g_{VA}^{eu} - \frac{1}{2}g_{VA}^{ed} \right) \approx \frac{9G_F}{5\sqrt{2}\pi\alpha} \left( \hat{s}_0^2 - \frac{1}{4} \right). \quad (10.37b)$$

The Jefferson Lab Hall A collaboration [156, 157] improved on the SLAC result by measuring  $A_{RL}$  at  $Q^2 = 1.085$  GeV $^2$  and  $1.901$  GeV $^2$ , and determined the weak mixing angle to 2% precision,  $\hat{s}_Z^2 = 0.2299 \pm 0.0043$ . In another polarized electron scattering experiment on deuterons, but in the quasi-elastic kinematic regime, the SAMPLE experiment [158, 159] at MIT-Bates extracted

the combination  $g_{VA}^{eu} - g_{VA}^{ed}$  at  $Q^2$  values of 0.038 GeV $^2$  and 0.091 GeV $^2$ . What was actually determined were nucleon form factors from which the quoted results were obtained by the removal of a multi-quark radiative correction [160]. Other linear combinations of the effective couplings have been determined in polarized lepton scattering at CERN in  $\mu$ - $^{12}\text{C}$  DIS [161] (the observable was the double charge-helicity cross-section asymmetry), at Mainz in  $e$ - $^9\text{Be}$  (quasi-elastic) [162], and at Bates in  $e$ - $^{12}\text{C}$  (elastic) [163]. More recent polarized electron scattering experiments, *i.e.*, SAMPLE, the PVA4 experiment at Mainz, and the HAPPEX and GØ experiments at Jefferson Lab, have focussed on the strange quark content of the nucleon [164].

$A_{RL}$  can also be measured in fixed target polarized Møller scattering,  $e^-e^- \rightarrow e^-e^-$ , and reads [165],

$$\frac{A_{RL}}{Q^2} = -2g_{AV}^{ee} \frac{G_F}{\sqrt{2\pi\alpha}} \frac{1-y}{1+y^4 + (1-y)^4}. \quad (10.38)$$

It has been determined at low  $Q^2 = 0.026$  GeV $^2$  in the SLAC E158 experiment [166], with the result,  $A_{RL} = (-1.31 \pm 0.14_{\text{stat.}} \pm 0.10_{\text{syst.}}) \times 10^{-7}$ . Expressed in terms of the weak mixing angle in the  $\overline{\text{MS}}$  scheme this yields  $\hat{s}^2(161 \text{ MeV}) = 0.2403 \pm 0.0013$ , and as shown in Fig. 10.2 established the scale dependence of the weak mixing angle at the level of  $6.4\sigma$ . One also extracts the model-independent effective coupling,  $g_{AV}^{ee} = 0.0190 \pm 0.0027$  [13]. One-loop radiative corrections and implications are discussed in Ref. [87].

In a similar experiment and at about the same  $Q^2 = 0.0248$  GeV $^2$ , the Q<sub>weak</sub> collaboration at Jefferson Lab obtained  $A_{RL} = (-2.265 \pm 0.073_{\text{stat.}} \pm 0.058_{\text{syst.}}) \times 10^{-7}$  [167, 168] in elastic  $e^-p \rightarrow e^-p$  scattering. To extract the physical quantity of interest, the weak charge of the proton [169], a large ( $\approx 30\%$ ) correction had to be applied to  $A_{RL}$  arising from electromagnetic, strange, and axial form factors. This was achieved by performing a global fit [170] including a large number of  $A_{RL}$  data points at larger  $Q^2$ , dominated by the HAPPEX result at  $Q^2 = 0.109$  GeV $^2$  [171]. Finally, the constraint,  $2g_{AV}^{eu} + g_{AV}^{ed} = 0.0356 \pm 0.0023$ , which translates into a weak mixing angle measurement of  $\hat{s}^2(157 \text{ MeV}) = 0.2382 \pm 0.0011$ , could be deduced, after correcting for a relatively large and uncertain contribution from the  $\gamma Z$  box diagram [172–175].

### 10.3.3 Atomic parity violation

There are precise measurements of atomic parity violation (APV) [9, 176, 177] in  $^{133}\text{Cs}$  [178, 179] (at the 0.4% level [178]),  $^{205}\text{Tl}$  [180, 181],  $^{208}\text{Pb}$  [182], and  $^{209}\text{Bi}$  [183]. The EW physics is contained in the nuclear weak charges  $Q_W(Z, N)$ , where  $Z$  and  $N$  are the numbers of protons and neutrons in the nucleus. In terms of the nucleon vector couplings,

$$g_{AV}^{ep} \equiv 2g_{AV}^{eu} + g_{AV}^{ed} \approx -\frac{1}{2} + 2\hat{s}_0^2, \quad (10.39a)$$

$$g_{AV}^{en} \equiv g_{AV}^{eu} + 2g_{AV}^{ed} \approx +\frac{1}{2}, \quad (10.39b)$$

one has,

$$Q_W(Z, N) \equiv -2[Z(g_{AV}^{ep} + 0.00005) + N(g_{AV}^{en} + 0.00006)] \left(1 - \frac{\alpha}{2\pi}\right), \quad (10.40)$$

where the numerically small adjustments are discussed in Ref. [13] and include the result of the  $\gamma Z$ -box correction from Ref. [184].

*E.g.*,  $Q_W(^{133}_{78}\text{Cs})$  is extracted by measuring experimentally the ratio of the parity violating amplitude,  $E_{\text{PNC}}$ , to the Stark vector transition polarizability,  $\beta$ , and by calculating theoretically  $E_{\text{PNC}}$  in terms of  $Q_W$ . One can then write,

$$Q_W(^{133}_{78}\text{Cs}) = N \left( \frac{\text{Im } E_{\text{PNC}}}{\beta} \right)_{\text{exp.}} \left( \frac{|e| a_B}{\text{Im } E_{\text{PNC}}} \frac{Q_W}{N} \right)_{\text{th.}} \left( \frac{\beta}{a_B^3} \right)_{\text{exp.+th.}} \left( \frac{a_B^2}{|e|} \right), \quad (10.41)$$

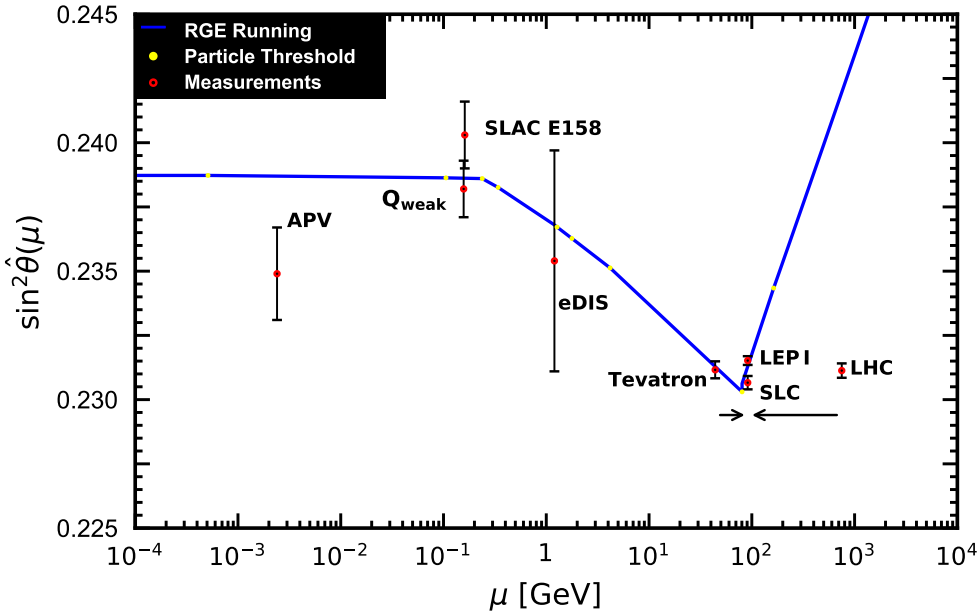


**Figure 10.2:** Scale dependence of the weak mixing angle defined in the  $\overline{\text{MS}}$  scheme [39,88] (for the scale dependence in a mass-dependent renormalization scheme, see Ref. [87]). The minimum of the curve corresponds to  $\mu = M_W$ , below which we switch to an effective theory with the  $W^\pm$  bosons integrated out, and where the  $\beta$ -function for  $\hat{s}^2(\mu)$  changes sign. At  $M_W$  and each fermion mass there are also discontinuities arising from scheme dependent matching terms, which are necessary to ensure that the various effective field theories within a given loop order describe the same physics. However, in the  $\overline{\text{MS}}$  scheme these are very small numerically and barely visible in the figure provided one decouples quarks at  $\mu = \hat{m}_q(\hat{m}_q)$ . The width of the curve exceeds the theory uncertainty from strong interaction effects which at low energies is at the level of  $\pm 2 \times 10^{-5}$  [39]. The Tevatron and LHC measurements are strongly dominated by invariant masses of the final-state di-lepton pair of  $\mathcal{O}(M_Z)$  and can thus be considered as additional  $Z$  pole data points. For clarity we displayed the Tevatron and LHC points horizontally to the left and right, respectively.

where  $a_B$  is the Bohr radius. There are currently two semi-empirical approaches to  $\beta$  of similar precision. The ratio of the off-diagonal hyperfine amplitude to the vector polarizability was measured directly by the Boulder group [185]. Combined with the hyperfine amplitude, computed precisely in Ref. [186], one finds  $\beta = (26.957 \pm 0.044_{\text{exp.}} \pm 0.027_{\text{th.}}) a_B^3$ . Alternatively, one can combine [187] the measurement of the ratio of scalar to vector transition polarizabilities [188] with the recent calculation of the scalar polarizability [189] to obtain  $\beta = (26.887 \pm 0.030_{\text{exp.}} \pm 0.021_{\text{th.}}) a_B^3$ , in agreement with earlier results [190, 191] based on this approach. The two determinations average to  $\beta = (26.911 \pm 0.025_{\text{exp.}} \pm 0.017_{\text{th.}}) a_B^3$ .

The uncertainties associated with the atomic wave function calculations are relatively small for cesium [9, 192–194]. State-of-the-art many-body atomic structure computations of the parity non-conserving amplitude,  $\text{Im } E_{\text{PNC}} = (0.8977 \pm 0.0040) \times 10^{-11} |e| a_B Q_W / N$  [195–200], together with the measurements [178, 179] which can be combined to give  $\text{Im } E_{\text{PNC}} / \beta = -1.5924 \pm 0.0055 \text{ mV/cm}$ , imply,

$$Q_W(^{133}_{78}\text{Cs}) = -72.41 \pm 0.26_{\text{exp.}} \pm 0.33_{\text{th.}}, \quad (10.42)$$

or equivalently the constraint,  $55g_{AV}^{ep} + 78g_{AV}^{en} = 36.25 \pm 0.21$ . Within the SM this can also be translated into a determination of the weak mixing angle,  $\hat{s}^2(2.4 \text{ MeV}) = 0.2349 \pm 0.0018$ , where the scale setting follows the estimate in Ref. [201] for the typical momentum transfer for parity violation experiments in Cs (the corresponding estimate for Tl amounts to 8 MeV). By comparing different hyperfine transitions, the Boulder experiment in cesium also observed the parity violating weak corrections to the nuclear electromagnetic vertex, called the nuclear anapole moment [202–204].

The theoretical atomic structure uncertainties are 3% for thallium [205] and even larger for the other atoms. However, they mostly cancel if one takes ratios of parity violation in different isotopes [206]. The first result of this type of experiment was announced recently by the Mainz group [207], who studied APV in  $^{100}\text{Yb}$ ,  $^{102}\text{Yb}$ ,  $^{104}\text{Yb}$ , and  $^{106}\text{Yb}$ , at the 0.5% level. The resulting three ratios can be interpreted as a measurement of  $\hat{s}_0^2 = 0.258 \pm 0.052$ , and represent a very complementary approach to search for BSM physics [208]. If the precision increases in the future, one would ultimately face uncertainties from differences in the neutron charge radii [209,210]. These can be constrained experimentally [211], *e.g.*, by measuring  $A_{RL}$  in heavier nuclei as done by the PREX collaboration at Jefferson Lab on  $^{208}\text{Pb}$  [212] and  $^{48}\text{Ca}$  [213].

## 10.4 Precision flavor physics

In addition to cross-sections, asymmetries, parity violation,  $W$ ,  $Z$ , Higgs and other collider physics, there is a large number of experiments and observables testing the flavor structure of the SM. These are addressed elsewhere in this *Review*, and are generally not included in this Section. However, we identify three precision observables with sensitivity to similar types of new physics as the other processes discussed here. The branching fraction of the flavor changing transition  $b \rightarrow s\gamma$  is of comparatively low precision, but since it is a loop-level process (in the SM) its sensitivity to new physics (and SM parameters, such as heavy quark masses) is enhanced. A discussion can be found in the 2010 edition of this *Review*.

The  $\tau$  lepton lifetime and leptonic branching ratios are primarily sensitive to  $\alpha_s$  and not affected significantly by many types of new physics. However, having an independent and reliable low energy measurement of  $\alpha_s$  in a global analysis allows the comparison with the  $Z$  lineshape determination of  $\alpha_s$  which shifts easily in the presence of new physics contributions. By far the most precise observable discussed here is the anomalous magnetic moment of the muon. Its combined experimental and theoretical uncertainty is smaller than typical electroweak scale contributions. The electron magnetic moment is measured to even greater precision, and as discussed in Sec. 10.2.2 can be used to determine  $\alpha$ . Its new physics sensitivity, however, is suppressed by an additional factor of  $m_e^2/m_\mu^2$ , unless there is a new light degree of freedom such as a dark  $Z$  [214] boson.

### 10.4.1 The $\tau$ lifetime

The extraction of  $\alpha_s$  from the  $\tau$  lifetime  $\tau_\tau$  [215,216] is standing out from other determinations because of a variety of independent reasons:

- (i) The  $\tau$ -scale is low, so that upon extrapolation to the  $Z$  scale (where it can be compared to the theoretically clean  $Z$  lineshape determinations) the  $\alpha_s$  error shrinks by about an order of magnitude.
- (ii) Yet, this scale is high enough that perturbation theory and the operator product expansion (OPE) can be applied.
- (iii) These observables are fully inclusive and thus free of fragmentation and hadronization effects that would have to be modeled or measured.
- (iv) Duality violation (DV) effects are most problematic near the branch cut but there they are suppressed by a double zero at  $s = m_\tau^2$ .
- (v) There are data [44,46,217] to constrain non-perturbative effects both within and breaking the

OPE.

- (vi) A complete four-loop order QCD calculation is available [218–222] in the massless limit.
- (vii) Large effects associated with the QCD  $\beta$ -function can be re-summed [223] in what has become known as contour improved perturbation theory (CIPT).

However, while CIPT certainly shows faster convergence in the lower (calculable) orders, doubts have been cast on the method by the observation of discrepancies in a specific model [224] and the realization that CIPT appears to be incompatible with the OPE [225, 226]. Moreover, it has been found that the construction of a renormalon-free scheme for the gluon condensate brings the CIPT results in agreement with ordinary fixed order perturbation theory (FOPT), without significantly modifying the latter [227, 228]. We therefore use the FOPT expressions [60, 222, 229],

$$\tau_\tau = \hbar \frac{1 - \mathcal{B}_\tau^s}{\Gamma_\tau^e + \Gamma_\tau^\mu + \Gamma_\tau^{ud}} = 290.75 \pm 0.36 \text{ fs} , \quad (10.43)$$

and

$$\begin{aligned} \Gamma_\tau^{ud} &= \frac{G_F^2 m_\tau^5 |V_{ud}|^2}{64\pi^3} S(m_\tau, M_Z) \left( 1 + \frac{3}{5} \frac{m_\tau^2 - m_\mu^2}{M_W^2} \right) \times \\ &\left[ 1 + \frac{\alpha_s^{(3)}(m_\tau)}{\pi} + 5.202 \frac{\alpha_s^2}{\pi^2} + 26.37 \frac{\alpha_s^3}{\pi^3} + 127.1 \frac{\alpha_s^4}{\pi^4} + \frac{\hat{\alpha}}{\pi} \left( \frac{85}{24} - \frac{\pi^2}{2} \right) + \delta_{\text{NP}} \right] , \end{aligned} \quad (10.44)$$

where  $\Gamma_\tau^e$  and  $\Gamma_\tau^\mu$  can be taken from Eq. (10.9) with obvious replacements. The relative fraction of strangeness changing ( $\Delta S = -1$ ) decays,  $\mathcal{B}_\tau^s = 0.0292 \pm 0.0004$ , is based on experimental data since the value for the strange quark mass,  $\hat{m}_s(m_\tau)$ , is not well known and the QCD expansion proportional to  $\hat{m}_s^2$  converges poorly and cannot be trusted.  $S(m_\tau, M_Z) = 1.01908 \pm 0.0003$  is a logarithmically enhanced EW correction factor [230] with higher orders re-summed [231].

$\delta_{\text{NP}}$  collects non-perturbative and quark-mass suppressed contributions, including the dimension four, six and eight terms in the OPE, as well as DV effects. We use the average  $\delta_{\text{NP}} = 0.0141 \pm 0.0072$  derived from the  $\tau$  decay spectral functions provided by OPAL [44] and ALEPH [46, 217], which give  $\delta_{\text{NP}} = 0.000 \pm 0.012$  and  $\delta_{\text{NP}} = 0.022 \pm 0.009$ , respectively. These numbers are based on the original analyses in Refs. [232, 233], but are modified to correspond to a strict FOPT analysis as is appropriate for our purpose<sup>10</sup> (for alternative analyses, see Section 9 on “Quantum Chromodynamics” in this *Review* ).

The dominant uncertainty arises from the truncation of the FOPT series and is conservatively taken as the  $\alpha_s^4$  term (this is re-calculated in each call of the fits, leading to an  $\alpha_s$ -dependent and thus asymmetric error) until a better understanding of the numerical differences between FOPT and CIPT has been gained. Our perturbative error covers almost the entire range from using CIPT to assuming that the nearly geometric series in Eq. (10.44) continues to higher orders. The experimental uncertainty in Eq. (10.43) is from the combination of the two leptonic branching ratios with the direct  $\tau_\tau$ . Included are also various smaller uncertainties ( $\pm 0.16$  fs) from other sources. Based on the method of Refs. [60, 234], we obtain in total

$$\alpha_s^{(4)}(m_\tau) = 0.312_{-0.013}^{+0.016} , \quad \alpha_s^{(5)}(M_Z) = 0.1171_{-0.0017}^{+0.0018} , \quad (10.45)$$

which represents a 1.5% determination of  $\alpha_s(M_Z)$ . For more details, see Refs. [232, 233] where the  $\tau$  spectral functions themselves and an estimate of the unknown  $\alpha_s^5$  term were used as additional inputs.

---

<sup>10</sup>We are indebted to Diogo Boito, Maarten Golterman, Kim Maltman and Santiago Peris for privately communicating these results to us.

### 10.4.2 The muon anomalous magnetic moment

The world average of the muon anomalous magnetic moment<sup>11</sup>,

$$a_\mu^{\text{exp}} = \frac{g_\mu - 2}{2} = (1165920.59 \pm 0.22) \times 10^{-9}, \quad (10.46)$$

is the combination of the final result of the BNL E821 collaboration [235] and the recent result of the Muon  $g - 2$  collaboration at Fermilab [236]. The QED contribution has been calculated to five loops [25, 27, 237–239] (fully analytic to three loops [240–244]). The estimated SM EW contribution [245–250],  $a_\mu^{\text{EW}} = (1.54 \pm 0.01) \times 10^{-9}$ , includes two-loop [251–255] and leading three-loop [256, 257] corrections and is at the level of more than four times the current total uncertainty.

The limiting factor in the interpretation of the result are the uncertainties from hadronic effects. The most recent evaluations of the leading-order (two-loop) hadronic vacuum polarization contribution using data from  $e^+e^- \rightarrow \text{hadrons}$  obtained  $a_\mu^{\text{had,VP}}(\alpha^2) = (68.81 \pm 0.41) \times 10^{-9}$  [258],  $a_\mu^{\text{had,VP}}(\alpha^2) = (69.23 \pm 0.33) \times 10^{-9}$  [259],  $a_\mu^{\text{had,VP}}(\alpha^2) = (69.40 \pm 0.40) \times 10^{-9}$  [41], and  $a_\mu^{\text{had,VP}}(\alpha^2) = (69.28 \pm 0.24) \times 10^{-9}$  [42]. Our analysis is based on the  $e^+e^-$  data compiled in Ref. [41], where by utilizing the assessment in Ref. [50], we add  $\tau$ -decay information and the very recent CMD-3 result [48] to estimate the dominant pion form factor contribution. We complement the contributions up to  $\sqrt{s} = 2$  GeV, for which we find  $a_\mu^{\text{had,VP}}(\alpha^2, 2 \text{ GeV}) = (65.12 \pm 0.30) \times 10^{-9}$ , with analytical PQCD expressions for energies beyond 2 GeV and for the  $c$  and  $b$  quark contributions [244, 260].

By now there are also precise results for  $a_\mu^{\text{had,VP}}(\alpha^2)$  from lattice QCD calculations [261]. We use the constraint,  $a_\mu^{\text{had,VP}}(\alpha^2, 2 \text{ GeV}) = (65.71 \pm 0.55) \times 10^{-9}$ , obtained from the result with the smallest quoted uncertainty (by the BMW collaboration [262]),  $a_\mu^{\text{had,VP}}(\alpha^2) = (70.75 \pm 0.55) \times 10^{-9}$ , by subtracting the perturbative QCD contribution including from charm and bottom quarks. It is important to note that there is a strong correlation (estimated to 86% in Ref. [51]) between  $a_\mu^{\text{had,VP}}(\alpha^2, 1.8 \text{ GeV})$  and  $\Delta\alpha_{\text{had}}^{(3)}(1.8 \text{ GeV})$  discussed in Sec. 10.2.2. As a result, using the lattice calculation from Ref. [49] as a constraint for  $\Delta\alpha_{\text{had}}$  has an impact on  $a_\mu^{\text{had,VP}}$  by slightly increasing it<sup>12</sup>. Incorporating this effect together with the BMW result,  $a_\mu^{\text{had,VP}}(\alpha^2, 2 \text{ GeV}) = (65.71 \pm 0.55) \times 10^{-9}$ , and the data-driven value,  $a_\mu^{\text{had,VP}}(\alpha^2, 2 \text{ GeV}) = (65.12 \pm 0.30) \times 10^{-9}$ , we obtain

$$a_\mu^{\text{had,VP}}(\alpha^2, 2 \text{ GeV}) = (65.44 \pm 0.25) \times 10^{-9}, \quad (10.47)$$

which we use as an input to our fits. The BMW result is roughly  $2\sigma$  higher than the value derived from the KLOE data [263], is slightly lower than that from CMD-3 [48], and agrees well with  $\tau$  decays. In fact, the discrepancy between KLOE and CMD-3 cross-sections exceeds  $5\sigma$  locally, and amounts to  $3.3\sigma$  if one considers the entire overlap region of the two experiments [50]. A more detailed analysis [264, 265] of the difference between BMW and the data-driven evaluation using KLOE input suggests that it originates mostly from hadronic contributions below 2 GeV to the vacuum polarization. The BMW result for this hadronic window is supported by findings from other lattice collaborations [266–272]. Possible explanations for this discrepancy include underestimated systematic uncertainties in the analysis of some of the available experimental data and higher-order initial-state radiation effects [50].

Sub-leading hadronic vacuum polarization effects at three-loop [273] and four-loop order [274] contribute  $a_\mu^{\text{had,VP}}(\alpha^3) = (-0.983 \pm 0.004) \times 10^{-9}$  [42] and  $a_\mu^{\text{had,VP}}(\alpha^4) = (0.124 \pm 0.001) \times 10^{-9}$  [274], respectively. To account for the larger vacuum polarization effects suggested by lattice QCD, we

<sup>11</sup>In what follows, we summarize the most important aspects of  $a_\mu$  and give some details on the evaluation in our fits. For more details and references, see Section 56 on the “Muon Anomalous Magnetic Moment” in this *Review*. There are some numerical differences, which are well understood and arise because internal consistency of the fits requires the calculation of all observables from analytical expressions and common inputs and fit parameters, so that an independent evaluation is necessary for this Section.

<sup>12</sup>Conversely, adding the BMW constraint for  $a_\mu^{\text{had,VP}}$  has the effect of increasing  $\Delta\alpha_{\text{had}}^{(3)}(2 \text{ GeV})$ .

increase both  $a_\mu^{\text{had},\text{VP}}(\alpha^3)$  and  $a_\mu^{\text{had},\text{VP}}(\alpha^4)$  by 1%. The correlations with the two-loop hadronic contribution and with  $\Delta\alpha(M_Z)$  (see Sec. 10.2) were considered in Ref. [244].

The other hadronic uncertainty is induced by the three-loop light-by-light scattering amplitude, where a number of independent model calculations yield results which are in reasonable agreement with each other,  $a_\mu^{\text{had},\gamma\times\gamma}(\alpha^3) = (1.36 \pm 0.25) \times 10^{-9}$  [275],  $a_\mu^{\text{had},\gamma\times\gamma}(\alpha^3) = 1.37^{+0.15}_{-0.27} \times 10^{-9}$  [276],  $a_\mu^{\text{had},\gamma\times\gamma}(\alpha^3) = (1.05 \pm 0.26) \times 10^{-9}$  [277], and  $a_\mu^{\text{had},\gamma\times\gamma}(\alpha^3) = (1.03 \pm 0.29) \times 10^{-9}$  [258], but the sign of this effect is opposite [278] to the one quoted in the 2002 edition of this *Review*. There is also an upper bound given by  $a_\mu^{\text{had},\gamma\times\gamma}(\alpha^3) < 1.59 \times 10^{-9}$  [276] but this requires an *ad hoc* assumption, too. Efforts to improve the evaluation by using experimental input where available yield the lower values,  $a_\mu^{\text{had},\gamma\times\gamma}(\alpha^3) = (0.87 \pm 0.13) \times 10^{-9}$  [279] and  $a_\mu^{\text{had},\gamma\times\gamma}(\alpha^3) = (0.92 \pm 0.19) \times 10^{-9}$  [261]. See also Ref. [280] for a recent discussion of the axial-vector contribution and short-distance constraints. Lattice calculations have reached similar levels of precision,  $a_\mu^{\text{had},\gamma\times\gamma}(\alpha^3) = (1.10 \pm 0.15) \times 10^{-9}$  [281, 282] and  $a_\mu^{\text{had},\gamma\times\gamma}(\alpha^3) = (1.25 \pm 0.15) \times 10^{-9}$  [283], and are consistent with the model and data-driven calculations. For our fits we average the two lattice results (with the systematic errors considered as fully correlated) and combine them with the data-driven result [261] to obtain,

$$a_\mu^{\text{had},\gamma\times\gamma}(\alpha^3) = (1.11 \pm 0.10) \times 10^{-9}, \quad (10.48)$$

which we have shifted by  $1 \times 10^{-11}$  to account for the perturbative charm quark treatment of Ref. [276]. Higher-order contributions with a hadronic light-by-light scattering subgraph have been estimated in Ref. [284] with the result,  $a_\mu^{\text{had},\gamma\times\gamma}(\alpha^4) = (0.02 \pm 0.01) \times 10^{-9}$  [261].

Altogether, the SM prediction is

$$a_\mu^{\text{theory}} = (1165919.46 \pm 0.27) \times 10^{-9}, \quad (10.49)$$

where the error is from the hadronic uncertainties excluding parametric ones, such as from  $\alpha_s$  and the heavy quark masses. We evaluate the correlation of the total (experimental plus theoretical) uncertainty in  $a_\mu$  with  $\Delta\alpha(M_Z)$  to amount to 43%. The overall  $3.2\sigma$  discrepancy between the experimental value (10.46) and the SM prediction,

$$a_\mu^{\text{exp}} - a_\mu^{\text{theory}} = (1.13 \pm 0.35) \times 10^{-9}, \quad (10.50)$$

could be due to fluctuations ( $a_\mu^{\text{exp}}$  is statistics dominated) or underestimates of the theoretical uncertainties. On the other hand, the deviation could also arise from physics beyond the SM, such as supersymmetric models with large  $\tan\beta$  and moderately light superparticle masses [285], or a dark  $Z$  boson [214].

## 10.5 Physics of the massive electroweak bosons

If the CM energy  $\sqrt{s}$  is large compared to the fermion mass  $m_f$ , the unpolarized Born cross-section for  $e^+e^- \rightarrow f\bar{f}$  [286] can be written as,

$$\frac{d\sigma}{d\cos\theta} = \frac{\pi\alpha^2(s)}{2s} \left[ F_1(1 + \cos^2\theta) + 2F_2\cos\theta \right] + B, \quad (10.51\text{a})$$

$$F_1 = Q_e^2 Q_f^2 - 2\chi Q_e Q_f \bar{g}_V^e \bar{g}_V^f \cos\delta_R + \chi^2 (\bar{g}_V^{e2} + \bar{g}_A^{e2})(\bar{g}_V^{f2} + \bar{g}_A^{f2}), \quad (10.51\text{b})$$

$$F_2 = -2\chi Q_e Q_f \bar{g}_A^e \bar{g}_A^f \cos\delta_R + 4\chi^2 \bar{g}_V^e \bar{g}_A^e \bar{g}_V^f \bar{g}_A^f, \quad (10.51\text{c})$$

where

$$\tan\delta_R = \frac{\bar{M}_Z \bar{\Gamma}_Z}{\bar{M}_Z^2 - s}, \quad \chi = \frac{G_F}{2\sqrt{2}\pi\alpha(s)} \frac{s \bar{M}_Z^2}{[(\bar{M}_Z^2 - s)^2 + \bar{M}_Z^2 \bar{\Gamma}_Z^2]^{1/2}}. \quad (10.52)$$

$B$  accounts for box graphs involving virtual  $Z$  and  $W$  bosons, and the  $\bar{g}_{V,A}^f$  are defined in Eq. (10.53) below.  $\bar{M}_Z$  and  $\bar{T}_Z$  correspond to mass and width definitions based on a Breit-Wigner shape with an energy-independent width (see Section 55 on the “ $Z$  Boson” in this *Review*). The differential cross-section receives important corrections from QED effects in the initial and final states, and interference between the two [287]. For  $q\bar{q}$  production, there are additional final-state QCD corrections, which are relatively large. Note also that the equations above are written in the CM frame of the incident  $e^+e^-$  system, which may be boosted due to the initial-state QED radiation.

Some of the leading virtual EW corrections are captured by the running QED coupling  $\alpha(s)$  and the Fermi constant  $G_F$ . The remaining corrections to the  $Zff$  interactions are absorbed by replacing the tree-level couplings in Eq. (10.7) with the  $s$ -dependent *effective couplings* [288],

$$\bar{g}_V^f = \sqrt{\rho_f} \left( t_{3L}^f - 2Q_f \kappa_f \sin^2 \theta_W \right) , \quad (10.53a)$$

$$\bar{g}_A^f = \sqrt{\rho_f} t_{3L}^f . \quad (10.53b)$$

In these equations, the effective couplings are to be taken at the scale  $\sqrt{s}$ , but for notational simplicity we do not show this explicitly. At tree-level,  $\rho_f = \kappa_f = 1$ , but inclusion of EW radiative corrections leads to  $\rho_f \neq 1$  and  $\kappa_f \neq 1$ , which depend on the fermion  $f$  and on the renormalization scheme. In the on-shell scheme, the quadratic  $m_t$  dependence is given by,

$$\rho_f \sim 1 + \rho_t , \quad \kappa_f \sim 1 + \frac{\rho_t}{\tan^2 \theta_W} , \quad (10.54)$$

while in  $\overline{\text{MS}}$ ,  $\hat{\rho}_f \sim \hat{\kappa}_f \sim 1$ , for  $f \neq b$ , and

$$\hat{\rho}_b \sim 1 - \frac{4}{3}\rho_t , \quad \hat{\kappa}_b \sim 1 + \frac{2}{3}\rho_t . \quad (10.55)$$

In the  $\overline{\text{MS}}$  scheme the normalization is changed according to  $G_F M_Z^2 / 2\sqrt{2}\pi \rightarrow \hat{\alpha} / 4\hat{s}_Z^2 \hat{c}_Z^2$  in the second Eq. (10.52).

As reviewed in Sec. 10.2.5, for the high precision  $Z$  pole observables discussed below, many additional bosonic and fermionic loop effects, vertex corrections, and higher order contributions, *etc.*, must be included. For example, in the  $\overline{\text{MS}}$  scheme one then has  $\hat{\rho}_\ell = 0.9977$ ,  $\hat{\kappa}_\ell = 1.0014$ ,  $\hat{\rho}_b = 0.9867$ , and  $\hat{\kappa}_b = 1.0068$ .

To connect to measured quantities, it is convenient to define an effective angle

$$s_f^2 \equiv \sin^2 \bar{\theta}_{Wf} \equiv \hat{\kappa}_f \hat{s}_Z^2 = \kappa_f s_W^2 , \quad (10.56)$$

in terms of which  $\bar{g}_V^f$  and  $\bar{g}_A^f$  are given by  $\sqrt{\rho_f}$  times their tree-level formulae. One finds that the  $\hat{\kappa}_f$  ( $f \neq b$ ) are almost independent of  $m_t$  and  $M_H$ , and thus one can write,

$$\bar{s}_\ell^2 = \hat{s}_Z^2 + 0.00032 , \quad (10.57)$$

while the  $\kappa_f$  for the on-shell scheme are  $m_t$  dependent.

### 10.5.1 The $Z$ boson mass

The mass of the  $Z$  boson,  $M_Z = 91.1876 \pm 0.0021$  GeV, has been determined from the  $Z$  lineshape scan at LEP 1 [288]. Very recently the CDF collaboration at the Tevatron [289] determined  $M_Z$  from fits to the dimuon and dielectron mass distributions. The dimuon channel strongly dominates so that our combination,  $M_Z = 91.192 \pm 0.007$  GeV, is insensitive (at the level of the quoted digits)

to variations in the assumption concerning possible cross-channel correlations. Combined we find the world average,

$$M_Z = 91.1880 \pm 0.0020 \text{ GeV} . \quad (10.58)$$

These values correspond to a definition based on a Breit-Wigner shape with an energy-dependent width, which differs from  $\bar{M}_Z$  in eq. (10.52)<sup>13</sup>.

### 10.5.2 Electroweak physics off the $Z$ pole

Experiments at PEP, PETRA and TRISTAN have measured the unpolarized forward-backward asymmetry,  $A_{FB}$ , and the total cross-section relative to pure QED,  $R$ , for  $e^+e^- \rightarrow \ell^+\ell^-$ ,  $\ell = \mu$  or  $\tau$  at CM energies  $\sqrt{s} < M_Z$ . They are defined as

$$A_{FB} \equiv \frac{\sigma_F - \sigma_B}{\sigma_F + \sigma_B} , \quad R = \frac{\sigma}{\mathcal{R}_{\text{ini}} \otimes \sigma_{\text{QED}}} , \quad (10.59)$$

where  $\sigma_F(\sigma_B)$  is the cross-section for  $\ell^-$  to travel forward (backward) with respect to the  $e^-$  direction,  $\sigma_{\text{QED}}$  is the tree-level cross-section from s-channel photon exchange, and  $\mathcal{R}_{\text{ini}} \otimes$  denotes convolution with initial-state QED corrections. Neglecting box graph contributions, they are given by,

$$A_{FB} = \frac{3}{4} \frac{F_2}{F_1} , \quad R = F_1 . \quad (10.60)$$

For the available data, it is sufficient to approximate the EW corrections through the leading running  $\alpha(s)$  and quadratic  $m_t$  contributions [290], as described above. Reviews and formulae for  $e^+e^- \rightarrow$  hadrons may be found in [9, 291, 292].

LEP 2 [294] ran at several energies above the  $Z$  pole up to  $\sim 209$  GeV. Measurements were made of a number of observables, including the total production cross-sections of  $f\bar{f}$  pairs for  $f = \mu, \tau$ , and  $q$  (hadrons), of four-fermion final states, of  $\gamma\gamma$ ,  $ZZ$ ,  $WW$  and  $WW\gamma$ . The differential cross-sections for all three lepton flavors, and the leptonic and hadronic  $W$  branching ratios were also extracted.

Among the most important LEP 2 results were the measurements [294] of the  $W$  boson mass,  $M_W$ , which were dominated by kinematic reconstruction, but included the complementary albeit statistics limited and thus much less precise determination from a  $WW$  threshold cross-section measurement. The kinematic method was also employed at the Tevatron [301] and by ATLAS [302] and LHCb [296] at the LHC. A recent combination [298] of all available  $M_W$  measurements, using a careful calibration of simulation tools and PDFs, obtained the world average,

$$M_W = 80.3946 \pm 0.0115 \text{ GeV} . \quad (10.61)$$

However, the  $\chi^2$  probability of this combination is 0.5% or less, depending on the chosen PDF set, which is mostly due to the  $W$  mass measurement by CDF from Run II at the Tevatron [289],  $M_W = 80.432 \pm 0.016$  GeV (adjusted to the common PDF set CT18 [303] in Ref. [298]). It differs by almost  $4\sigma$  from the other measurements of  $M_W$ , while the latter agree well among each other, with the average [298]

$$M_W = 80.3692 \pm 0.0133 \text{ GeV} , \quad (10.62)$$

without CDF II. Subsequently, the ATLAS result has been updated [295], resulting in a significant downward shift of  $M_W$ . It also included a measurement of the  $W$  boson width,  $\Gamma_W$ , together with a strong 30% anticorrelation with  $M_W$ . The new ATLAS  $\Gamma_W$  value differs by about  $2\sigma$  from

---

<sup>13</sup>Note that  $\bar{M}_Z$  is defined through the complex pole of the propagator, which ensures that it is gauge-invariant and theoretically consistent, and which leads to a Breit-Wigner shape with a constant width. The two definitions differ numerically, and this difference has to be accounted for in theoretical calculations.

**Table 10.4:** Non- $Z$  pole observables, compared with the SM best fit predictions. The SM prediction for  $\Gamma_H$  is without electroweak corrections as in Ref. [293]. The first and second  $M_W$  and  $\Gamma_W$  values are from LEP 2 [294] and ATLAS [295], respectively. The remaining  $M_W$  values are from LHCb [296], DØ [297], and CDF [289], respectively, adjusted according to Ref. [298], and where the last one [in brackets] is omitted from the fits (see text and Sec. 10.8). The third  $\Gamma_W$  is the Tevatron combination [299], shifted to correspond to the current SM prediction of  $M_W$  (what is actually measured is a linear combination containing an  $M_W$  term). The hadronic branching ratio for  $W$  decays combines LEP 2 [294] and CMS [300] and assumes lepton flavor universality. The world averages for  $g_{V,A}^{\nu e}$  are dominated by the CHARM II [139] results,  $g_V^{\nu e} = -0.035 \pm 0.017$  and  $g_A^{\nu e} = -0.503 \pm 0.017$ . The  $\tau_\tau$  value is the  $\tau$  lifetime world average computed by combining the direct measurements with values derived from the leptonic branching ratios [60]; in this case, the theory error is included in the SM prediction. In all other SM predictions, the uncertainty is parametric from  $M_Z$ ,  $M_H$ ,  $m_t$ ,  $m_b$ ,  $m_c$ ,  $\hat{\alpha}(M_Z)$ , and  $\alpha_s$ , and theoretical from unknown higher orders [83], where correlations due to both types have been accounted for. The column denoted by Pull gives the standard deviations.

Quantity	Value	Standard Model	Pull
$m_t$ [GeV]	$172.61 \pm 0.58$	$172.85 \pm 0.55$	-0.4
$M_H$ [GeV]	$125.10 \pm 0.09$	$125.10 \pm 0.09$	0.0
$\Gamma_H$ [MeV]	$3.5 \pm 1.5$	$4.09 \pm 0.05$	-0.4
$M_W$ [GeV]	$80.376 \pm 0.033$	$80.356 \pm 0.005$	0.6
	$80.355 \pm 0.016$		-0.1
	$80.347 \pm 0.033$		-0.3
	$80.372 \pm 0.026$		0.6
	[ $80.432 \pm 0.016$ ]		—
$\Gamma_W$ [GeV]	$2.195 \pm 0.083$	$2.089 \pm 0.001$	1.3
	$2.198 \pm 0.049$		2.2
	$2.059 \pm 0.049$		-0.6
$\mathcal{B}(W \rightarrow \text{hadrons})$	$0.6736 \pm 0.0018$	$0.6751 \pm 0.0001$	-0.8
$g_V^{\nu e}$	$-0.040 \pm 0.015$	$-0.0395 \pm 0.0001$	0.0
$g_A^{\nu e}$	$-0.507 \pm 0.014$	$-0.5063$	0.0
$Q_W(e)$	$-0.0403 \pm 0.0053$	$-0.0469 \pm 0.0002$	1.3
$Q_W(p)$	$0.0719 \pm 0.0045$	$0.0705 \pm 0.0002$	0.3
$Q_W(\text{Cs})$	$-72.41 \pm 0.42$	$-73.26 \pm 0.01$	2.0
$Q_W(\text{Tl})$	$-116.4 \pm 3.6$	$-116.93 \pm 0.01$	0.1
$\hat{s}_Z^2(\text{eDIS})$	$0.2299 \pm 0.0043$	$0.23129 \pm 0.00004$	-0.3
$\tau_\tau$ [fs]	$290.75 \pm 0.36$	$288.59 \pm 2.31$	0.9
$\frac{1}{2}(g_\mu - 2 - \frac{\alpha}{\pi})$	$(4510.86 \pm 0.35) \times 10^{-9}$	$(4509.73 \pm 0.03) \times 10^{-9}$	3.2

the Tevatron width result [299] and the SM prediction. To include it in the global fit, instead of employing (10.62) *verbatim*, we combine (i) the adjusted results for DØ and LHCb quoted in Ref. [298], (ii) LEP [294], (iii) the new ATLAS results [295], and (iv) the Tevatron width determination [299], keeping the approximate 49% PDF anticorrelation between ATLAS and LHCb. Including further small correlations between DØ and the LHC experiments, this results in the

updated overall averages (without  $M_W$  from CDF as recommended by the authors of Ref. [298]<sup>14)</sup>,

$$M_W = 80.360 \pm 0.012 \text{ GeV} , \quad (10.63)$$

$$\Gamma_W = 2.136 \pm 0.032 \text{ GeV} , \quad (10.64)$$

with a correlation coefficient of close to  $-0.3$ . Alternatively, fixing  $\Gamma_W$  to the SM prediction gives

$$M_W = 80.366 \pm 0.012 \text{ GeV} . \quad (10.65)$$

For details and references, see Section 54 on the “Mass and Width of the  $W$  Boson” in this *Review*.

Strong constraints on anomalous triple and quartic gauge couplings have been obtained at LEP 2, the Tevatron, and the LHC. These are described in detail in “Extraction of Triple Gauge Couplings (TGCs)”, “Anomalous  $W/Z$  Quartic Couplings (QGCs)” notes in the  $W$  particle listing and in “Anomalous  $ZZ\gamma$ ,  $Z\gamma\gamma$ , and  $ZZV$  Couplings” note in the  $Z$  particle listing.

After their discovery of the Higgs boson [304, 305], the LHC experiments are now performing high precision measurements of its mass,  $M_H$ . We average the results,  $M_H = 125.11 \pm 0.09_{\text{stat.}} \pm 0.06_{\text{syst.}}$  GeV from ATLAS [306], and  $M_H = 125.08 \pm 0.10_{\text{stat.}} \pm 0.07_{\text{syst.}}$  GeV from CMS [307], by treating the smaller systematic error as common among the two determinations, and arrive at,

$$M_H = 125.10 \pm 0.07_{\text{stat.}} \pm 0.06_{\text{syst.}} \text{ GeV (LHC)} . \quad (10.66)$$

There are also first measurements of the Higgs boson width,  $\Gamma_H = 2.9^{+1.9}_{-1.4}$  MeV from CMS [307] and  $\Gamma_H = 4.5^{+3.3}_{-2.5}$  MeV from ATLAS [308]. We perform a simple Gaussian average using the upper error of CMS and the lower error of ATLAS. For further references and more details on Higgs boson properties, see Section 11 on the “Status of Higgs Boson Physics” in this *Review*.

The principal non- $Z$  pole observables discussed here and in Sections 10.2–10.4 are summarized in Table 10.4.

### 10.5.3 $Z$ pole physics

High precision measurements of various  $Z$  pole ( $\sqrt{s} \approx M_Z$ ) observables [9, 318, 319] have been performed at LEP 1 and SLC [288, 315, 316, 320, 321], as summarized in Table 10.5. These include the  $Z$  mass and total width,  $\Gamma_Z$ , and partial widths  $\Gamma_{f\bar{f}}$  for  $Z \rightarrow f\bar{f}$ , where  $f = e, \mu, \tau$ , light hadrons,  $b$ , and  $c$ . It is convenient to use the variables  $M_Z$ ,  $\Gamma_Z$ ,

$$\sigma_{\text{had}} \equiv \frac{12\pi\Gamma_{e^+e^-}\Gamma_{\text{had}}}{M_Z^2\Gamma_Z^2} , \quad R_\ell \equiv \frac{\Gamma_{\text{had}}}{\Gamma_{\ell^+\ell^-}} , \quad R_q \equiv \frac{\Gamma_{q\bar{q}}}{\Gamma_{\text{had}}} , \quad (10.67)$$

for  $\ell = e, \mu$  or  $\tau$ , and  $q = b$  or  $c$ , where  $\Gamma_{\text{had}}$  is the partial decay width into hadrons. Most of these are weakly correlated experimentally. The three values for  $R_\ell$  are consistent with lepton universality<sup>15</sup> (although  $R_\tau$  is somewhat low compared to  $R_e$  and  $R_\mu$ ), but we use the general analysis in which the three observables are treated as independent. Similar remarks apply to  $A_{FB}^{0,\ell}$  defined through Eq. (10.68) with  $P_e = 0$ , where  $A_{FB}^{0,\tau}$  is somewhat high. Initial-state radiation reduces the peak cross-section by more than 25%, where  $\mathcal{O}(\alpha^3)$  QED effects induce a large anti-correlation ( $-30\%$ ) between  $\Gamma_Z$  and  $\sigma_{\text{had}}$ . The anti-correlation between  $R_b$  and  $R_c$  amounts to  $-18\%$  [288]. The  $R_\ell$  are insensitive to  $m_t$  except for the  $Z \rightarrow b\bar{b}$  vertex, final-state corrections, and the implicit dependence through  $\sin^2\theta_W$ . Thus, they are especially useful for constraining  $\alpha_s$ .

Very important constraints follow from measurements of various  $Z$  pole asymmetries. These include the forward-backward asymmetry,  $A_{FB}$ , and the polarization or left-right asymmetry,  $A_{LR}$ ,

<sup>14</sup>See Sec. 10.8 for the impact of including the CDF  $W$  mass result.

<sup>15</sup>The ratio of branching fractions for  $Z$  bosons decaying into  $e^+e^-$  relative to  $\mu^+\mu^-$  final states has also been measured by ATLAS [322], obtaining  $R_{e/\mu} = 1.0026 \pm 0.0050$ , in perfect agreement with lepton universality.

**Table 10.5:** Principal  $Z$  pole observables and their SM predictions (*cf.* Table 10.4). The first  $M_Z$  is from LEP 1 [288] and the second from CDF [289]. The first  $\bar{s}_\ell^2$  is the effective weak mixing angle extracted from the hadronic charge asymmetry at LEP 1 [288], the second is the combined value from the Tevatron [309], and the third is from the LHC [310–314]. The values of  $A_e$  are (i) from  $A_{LR}$  for hadronic final states [315]; (ii) from  $A_{LR}$  for leptonic final states and from polarized Bhabha scattering [316]; and (iii) from the angular distribution of the  $\tau$  polarization at LEP 1 [288]. The  $A_\tau$  values are from SLD [316], the total  $\tau$  polarization from LEP [288], and from CMS [317], respectively. Note that the SM errors in  $\Gamma_Z$ , the  $R_\ell$ , and  $\sigma_{\text{had}}$  are largely dominated by the uncertainty in  $\alpha_s$ .

Quantity	Value	Standard Model	Pull
$M_Z$ [GeV]	$91.1876 \pm 0.0021$	$91.1884 \pm 0.0019$	-0.4
	$91.192 \pm 0.007$		0.6
$\Gamma_Z$ [GeV]	$2.4955 \pm 0.0023$	$2.4940 \pm 0.0009$	0.7
$\sigma_{\text{had}}$ [nb]	$41.481 \pm 0.033$	$41.481 \pm 0.009$	0.0
$R_e$	$20.804 \pm 0.050$	$20.736 \pm 0.010$	1.4
$R_\mu$	$20.784 \pm 0.034$	$20.736 \pm 0.010$	1.4
$R_\tau$	$20.764 \pm 0.045$	$20.781 \pm 0.010$	-0.4
$R_b$	$0.21629 \pm 0.00066$	$0.21583 \pm 0.00002$	0.7
$R_c$	$0.1721 \pm 0.0030$	$0.17221 \pm 0.00003$	0.0
$A_{FB}^{(0,e)}$	$0.0145 \pm 0.0025$	$0.01606 \pm 0.00006$	-0.6
$A_{FB}^{(0,\mu)}$	$0.0169 \pm 0.0013$		0.6
$A_{FB}^{(0,\tau)}$	$0.0188 \pm 0.0017$		1.6
$A_{FB}^{(0,b)}$	$0.0996 \pm 0.0016$	$0.1026 \pm 0.0002$	-1.8
$A_{FB}^{(0,c)}$	$0.0707 \pm 0.0035$	$0.0732 \pm 0.0002$	-0.7
$A_{FB}^{(0,s)}$	$0.0976 \pm 0.0114$	$0.1027 \pm 0.0002$	-0.4
$\bar{s}_\ell^2$	$0.2324 \pm 0.0012$	$0.23161 \pm 0.00004$	0.7
	$0.23148 \pm 0.00033$		-0.4
	$0.23145 \pm 0.00028$		-0.6
$A_e$	$0.15138 \pm 0.00216$	$0.1463 \pm 0.0003$	2.3
	$0.1544 \pm 0.0060$		1.3
	$0.1498 \pm 0.0049$		0.7
$A_\mu$	$0.142 \pm 0.015$		-0.3
$A_\tau$	$0.136 \pm 0.015$		-0.7
	$0.1439 \pm 0.0043$		-0.6
	$0.144 \pm 0.015$		-0.2
$A_b$	$0.923 \pm 0.020$	$0.9347$	-0.6
$A_c$	$0.670 \pm 0.027$	$0.6674 \pm 0.0001$	0.1
$A_s$	$0.895 \pm 0.091$	$0.9356$	-0.4

defined analogously to Eq. (10.35). The latter was measured precisely by the SLD collaboration at the SLC [315], and has the advantages of being very sensitive to  $\bar{s}_\ell^2$  and that systematic uncertain-

ties largely cancel. After removing initial-state QED corrections and contributions from photon exchange,  $\gamma$ - $Z$  interference, as well as the EW boxes in Eq. (10.51a), one can use the effective tree-level expressions,

$$A_{LR} = A_e P_e , \quad A_{FB} = \frac{3}{4} A_f \frac{A_e + P_e}{1 + P_e A_e} , \quad (10.68)$$

where,

$$A_f \equiv \frac{2\bar{g}_V^f \bar{g}_A^f}{\bar{g}_V^{f2} + \bar{g}_A^{f2}} = \frac{1 - 4|Q_f|\bar{s}_f^2}{1 - 4|Q_f|\bar{s}_f^2 + 8Q_f^2\bar{s}_f^4} . \quad (10.69)$$

$P_e$  is the initial  $e^-$  polarization, so that the second equality in Eq. (10.70) is reproduced for  $P_e = 1$ , and the  $Z$  pole forward-backward asymmetries at LEP 1 ( $P_e = 0$ ) are given by  $A_{FB}^{(0,f)} = \frac{3}{4} A_e A_f$  for  $f = e, \mu, \tau, b, c, s$  [288], and  $q$ , and where  $A_{FB}^{(0,q)}$  refers to the hadronic charge asymmetry. Corrections for  $t$ -channel exchange and  $s/t$ -channel interference cause  $A_{FB}^{(0,e)}$  to be strongly anti-correlated with  $R_e$  ( $-37\%$ ). Recently, the  $m_b$ -dependence [323] of the  $\mathcal{O}(\alpha_s^2)$  QCD correction [324], affecting the reference axis of the  $b$  quark asymmetry [325], increased the extracted<sup>16</sup>  $A_{FB}^{(0,b)}$  by about  $0.2\sigma$ . The correlation between  $A_{FB}^{(0,b)}$  and  $A_{FB}^{(0,c)}$  amounts to  $15\%$ .

In addition, SLD extracted the final-state couplings  $A_b$ ,  $A_c$  [288],  $A_s$  [320],  $A_\tau$ , and  $A_\mu$  [316], from left-right forward-backward asymmetries, using

$$A_{LR}^{FB}(f) = \frac{\sigma_{LF}^f - \sigma_{LB}^f - \sigma_{RF}^f + \sigma_{RB}^f}{\sigma_{LF}^f + \sigma_{LB}^f + \sigma_{RF}^f + \sigma_{RB}^f} = \frac{3}{4} A_f , \quad (10.70)$$

where, for example,  $\sigma_{LF}^f$  is the cross-section for a left-handed incident electron to produce a fermion  $f$  traveling in the forward hemisphere. Similarly,  $A_\tau$  and  $A_e$  were measured at LEP 1 [288] ( $A_\tau$  also very recently by CMS [317]) through the  $\tau$  polarization,  $\mathcal{P}_\tau$ , as a function of the scattering angle  $\theta$ , which can be written as,

$$\mathcal{P}_\tau = -\frac{A_\tau(1 + \cos^2 \theta) + 2A_e \cos \theta}{(1 + \cos^2 \theta) + 2A_\tau A_e \cos \theta} . \quad (10.71)$$

The average polarization,  $\langle \mathcal{P}_\tau \rangle$ , obtained by integrating over  $\cos \theta$  in the numerator and denominator of Eq. (10.71), yields  $\langle \mathcal{P}_\tau \rangle = -A_\tau$ , and  $A_e$  can be extracted from the  $\mathcal{P}_\tau$  angular distribution. The initial-state coupling,  $A_e$ , was also determined through the left-right charge asymmetry [321] and in polarized Bhabha scattering [316] at the SLC. Because  $\bar{g}_V^\ell$  is very small, not only  $A_{LR}^0 = A_e$ ,  $A_{FB}^{(0,\ell)}$ , and  $\mathcal{P}_\tau$ , but also  $A_{FB}^{(0,q)}$  for  $q = b, c$ , and  $s$ , as well as the hadronic asymmetries are mainly sensitive to  $\bar{s}_\ell^2$ . The combination of all LEP and SLC asymmetries (but excluding other observables such as  $R_\ell$ ) yields,

$$\bar{s}_\ell^2 = 0.23151 \pm 0.00016 \text{ (LEP + SLC)} . \quad (10.72)$$

As an example of the precision of the  $Z$  pole observables, the values of  $\bar{g}_A^f$  and  $\bar{g}_V^f$  for  $f = e, \mu, \tau$ , and  $\ell$ , extracted from the LEP and SLC lineshape and asymmetry data, are shown in Fig. 10.3. It may be compared with Fig. 10.1 as the two sets of parameters coincide at the SM at tree-level.

As for hadron colliders, the forward-backward asymmetry,  $A_{FB}$ , for  $e^+e^-$  and  $\mu^+\mu^-$  final states (with invariant masses restricted to or dominated by values around  $M_Z$ ) in  $p\bar{p}$  collisions has been measured by the CDF [326] and DØ [327] collaborations, and the values  $\bar{s}_\ell^2 = 0.23221 \pm 0.00046$

<sup>16</sup>We are grateful to Werner Bernreuther and Long Chen for the re-calculation of their result employing the more appropriate  $\overline{\text{MS}}$  mixing angle,  $\hat{s}_Z^2$ , instead of the on-shell quantity,  $s_W^2$ .

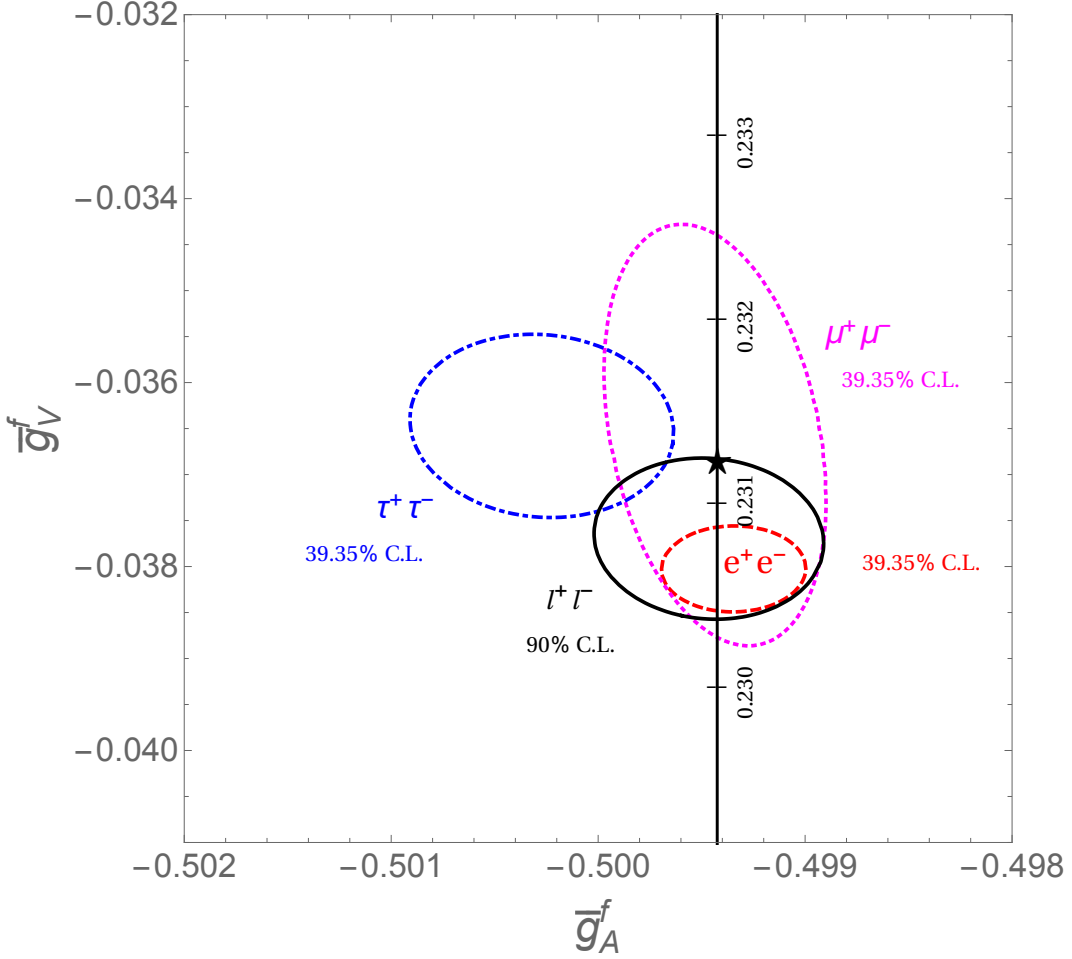


**Figure 10.3:**  $1\sigma$  (39.35% CL) contours of the effective couplings  $\bar{g}_A^f$  and  $\bar{g}_V^f$  for  $f = e, \mu$  and  $\tau$  from LEP and SLC, compared to the SM expectation as a function of  $\hat{s}_Z^2$ . (The SM best fit value  $\hat{s}_Z^2 = 0.23129$  is also indicated.) Also shown is the 90% CL allowed region in  $\bar{g}_{A,V}^f$  obtained assuming lepton universality.

and  $\bar{s}_\ell^2 = 0.23095 \pm 0.00040$  were extracted, respectively. The combination of these measurements (which differ by more than  $2\sigma$ ) yields [309],

$$\bar{s}_\ell^2 = 0.23148 \pm 0.00033 \text{ (Tevatron)} . \quad (10.73)$$

By varying the invariant mass and the scattering angle (and assuming the electron couplings), information on the effective  $Z$  couplings to light quarks,  $\bar{g}_{V,A}^{u,d}$ , could also be obtained [328,329], but with large uncertainties, mutual correlations, and not independently of  $\bar{s}_\ell^2$  above. Similar analyses have also been reported by the H1 [330] and ZEUS [331] collaborations at HERA and by the LEP collaborations [288]. This kind of measurement is harder in the  $pp$  environment due to the difficulty to assign the initial quark and antiquark in the underlying Drell-Yan process to the protons, thus requiring excellent control of uncertainties from parton distribution functions. ATLAS obtained  $\bar{s}_\ell^2 = 0.2308 \pm 0.0012$  using 7 TeV data [310] and a preliminary result  $\bar{s}_\ell^2 = 0.23140 \pm 0.00036$  at 8 TeV [311], while CMS measured  $\bar{s}_\ell^2 = 0.23101 \pm 0.00053$  (8 TeV) [312] and a preliminary result  $\bar{s}_\ell^2 = 0.23157 \pm 0.00031$  (13 TeV) [313], and LHCb reported  $\bar{s}_\ell^2 = 0.23142 \pm 0.00106$  (from both 7 and

**Table 10.6:** Results derived from Table 10.5 and the corresponding covariance matrices [288, 332], and the SM predictions for the partial and total  $Z$  decay widths [in MeV]. In the (second) third column lepton universality is (not) assumed.

Quantity	Value	Value (universal)	Standard Model
$\Gamma_{e^+e^-}$	$83.87 \pm 0.12$	$83.942 \pm 0.085$	$83.955 \pm 0.009$
$\Gamma_{\mu^+\mu^-}$	$83.95 \pm 0.18$	$83.941 \pm 0.085$	$83.955 \pm 0.009$
$\Gamma_{\tau^+\tau^-}$	$84.03 \pm 0.21$	$83.759 \pm 0.085$	$83.772 \pm 0.009$
$\Gamma_{\text{inv}}$	$498.9 \pm 2.5$	$500.5 \pm 1.5$	$501.435 \pm 0.045$
$\Gamma_{u\bar{u}}$	—	—	$299.87 \pm 0.20$
$\Gamma_{c\bar{c}}$	$300.3 \pm 5.3$	$300.0 \pm 5.2$	$299.81 \pm 0.20$
$\Gamma_{d\bar{d}}, \Gamma_{s\bar{s}}$	—	—	$382.75 \pm 0.14$
$\Gamma_{b\bar{b}}$	$377.4 \pm 1.3$	$377.0 \pm 1.2$	$375.73 \mp 0.18$
$\Gamma_{\text{had}}$	$1744.8 \pm 2.6$	$1743.2 \pm 1.9$	$1740.88 \pm 0.86$
$\Gamma_Z$	$2495.5 \pm 2.3$	$2495.5 \pm 2.3$	$2494.00 \pm 0.87$

8 TeV data, but only analyzing  $\mu^+\mu^-$  final state) [314]. Assuming that the smallest theoretical and PDF uncertainty ( $\pm 0.00024$  from ATLAS [311]) is fully correlated among the five determinations, they combine to

$$\bar{s}_\ell^2 = 0.23145 \pm 0.00028 \text{ (LHC)} . \quad (10.74)$$

Combining Eqs. (10.72), (10.73), and (10.74) gives,

$$\bar{s}_\ell^2 = 0.23149 \pm 0.00013 \text{ (collider average)} . \quad (10.75)$$

#### 10.5.4 $W$ and $Z$ decays

The partial decay widths for gauge bosons to decay into massless fermions  $f_1\bar{f}_2$  (the numerical values include the small EW radiative corrections and final-state mass effects) are given by,

$$\Gamma(W^+ \rightarrow e^+\nu_e) = \frac{M_W^3}{12\pi v^2} = 226.29 \pm 0.04 \text{ MeV} , \quad (10.76a)$$

$$\Gamma(W^+ \rightarrow u_i\bar{d}_j) = \frac{M_W^3}{12\pi v^2} |V_{ij}|^2 \mathcal{R}_V^q = (705.3 \pm 0.4 \text{ MeV}) |V_{ij}|^2 , \quad (10.76b)$$

$$\Gamma(Z \rightarrow f\bar{f}) = \frac{M_Z^3}{12\pi v^2} [\mathcal{R}_V^f \bar{g}_V^{f2} + \mathcal{R}_A^f \bar{g}_A^{f2}] , \quad (10.76c)$$

where the result for the latter are shown in Table 10.6. Final-state QED and QCD corrections [333] to the vector and axial-vector form factors are given by,

$$\mathcal{R}_{V,A}^f = N_C \left[ 1 + \frac{3}{4} \left( Q_f^2 \frac{\alpha(s)}{\pi} + \frac{N_C^2 - 1}{2N_C} \frac{\alpha_s(s)}{\pi} \right) + \dots \right] , \quad (10.77)$$

where  $N_C = 3$  (1) is the color factor for quarks (leptons) and the dots indicate finite fermion mass effects proportional to  $m_f^2/s$  which are different for  $\mathcal{R}_V^f$  and  $\mathcal{R}_A^f$ , as well as higher-order QCD corrections [334], which are known to  $\mathcal{O}(\alpha_s^4)$  [222]. For the  $Z$  boson, these include singlet contributions starting from two-loop order which are large, strongly top quark mass dependent, family universal,

and flavor non-universal [335–339]. The  $\mathcal{O}(\alpha^2)$  self-energy corrections from Ref. [340] are also taken into account.

For the  $W$  decay into quarks, Eq. (10.76b), only the universal massless part (non-singlet and  $m_q = 0$ ) of the final-state QCD radiator function in  $\mathcal{R}_V$  from Eq. (10.77) is used, and the QED corrections are modified. Expressing the widths in terms of  $G_F M_{W,Z}^3$  incorporates the largest radiative corrections from the running QED coupling. EW corrections to the  $Z$  widths are then taken into account through the effective couplings  $\bar{g}_{V,A}^{i2}$ . Hence, in the on-shell scheme the  $Z$  widths are proportional to  $\rho_i \sim 1 + \rho_t$ . There is additional (negative) quadratic  $m_t$  dependence in the  $Z \rightarrow b\bar{b}$  vertex corrections [341, 342] which causes  $\Gamma_{b\bar{b}}$  to decrease with  $m_t$ . The dominant effect is to multiply  $\Gamma_{b\bar{b}}$  by the vertex correction  $1 + \delta\rho_{b\bar{b}}$ , where  $\delta\rho_{b\bar{b}} \sim 10^{-2}(-\frac{1}{2}m_t^2/M_Z^2 + \frac{1}{5})$ . In practice, the corrections are included in  $\hat{\rho}_b$  and  $\hat{\kappa}_b$ , as discussed in Sec. 10.5.

Starting at  $\mathcal{O}(\alpha\alpha_s)$ , the factorized form indicated in Eq. (10.76) is violated and corrections need to be included [343–345]. They add coherently, resulting in a sizable effect, and shift  $\alpha_s(M_Z)$  when extracted from  $Z$  lineshape observables by about  $+0.0007$ . Similar non-factorizable corrections are also known for mixed QED-EW corrections [111, 112, 114, 346].

For three fermion families the total widths of the  $Z$  [347–351] and  $W$  [352, 353] bosons are predicted to be,

$$\Gamma_Z = 2.4940 \pm 0.0009 \text{ GeV} , \quad \Gamma_W = 2.0892 \pm 0.0008 \text{ GeV} . \quad (10.78)$$

The uncertainties in these predictions are almost entirely induced by the parametric error in  $\alpha_s(M_Z) = 0.1187 \pm 0.0017$  from the global fit. These predictions can be compared with the experimental results,  $\Gamma_Z = 2.4955 \pm 0.0023$  GeV [288, 332] and  $\Gamma_W = 2.137 \pm 0.032$  GeV in (10.78). Note regarding the latter that in this Section we include the very recent result from ATLAS [295] and an updated value of the Tevatron result [299], which differ from the treatment in the Gauge & Higgs Bosons Particle Listings and Section 54 on the “Mass and Width of the  $W$  Boson” in this *Review*. The hadronic branching ratio of the  $W$  boson,  $\mathcal{B}(W \rightarrow \text{hadrons})$  has been measured by both LEP 2 [294] and CMS [300]. The measurements of the total and partial widths are generally in good agreement with the SM. The exceptions are  $\Gamma_W$ , which is  $1.5\sigma$  larger than the SM prediction, and the branching ratio  $W \rightarrow \tau + \nu_\tau$  from LEP 2, which is  $2.6\sigma$  larger than the electron-muon average [294]<sup>17</sup>.

The invisible decay width,  $\Gamma_{\text{inv}} = \Gamma_Z - \Gamma_{e^+e^-} - \Gamma_{\mu^+\mu^-} - \Gamma_{\tau^+\tau^-} - \Gamma_{\text{had}}$ , can be used to determine the number of neutrino flavors,  $N_\nu$ , much lighter than  $M_Z/2$ . The hadronic peak cross-section, and therefore the extracted  $\Gamma_{\text{had}}$ , depends strongly on the knowledge of the LEP 1 luminosity derived from small-angle Bhabha scattering. However, the prediction for the Bhabha cross-section was recently found to be overestimated, and consequently the luminosity underestimated [332]. The updated analysis involved an improved  $Z$  lineshape fit, significantly reducing  $\sigma_{\text{had}}$ , while slightly increasing  $\Gamma_Z$ , with the result,  $N_\nu = 2.9963 \pm 0.0074$  [332]. In practice, we determine  $N_\nu$  by allowing it as an additional fit parameter and obtain,

$$N_\nu = 3.0025 \pm 0.0061 , \quad (10.79)$$

which is now in perfect agreement with the observed number of fermion generations and  $N_\nu = 3$  (a  $1.3\sigma$  deviation was observed in the 2018 edition of this *Review* before including the correction in the luminosity determination).

## 10.6 Global fit results

In this section, we present the results of global fits, subject to the experimental data and theoretical constraints discussed in Section 10.2–10.5. For earlier analyses, see Refs. [83, 288, 355–

---

<sup>17</sup> $W$ -boson branching ratio measurements from CMS and ATLAS are in good agreement with lepton universality and slightly more precise than LEP-2 [300, 354].

**Table 10.7:** Principal electroweak SM fit result including mutual correlations.

$M_Z$ [GeV]	$91.1884 \pm 0.0019$	1.00	-0.08	0.00	0.00	0.02	0.02
$\hat{m}_t(\hat{m}_t)$ [GeV]	$163.18 \pm 0.54$	-0.08	1.00	0.00	-0.12	-0.23	0.04
$\hat{m}_b(\hat{m}_b)$ [GeV]	$4.180 \pm 0.008$	0.00	0.00	1.00	0.19	-0.02	0.01
$\hat{m}_c(\hat{m}_c)$ [GeV]	$1.274 \pm 0.009$	0.00	-0.12	0.19	1.00	0.48	0.01
$\alpha_s(M_Z)$	$0.1187 \pm 0.0017$	0.02	-0.23	-0.02	0.48	1.00	-0.04
$\Delta\alpha_{\text{had}}^{(3)}(2 \text{ GeV})$	$0.00608 \pm 0.00004$	0.02	0.04	0.01	0.01	-0.04	1.00

[358] and previous editions of this *Review*. Recent global fits by other groups [359–361] find a similar pattern of agreement as discussed below, with some discrepancies beyond the  $2\sigma$  level for a few quantities entering into the fit. They differ, however, from the fit presented here by (i) not including inputs from low-energy parity-violation data and the muon magnetic moment<sup>18</sup>; (ii) the set of input data; (iii) the implementation of radiative corrections; and (iv) the fitting tools used.

For the results in this *Review*, the values for  $m_t$  (see Sec. 10.2.3),  $M_H$  [364, 365],  $\Gamma_H$  [308, 366],  $M_W$  [295, 298],  $\Gamma_W$  [294, 295, 299],  $\mathcal{B}(W \rightarrow \text{hadrons})$  [294, 300], the weak charges of the electron [166], the proton [167], cesium [178, 179] and thallium [180, 181], the weak mixing angle extracted from eDIS [156],  $\nu_\mu(\bar{\nu}_\mu)\text{-e}$  scattering [137–139], the  $\tau$  lifetime, and the  $\mu$  anomalous magnetic moment [367] are listed in Table 10.4. Likewise, Table 10.5 summarizes the principal  $Z$  pole observables, where the LEP 1 averages of the ALEPH, DELPHI, L3, and OPAL results include common systematic uncertainties and correlations [288, 332]. The heavy flavor results [288, 323] of LEP 1 and SLD are based on common inputs, and are thus correlated, as well.

Also shown in both tables are the SM predictions for the values of  $M_Z$ ,  $\alpha_s(M_Z)$ ,  $\Delta\alpha_{\text{had}}^{(3)}$  and the heavy quark masses shown in Table 10.7. The predictions result from a global least-square ( $\chi^2$ ) fit to all data using the minimization package MINUIT [368] and the EW library GAPP [34]. In most cases, we treat all input errors (the uncertainties of the values) as Gaussian. The reason is not that we assume that theoretical and systematic errors are intrinsically bell-shaped (which they are not) but because in most cases the input errors are either dominated by the statistical components or they are combinations of many different (including statistical) error sources, which should yield approximately Gaussian *combined* errors by the large number theorem. An exception is the theory dominated error on the  $\tau$  lifetime, which we recalculate in each  $\chi^2$ -function call since it depends itself on  $\alpha_s$ . Sizes and shapes of the output errors (the uncertainties of the predictions and the SM fit parameters) are fully determined by the fit, and  $1\sigma$  errors are defined to correspond to  $\Delta\chi^2 = \chi^2 - \chi^2_{\min} = 1$ , and do not necessarily correspond to the 68.3% probability range or the 39.3% probability contour (for 2 parameters).

The agreement is generally very good. Despite the few discrepancies addressed in the following, the global electroweak fit describes the data well, with a very good  $\chi^2/\text{d.o.f.} = 49.5/47$ . The probability of a larger  $\chi^2$  is 37%, and only  $g_\mu - 2$  is currently showing a larger ( $3.2\sigma$ ) conflict. In addition,  $A_{LR}^0$  (SLD) from hadronic final states,  $A_{FB}^{(0,b)}$  (LEP 1),  $\Gamma_W$  (ATLAS) and  $Q_W(\text{Cs})$  deviate at the  $2\sigma$  level.  $g_L^2$  from NuTeV is nominally in conflict with the SM, as well, but the precise status is unresolved (see Sec. 10.3.1). Also, there is currently no understanding as to why the  $M_W$  value reported by the CDF collaboration is significantly larger than the findings by other groups. In this context, we refer to Sec. 10.8 for a discussion of fits involving alternative data inputs. We also emphasize that there are a number of discrepancies among individual measurements of certain

<sup>18</sup>Refs. [51, 362, 363] report on specialized fits to study the impact of a shift of the hadronic vacuum polarization in the running of the electromagnetic coupling, where such shift is motivated by the apparent mismatch of the direct measurement and the data-driven SM prediction of  $g_\mu - 2$ , but they do not include  $g_\mu - 2$  itself in the fit.

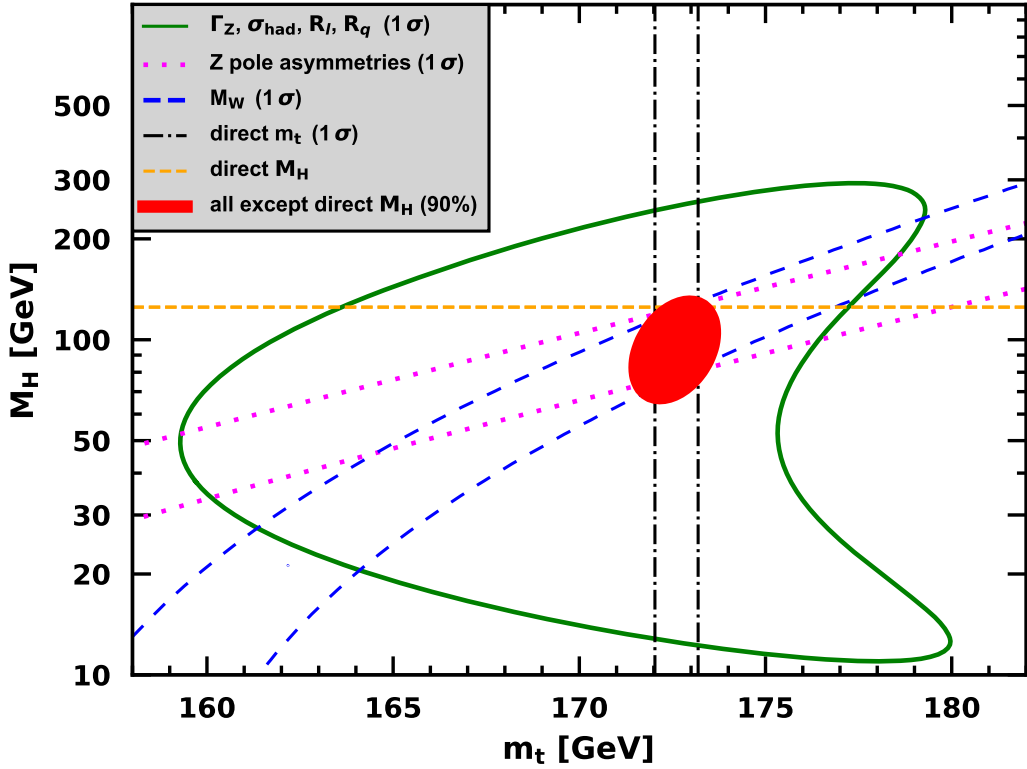


**Figure 10.4:** Fit result and one-standard-deviation (approximately 39.35% for the closed contours and 68% for the others) uncertainties in  $M_H$  as a function of  $m_t$  for various inputs, and the 90% CL region ( $\Delta\chi^2 = 4.605$ ) allowed by all data.  $\alpha_s(M_Z) = 0.1187$  is assumed except for the fits including the  $Z$  lineshape. The width of the horizontal dashed band is not visible on the scale of the plot.

quantities, as discussed in previous sections, but that they are not reflected in the overall  $\chi^2$  of the fit as only the corresponding combinations are used as constraints.

$A_b$  can be extracted from  $A_{FB}^{(0,b)}$  when  $A_e = 0.1501 \pm 0.0016$  is taken from a fit to leptonic asymmetries (using lepton universality). The result,  $A_b = 0.885 \pm 0.017$ , is  $2.9\sigma$  below the SM prediction<sup>19</sup> and also  $1.4\sigma$  below  $A_b = 0.923 \pm 0.020$  obtained from  $A_{LR}^{FB}(b)$  at SLD. Thus, it appears that at least some of the problem in  $A_b$  is due to a statistical fluctuation or other experimental effect in one of the asymmetries. Note, however, that the uncertainty in  $A_{FB}^{(0,b)}$  is strongly statistics dominated. The combined value,  $A_b = 0.901 \pm 0.013$  deviates by  $2.6\sigma$ .

The left-right asymmetry,  $A_{LR}^0 = 0.15138 \pm 0.00216$  [315], from hadronic decays at SLD, differs by  $2.3\sigma$  from the SM expectation of  $0.1463 \pm 0.0003$ . The combined value of  $A_\ell = 0.1513 \pm 0.0021$  from SLD (using lepton-family universality and including correlations) is also  $2.4\sigma$  above the SM prediction; but there is experimental agreement between this SLD value and the LEP 1 value,  $A_\ell = 0.1481 \pm 0.0027$ , obtained from a fit to  $A_{FB}^{(0,\ell)}$ ,  $A_e(\mathcal{P}_\tau)$ , and  $A_\tau(\mathcal{P}_\tau)$ , again assuming universality.

The observables in Table 10.4 and Table 10.5, as well as some other less precise observables, are used in the global fits described below. In all fits, the errors include full statistical, systematic, and theoretical uncertainties. The correlations from the LEP 1 lineshape and  $\tau$  polarization measurements, the LEP/SLD heavy flavor observables, the SLD lepton asymmetries, and the  $\nu$ - $e$

<sup>19</sup>Alternatively, one can use  $A_\ell = 0.1481 \pm 0.0027$ , which is from LEP 1 alone and in excellent agreement with the SM, and obtain  $A_b = 0.897 \pm 0.022$  which is  $1.7\sigma$  low. This illustrates that some of the discrepancy is related to the one in  $A_{LR}$ .

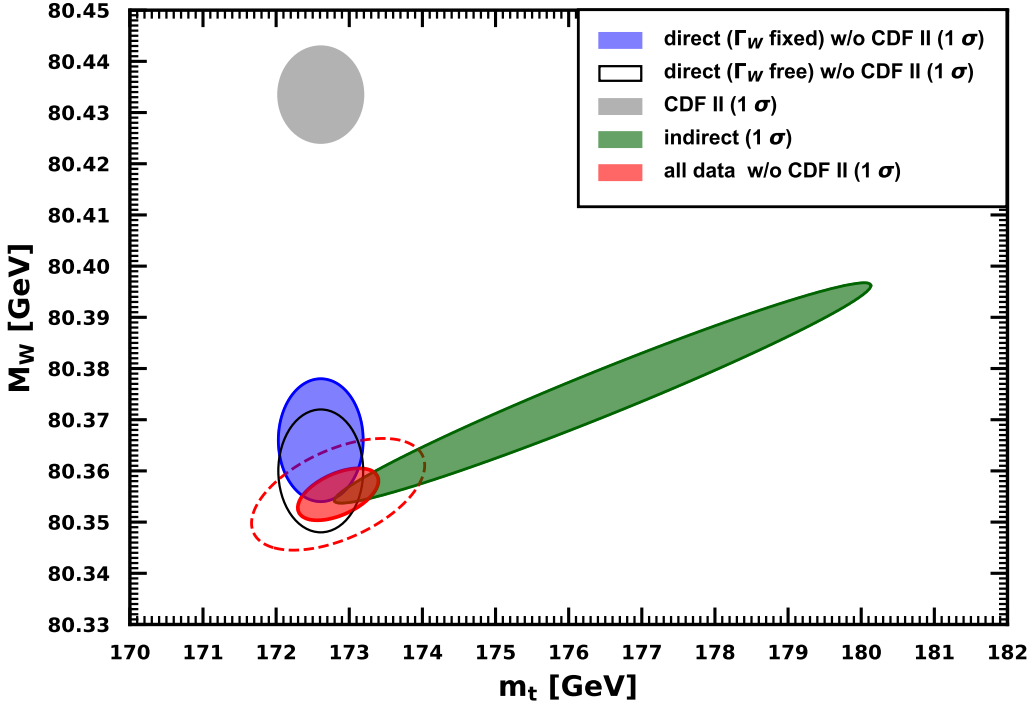


**Figure 10.5:** One-standard-deviation (39.35%) regions in  $M_W$  as a function of  $m_t$  for the indirect data from the fit (green), the direct data for  $m_t$  and  $M_W$  without the CDF II measurement (blue and black contour, respectively, for two differently treatments of the  $W$ -boson width), and the combination thereof (red). For the combination, the 90% CL region ( $\Delta\chi^2 = 4.605$ ) is also shown as a red dashed contour. The grey region uses only the  $M_W$  value from CDF II. Compared to previous editions of this *Review*, this plot additionally includes theoretical uncertainties and subleading parameter dependencies.

scattering observables, are included. The theoretical correlations between  $\Delta\alpha_{\text{had}}^{(5)}$ ,  $\hat{s}_0^2$ , and  $g_\mu - 2$ , and between the  $M_W$  and  $\Gamma_W$  extractions from the LHC and the Tevatron, are also accounted for.

The electroweak data allow a simultaneous determination of  $M_Z$ ,  $m_t$ , and  $\alpha_s(M_Z)$ . The direct measurements of  $M_H$  at the LHC [364, 365] have reached a precision that the global fit result for  $M_H$  coincides with the constraint in Eq. (10.66) with negligible correlations with the other fit parameters.  $\hat{m}_c$ ,  $\hat{m}_b$ , and  $\Delta\alpha_{\text{had}}^{(3)}$  are also allowed to float in the fits, subject to the theoretical constraints [33, 58] described in Sec. 10.2, and are correlated with  $\alpha_s$ , which in turn is determined mainly through  $R_\ell$ ,  $\Gamma_Z$ ,  $\sigma_{\text{had}}$ , and  $\tau_\tau$ , but  $\Gamma_W$  and  $\mathcal{B}(W \rightarrow \text{hadrons})$  also have an impact. The global fit to all data, including the hadron collider  $m_t$  average in Eq. (10.21), yields the results in Table 10.7, while those for the weak mixing angle in various schemes are summarized in Table 10.2.

Removing the kinematic constraint on  $M_H$  from LHC gives the loop-level determination from the precision data,

$$M_H = 97_{-16}^{+18} \text{ GeV} , \quad (10.80)$$

which is  $1.6\sigma$  below the value in Eq. (10.66). The latter is just inside the 90% central confidence range,

$$71 \text{ GeV} < M_H < 126 \text{ GeV} . \quad (10.81)$$

It is instructive to study the effect of doubling the uncertainty in Eq. (10.14) on the loop-level

**Table 10.8:** Values of  $\hat{s}_Z^2$ ,  $s_W^2$ ,  $\alpha_s$ ,  $m_t$  and  $M_H$  for various data sets. In the fit to the LHC data, the  $\alpha_s$  constraint is from an NNLO analysis of the transverse momentum distribution of  $Z$  bosons [369]. For the Tevatron fit we use the  $\alpha_s$  result from the inclusive jet cross-section at D $\emptyset$  [370] and add the  $M_W$  result from CDF [289] as adjusted in Ref. [298].

data set	$\hat{s}_Z^2$	$s_W^2$	$\alpha_s(M_Z)$	$m_t$ [GeV]	$M_H$ [GeV]
all data	0.23129(4)	0.22348(10)	0.1187(17)	$172.9 \pm 0.6$	125
all data except $M_H$	0.23118(8)	0.22327(18)	0.1190(17)	$172.6 \pm 0.6$	$97^{+18}_{-16}$
all data except $M_Z$	0.23121(6)	0.22346(10)	0.1187(17)	$172.6 \pm 0.6$	125
all data except $M_W, \Gamma_W$	0.23130(4)	0.22353(11)	0.1188(17)	$172.7 \pm 0.6$	125
all data except $m_t$	0.23123(6)	0.22324(20)	0.1191(17)	$175.2 \pm 1.8$	125
$M_{H,Z} + \Gamma_{H,Z} + m_t$	0.23134(8)	0.22361(16)	0.1221(45)	$172.6 \pm 0.6$	125
LHC	0.23122(8)	0.22349(11)	0.1183 (9)	$172.3 \pm 0.6$	125
Tevatron	0.23085(13)	0.22254(28)	0.1159(45)	$174.4 \pm 0.8$	$67^{+25}_{-20}$
LEP 1 + LEP 2	0.23138(19)	0.22350(46)	0.1233(29)	$177 \pm 11$	$173^{+237}_{-96}$
LEP 1 + SLD	0.23116(17)	0.22340(58)	0.1221(27)	$169 \pm 10$	$71^{+87}_{-33}$
SLD + $M_Z + \Gamma_Z + m_t$	0.23064(29)	0.22224(54)	0.1196(52)	$172.6 \pm 0.6$	$31^{+27}_{-22}$
$A_{FB}^{(b,c)} + M_Z + \Gamma_Z + m_t$	0.23190(30)	0.22492(70)	0.1279(49)	$172.6 \pm 0.6$	$306^{+164}_{-111}$
$M_{W,Z} + \Gamma_{W,Z} + m_t$	0.23119(11)	0.22329(23)	0.1212(42)	$172.6 \pm 0.6$	$96^{+23}_{-20}$
low energy + $M_{H,Z}$	0.23173(94)	0.2252(35)	0.1172(18)	$159 \pm 29$	125

determination of the Higgs boson mass. The result,  $M_H = 94^{+19}_{-16}$  GeV, reduces the small tension compared to Eq. (10.80) only slightly ( $1.5\sigma$ ) and demonstrates that the uncertainty in  $\Delta\alpha_{\text{had}}$  is currently of only secondary importance. In fact, even removing  $\Delta\alpha_{\text{had}}^{(3)}(2 \text{ GeV})$  altogether as a fit constraint still gives the bound  $M_H < 135$  GeV at the 95% CL. The hadronic contribution to  $\alpha(M_Z)$  is correlated with  $g_\mu - 2$  (see Sec. 10.4). The measurement of the latter is higher than the SM prediction, and its inclusion in the fit favors a larger  $\alpha(M_Z)$  and a lower  $M_H$  from the precision data (currently by 3.2 GeV).

Alternatively, one can carry out a fit without including the direct constraint from the hadron colliders. One obtains  $m_t = 175.2 \pm 1.8$  GeV, which is  $1.4\sigma$  higher than the collider average  $m_t = 172.61 \pm 0.58$  GeV, and a reflection of the low value in Eq. (10.80). (The indirect prediction is for the  $\overline{\text{MS}}$  mass definition,  $\hat{m}_t(\hat{m}_t) = 165.4 \pm 1.7$  GeV, which is in the end converted to the pole mass.) Finally, one can remove the explicit  $M_W$  and  $\Gamma_W$  constraints from the global fit and use  $M_H = 125.10 \pm 0.09$  GeV to obtain  $M_W = 80.353 \pm 0.006$  GeV, in very good agreement with the experimental measurements except the one from CDF II. The situation is summarized in Fig. 10.4 and in Fig. 10.5, showing the  $m_t$  dependence of  $M_H$  and  $M_W$ , respectively.

The weak mixing angle can be determined from  $Z$  pole observables,  $M_W$ , and a variety of neutral-current processes spanning a very wide  $Q^2$  range. The results (for older low energy neutral-current data see Refs. [355–358], as well as earlier editions of this *Review*) shown in Table 10.8 are in reasonable agreement with each other, indicating the quantitative success of the SM. One of the largest discrepancies is the value  $\hat{s}_Z^2 = 0.23064 \pm 0.00028$  from the SLD asymmetries (combined with  $M_Z$ ,  $\Gamma_Z$ , and  $m_t$ ), which is  $2.3\sigma$  below the value  $0.23129 \pm 0.00004$  from the global fit to all data. On the other hand,  $\hat{s}_Z^2 = 0.23176 \pm 0.00027$  from  $A_{FB}^{(0,b)}$  and  $A_{FB}^{(0,c)}$  is  $1.7\sigma$  high.

The extracted  $Z$  pole value of  $\alpha_s(M_Z)$  is based on a formula with negligible theoretical un-

**Table 10.9:** Values of model-independent neutral-current parameters, compared with the SM predictions, where the uncertainties in the latter are  $\lesssim 0.0001$ , throughout.

Quantity	Experimental Value	Standard Model	Correlation	
$g_{LV}^{\nu e}$	$-0.040 \pm 0.015$	$-0.0395$	$-0.05$	
$g_{LA}^{\nu e}$	$-0.507 \pm 0.014$	$-0.5063$		
$g_{AV}^{eu} + 2g_{AV}^{ed}$	$0.4927 \pm 0.0031$	$0.4950$	$-0.88$	$0.20$
$2g_{AV}^{eu} - g_{AV}^{ed}$	$-0.7165 \pm 0.0068$	$-0.7189$	$-0.22$	
$2g_{VA}^{eu} - g_{VA}^{ed}$	$-0.13 \pm 0.06$	$-0.0944$		
$g_{VA}^{ee}$	$0.0190 \pm 0.0027$	$0.0224$		

certainty if one assumes the exact validity of the SM. One should keep in mind, however, that this value,  $\alpha_s(M_Z) = 0.1221 \pm 0.0027$ , which increased after the updated analysis in Ref. [332], is very sensitive to certain types of new physics such as non-universal vertex corrections. A fit to the wider set of high-energy data, *i.e.*, including  $W$ -decays but without  $\tau_\tau$  and  $g_\mu - 2$ , returns  $\alpha_s(M_Z) = 0.1211 \pm 0.0025$ . In contrast, the value derived from  $\tau$  decays,  $\alpha_s(M_Z) = 0.1171^{+0.0018}_{-0.0017}$ , is theory dominated but less sensitive to new physics. The agreement between these values is only marginal, but the latter does agree well with the averages deduced from heavy quarkonia spectroscopy ( $0.1181 \pm 0.0037$ ), DIS and global PDF fits ( $0.1161 \pm 0.0022$ ), hadronic final states of  $e^+e^-$  annihilations ( $0.1189 \pm 0.0037$ ), hadron colliders ( $0.1168 \pm 0.0027$ ), as well as lattice QCD simulations ( $0.1184 \pm 0.0008$ ). For more details, other determinations, and references, see Section 9 on “Quantum Chromodynamics” in this *Review*. We also provide the values, computed with five-loop beta functions and four-loop matching,

$$\alpha_s^{(4)}(m_\tau) = 0.325 \pm 0.014 , \quad (10.82)$$

$$\alpha_s^{(5)}(M_W) = 0.1210 \pm 0.0017 , \quad (10.83)$$

$$\alpha_s^{(5)}(M_H) = 0.1132 \pm 0.0015 , \quad (10.84)$$

$$\alpha_s^{(6)}(\hat{m}_t) = 0.1090 \pm 0.0014 , \quad (10.85)$$

to be used in precision calculations.

Using  $\alpha(M_Z)$  and  $\hat{s}_Z^2$  as inputs, one can predict  $\alpha_s(M_Z)$  assuming grand unification. One finds  $\alpha_s(M_Z) = 0.13 \pm 0.01$  [371, 372] for the simplest theories based on the minimal supersymmetric extension of the SM, where the uncertainty is from the unknown particle thresholds. This is slightly larger, but consistent with  $\alpha_s(M_Z) = 0.1187 \pm 0.0017$  from our fit and most other determinations, while minimal non-supersymmetric theories predict much lower and excluded values (see Section 93 on “Grand Unified Theories” in this *Review*).

Most of the parameters relevant to  $\nu$ -hadron,  $\nu$ - $e$ ,  $e$ -hadron, and  $e$ - $e$  processes are determined uniquely and precisely from the data in “model-independent” fits, *i.e.*, fits allowing for an arbitrary EW gauge theory. The values for the parameters defined in Eq. (10.29) are given in Table 10.9 along with the predictions of the SM. The agreement is very good. (The  $\nu$ -hadron results including NuTeV [151] and other  $\nu$ -DIS data can be found in the 2006 edition of this *Review*, and fits with modified NuTeV constraints in the 2008 and 2010 editions.)

## 10.7 Constraints on new physics

The masses and decay properties of the electroweak bosons and low energy data can be used to search for and set limits on deviations from the SM. We will mainly discuss the effects of exotic

particles (with heavy masses  $M_{\text{new}} \gg M_Z$  in an expansion in  $M_Z/M_{\text{new}}$ ) on the gauge boson self-energies. (Brief remarks are made on new physics which is not of this type.) Most of the effects on precision measurements can be described by three gauge self-energy parameters  $S$ ,  $T$ , and  $U$ . We will define these, as well as the related parameters  $\rho_0$  and  $\hat{\epsilon}_i$ , to arise from new physics only. In other words, they are equal to zero ( $\rho_0 = 1$ ) exactly in the SM, and do not include any (loop induced) contributions that depend on  $m_t$  or  $M_H$ , which are treated separately. Our treatment differs from most of the original papers.

The dominant effect of many extensions of the SM can be described by the  $\rho_0$  parameter,

$$\rho_0 \equiv \frac{M_W^2}{M_Z^2 \hat{c}_Z^2 \hat{\rho}}, \quad (10.86)$$

which describes new sources of SU(2) breaking that cannot be accounted for by the SM Higgs doublet or by  $m_t$  effects.  $\hat{\rho}$  is calculated as in Eq. (10.26) assuming the validity of the SM. In the presence of  $\rho_0 \neq 1$ , Eq. (10.86) generalizes the second Eq. (10.26) while the first remains unchanged. Provided that the new physics which yields  $\rho_0 \neq 1$  is a small perturbation which does not significantly affect other radiative corrections,  $\rho_0$  can be regarded as a phenomenological parameter which multiplies  $G_F$  in Eqs. (10.29) and (10.52), as well as  $\Gamma_Z$  in Eq. (10.76c). From the global fit,

$$\rho_0 = 1.00031 \pm 0.00019, \quad (10.87a)$$

$$\alpha_s(M_Z) = 0.1189 \pm 0.0017, \quad (10.87b)$$

where as before the uncertainty is from the experimental inputs and includes an estimate of the error from unknown higher-order electroweak corrections. The result in Eq. (10.87a) is  $1.6\sigma$  above the SM expectation,  $\rho_0 = 1$ , and not unrelated to the small tension observed in the context with Eq. (10.80). It can be used to constrain higher-dimensional Higgs representations to have vacuum expectation values of less than a few percent of those of the doublets. Indeed, the relation between  $M_W$  and  $M_Z$  is modified if there are Higgs multiplets with weak isospin  $> 1/2$  and significant vacuum expectation values. For a general (charge-conserving) Higgs structure,

$$\rho_0 = \frac{\sum_i [t_i(t_i + 1) - t_{3i}^2] |v_i|^2}{2 \sum_i t_{3i}^2 |v_i|^2}, \quad (10.88)$$

where  $v_i$  is the expectation value of the neutral component of a Higgs multiplet with weak isospin  $t_i$  and third component  $t_{3i}$ . In order to calculate to higher orders in such theories one must define a set of four fundamental renormalized parameters which one may conveniently choose to be  $\alpha$ ,  $G_F$ ,  $M_Z$ , and  $M_W$ , since  $M_W$  and  $M_Z$  are directly measurable. Then  $\hat{s}_Z^2$  and  $\rho_0$  can be considered dependent parameters.

Eq. (10.87a) can also be used to constrain other types of new physics. For example, non-degenerate multiplets of heavy fermions or scalars break the vector part of weak SU(2) and lead to a decrease in the value of  $M_Z/M_W$ . Each non-degenerate SU(2) doublet  $\begin{pmatrix} f_1 \\ f_2 \end{pmatrix}$  yields a positive contribution to  $\rho_0$  [373–375] of

$$\frac{N_C G_F}{8\sqrt{2}\pi^2} \Delta m^2, \quad (10.89)$$

where

$$\Delta m^2 \equiv m_1^2 + m_2^2 - \frac{4m_1^2 m_2^2}{m_1^2 - m_2^2} \ln \frac{m_1}{m_2} \geq (m_1 - m_2)^2, \quad (10.90)$$

and  $N_C = 1$  (3) for color singlets (triplets). Eq. (10.87a) taken together with Eq. (10.89) implies the following constraint on the mass splitting at the 90% CL,

$$(2 \text{ GeV})^2 < \sum_i \frac{N_C^i}{3} \Delta m_i^2 < (44 \text{ GeV})^2 , \quad (10.91)$$

where the sum runs over all new-physics doublets, for example fourth-family quarks or leptons,  $\binom{t'}{b'}$  or  $\binom{\ell'}{\ell'-}$ , vector-like fermion doublets (which contribute to the sum in Eq. (10.91) with an extra factor of 2), and scalar doublets such as  $\binom{t}{b}$  in Supersymmetry (in the absence of  $L$ - $R$  mixing).

Non-degenerate multiplets usually imply  $\rho_0 > 1$ . Similarly, heavy  $Z'$  bosons decrease the prediction for  $M_Z$  due to mixing and generally lead to  $\rho_0 > 1$  [376]. On the other hand, extra Higgs doublets participating in spontaneous symmetry breaking [377–379] or heavy lepton doublets involving Majorana neutrinos [380], both of which have more complicated expressions, and the  $v_i$  of higher-dimensional Higgs representations can contribute to  $\rho_0$  with either sign.

A number of authors [381–383] have considered the general effects on neutral-current,  $Z$  and  $W$  boson observables of various types of heavy (*i.e.*,  $M_{\text{new}} \gg M_Z$ ) physics which contribute to the  $W$  and  $Z$  self-energies but which do not have any direct coupling to the ordinary fermions (an alternative formulation is given by Ref. [384]). In addition to non-degenerate multiplets, which break the vector part of weak SU(2), these include heavy degenerate multiplets of chiral fermions which break the axial generators.

Such effects can be described by just three parameters,  $S$ ,  $T$ , and  $U$  [385], at the (EW) one-loop level<sup>20</sup>.  $T$  is proportional to the difference between the  $W$  and  $Z$  self-energies at  $Q^2 = 0$  (*i.e.*, vector SU(2)-breaking), while  $S$  ( $S + U$ ) is associated with the difference between the  $Z$  ( $W$ ) self-energy at  $Q^2 = M_{Z,W}^2$  and  $Q^2 = 0$  (axial SU(2)-breaking). Denoting the contributions of new physics to the various self-energies by  $\Pi_{ij}^{\text{new}}$ , we have

$$\hat{\alpha}(M_Z)T \equiv \frac{\Pi_{WW}^{\text{new}}(0)}{M_W^2} - \frac{\Pi_{ZZ}^{\text{new}}(0)}{M_Z^2} , \quad (10.92a)$$

$$\frac{\hat{\alpha}(M_Z)}{4\hat{s}_Z^2\hat{c}_Z^2}S \equiv \frac{\Pi_{ZZ}^{\text{new}}(M_Z^2) - \Pi_{ZZ}^{\text{new}}(0)}{M_Z^2} - \frac{\hat{c}_Z^2 - \hat{s}_Z^2}{\hat{c}_Z\hat{s}_Z} \frac{\Pi_{Z\gamma}^{\text{new}}(M_Z^2)}{M_Z^2} - \frac{\Pi_{\gamma\gamma}^{\text{new}}(M_Z^2)}{M_Z^2} , \quad (10.92b)$$

$$\frac{\hat{\alpha}(M_Z)}{4\hat{s}_Z^2}(S + U) \equiv \frac{\Pi_{WW}^{\text{new}}(M_W^2) - \Pi_{WW}^{\text{new}}(0)}{M_W^2} - \frac{\hat{c}_Z}{\hat{s}_Z} \frac{\Pi_{Z\gamma}^{\text{new}}(M_Z^2)}{M_Z^2} - \frac{\Pi_{\gamma\gamma}^{\text{new}}(M_Z^2)}{M_Z^2} . \quad (10.92c)$$

$S$ ,  $T$ , and  $U$  are defined with a factor proportional to  $\hat{\alpha}$  removed, so that they are expected to be of order unity in the presence of new physics. In the  $\overline{\text{MS}}$  scheme as defined in Ref. [85], the last two terms in Eqs. (10.92b) and (10.92c) can be omitted, as was done in some earlier editions of this *Review*. These parameters are related to other parameter sets,  $S_i$  [85],  $\hat{\epsilon}_i$  [389], and  $h_i$  [390], by

$$T = h_V = \frac{\hat{\epsilon}_1}{\hat{\alpha}(M_Z)} , \quad (10.93a)$$

$$S = h_{AZ} = S_Z = 4\hat{s}_Z^2 \frac{\hat{\epsilon}_3}{\hat{\alpha}(M_Z)} , \quad (10.93b)$$

$$U = h_{AW} - h_{AZ} = S_W - S_Z = -4\hat{s}_Z^2 \frac{\hat{\epsilon}_2}{\hat{\alpha}(M_Z)} . \quad (10.93c)$$

<sup>20</sup>Three additional parameters are needed if the new physics scale is comparable to  $M_Z$  [386]. Further generalizations, including effects relevant to LEP 2 and Drell-Yan production at the LHC, are described in Refs. [387] and [388], respectively.

A heavy non-degenerate multiplet of fermions or scalars contributes positively to  $T$  as

$$\rho_0 - 1 = \frac{1}{1 - \hat{\alpha}(M_Z)T} - 1 \approx \hat{\alpha}(M_Z)T , \quad (10.94)$$

where  $\rho_0 - 1$  is given in Eq. (10.89). The effects of non-standard Higgs representations cannot be separated from heavy non-degenerate multiplets unless the new physics has other consequences, such as vertex corrections. Most of the original papers defined  $T$  to include the effects of loops only. However, we will redefine  $T$  to include all new sources of SU(2) breaking, including non-standard Higgs, so that  $T$  and  $\rho_0$  are equivalent by Eq. (10.94).

A multiplet of heavy degenerate chiral fermions yields

$$S = \frac{N_C}{3\pi} \sum_i \left( t_{3i}^L - t_{3i}^R \right)^2 , \quad (10.95)$$

where  $t_{3i}^{L,R}$  is the 3<sup>rd</sup> component of weak isospin of the left-(right-)handed component of fermion  $i$ . For example, a heavy degenerate ordinary or mirror family would contribute  $2/3\pi$  to  $S$ . In models with warped extra dimensions [391], sizeable corrections to the  $S$  parameter are generated through mixing between the SM gauge bosons and their Kaluza-Klein (KK) excitations, and one finds  $S \approx 30 v^2 M_{KK}^{-2}$  [392], where  $M_{KK}$  is the mass scale of the KK gauge bosons. Large positive values of  $S$  can also be generated in models with dynamical electroweak symmetry breaking, where the Higgs boson is composite. In simple composite Higgs models, the dominant contribution stems from heavy spin-1 resonances of the strong dynamics leading to  $S \approx 4\pi v^2(M_V^{-2} + M_A^{-2})$ , where  $M_{V,A}$  are the masses of the lightest vector and axial-vector resonances, respectively [393].

Negative values of  $S$  are possible, for example, in composite Higgs models with larger gauge group representations [394, 395], or from loops involving scalars or Majorana particles [396–398]. The simplest origin of  $S < 0$  would probably be an additional heavy  $Z'$  boson [376]. Supersymmetric extensions of the SM [399, 400] generally give very small effects. For more details and references, see Refs. [401–410] and Sections 88,89 on “Supersymmetry” in this *Review*. Most simple types of new physics yield  $U = 0$ , although there are counter-examples, such as the effects of anomalous triple gauge vertices [389].

The SM expressions for observables are replaced by,

$$M_Z^2 = M_{Z0}^2 \frac{1 - \hat{\alpha}(M_Z)T}{1 - G_F M_{Z0}^2 S / 2\sqrt{2}\pi} , \quad (10.96a)$$

$$M_W^2 = M_{W0}^2 \frac{1}{1 - G_F M_{W0}^2 (S + U) / 2\sqrt{2}\pi} , \quad (10.96b)$$

where  $M_{Z0}$  and  $M_{W0}$  are the SM expressions (as functions of  $m_t$  and  $M_H$ ) in the  $\overline{\text{MS}}$  scheme. Furthermore,

$$\Gamma_Z = \frac{M_Z^3 \beta_Z}{1 - \hat{\alpha}(M_Z)T} , \quad (10.97a)$$

$$\Gamma_W = M_W^3 \beta_W , \quad (10.97b)$$

$$A_i = \frac{A_{i0}}{1 - \hat{\alpha}(M_Z)T} , \quad (10.97c)$$

where  $\beta_{Z,W}$  are the SM expressions for the reduced widths  $\Gamma_{Z0}/M_{Z0}^3$  and  $\Gamma_{W0}/M_{W0}^3$ ,  $M_Z$  and  $M_W$  are the physical masses, and  $A_i$  ( $A_{i0}$ ) is a neutral-current amplitude (in the SM).

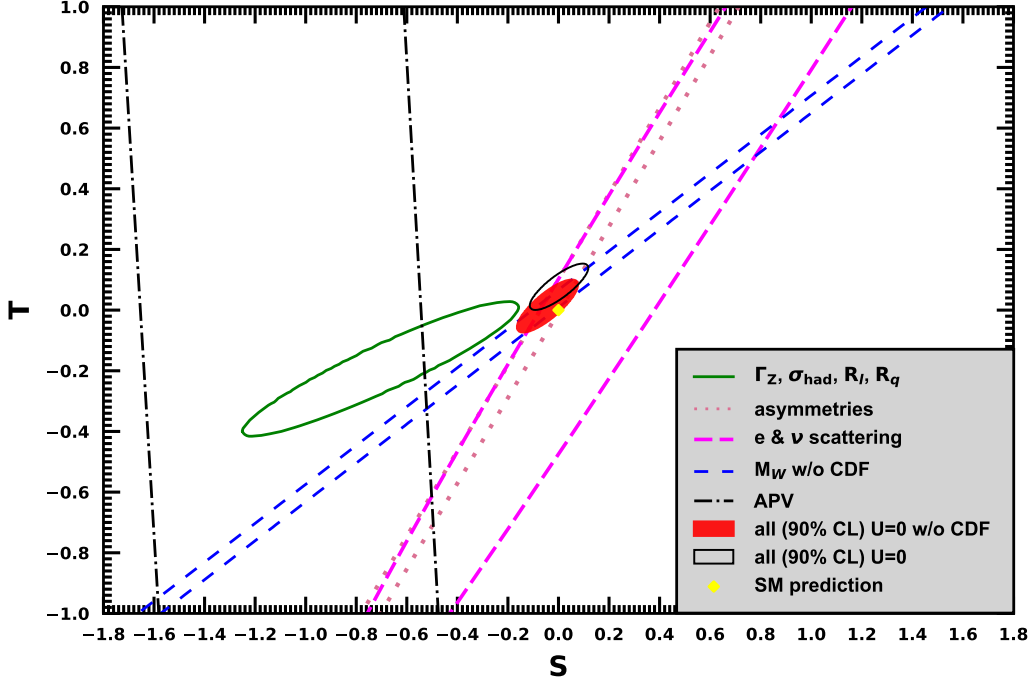


**Figure 10.6:**  $1\sigma$  constraints (39.35% for the closed contours and 68% for the others) on  $S$  and  $T$  (for  $U = 0$ ) from various inputs combined with  $M_Z$ .  $S$  and  $T$  represent the contributions of new physics only. Data sets not involving  $M_W$  or  $\Gamma_W$  are insensitive to  $U$ . With the exception of the fit to all data, we fix  $\alpha_s = 0.1187$ . The yellow dot indicates the Standard Model values  $S = T = 0$ . The fits to all data are at the 90% CL, with the open black ellipse corresponding to the alternative scenario discussed in Sec. 10.8, *i.e.* including the  $M_W$  result from CDF.

The data allows for a simultaneous determination of  $M_H$  and  $m_t$  (from the hadron colliders),  $S$  (from  $M_Z$ ),  $T$  (mainly from  $\Gamma_Z$ ),  $U$  (from  $M_W$ ),  $\hat{s}_Z^2 = 0.23113 \pm 0.00013$  (from the  $Z$  pole asymmetries), and  $\alpha_s(M_Z) = 0.1191 \pm 0.0018$  (mostly from  $R_\ell$ ,  $\sigma_{had}$ , and  $\tau_\tau$ ), giving,

$$S = -0.04 \pm 0.10 , \quad (10.98a)$$

$$T = 0.01 \pm 0.12 , \quad (10.98b)$$

$$U = -0.01 \pm 0.09 , \quad (10.98c)$$

where the correlations among the SM parameters are similar to those in Table 10.7, and where the uncertainties are from unknown higher orders in the SM predictions and the inputs. The parameters in Eq. (10.98), which by definition are due to new physics only, are in excellent agreement with the SM values of zero. Fixing  $U = 0$ , which is motivated by the fact that  $U$  is suppressed by an additional factor  $M_{new}^2/M_Z^2$  compared to  $S$  and  $T$  [411], greatly improves the precision on  $S$  and particularly  $T$ ,

$$S = -0.05 \pm 0.07 , \quad (10.99a)$$

$$T = 0.00 \pm 0.06 . \quad (10.99b)$$

Using Eq. (10.94), the value of  $\rho_0$  corresponding to  $T$  in Eq. (10.98b) is  $1.0001 \pm 0.0009$ , while the one corresponding to Eq. (10.99b) is  $1.0000 \pm 0.0005$ . Thus, the multi-parameter fits are consistent

with  $\rho_0 = 1$ , in contrast to the fit with  $S = U = 0$  in Eq. (10.87a). There is a strong correlation (93%) between the  $S$  and  $T$  parameters. The  $U$  parameter is  $-70\%$  ( $-87\%$ ) anti-correlated with  $S$  ( $T$ ). The allowed regions in  $S-T$  (for  $U = 0$ ) are shown in Fig. 10.6. From Eqs. (10.98) one obtains  $S \leq 0.11$  and  $T \leq 0.20$  at 95% CL, where the former puts the constraint  $M_{KK} \gtrsim 4$  TeV on the masses of KK gauge bosons in warped extra dimensions. In minimal composite Higgs models, the bound on  $S$  requires  $M_V \gtrsim 4.8$  TeV, which is obtained from a one-sided 95% CL bound on  $S > 0$  for  $T = 0$  and using Weinberg sum rules [412]. However, this constraint can be relaxed, *e.g.*, if the fermionic sector is also allowed to be partially composite [413, 414] and in soft-wall models [415].

The  $S$  parameter can also be used to constrain the number of fermion families, *under the assumption* that there are no new contributions to  $T$  or  $U$  and therefore that any new families are degenerate; then an extra generation of SM fermions is excluded with almost  $9\sigma$  confidence, corresponding to  $N_F = 2.75 \pm 0.14$ . This can be compared to the fit to the number of light neutrinos given in Eq. (10.79),  $N_\nu = 3.0025 \pm 0.0061$ , but the  $S$  parameter fits are valid even for a very heavy fourth family neutrino. Allowing  $T$  to vary as well, the constraint on a fourth family is weaker [416]. However, a heavy fourth family would increase the Higgs production cross-section through gluon fusion by a factor of about 9 [417], which is in considerable tension with the observed Higgs signal at the LHC [418]. Combining the limits from electroweak precision data with the measured Higgs production rate and limits from direct searches for heavy quarks [419], a fourth family of chiral fermions is now excluded by more than five standard deviations [420, 421]. Similar remarks apply to a heavy mirror family [422] involving right-handed SU(2) doublets and left-handed singlets. In contrast, new doublets that receive most of their mass from a different source than the Higgs vacuum expectation value, such as vector-like fermion doublets or scalar doublets in Supersymmetry, give small or no contribution to  $S$ ,  $T$ ,  $U$ , and the Higgs production cross-section and are therefore still allowed. Partial or complete vector-like fermion families are predicted in many Grand Unified Theories [423] (see Section 93 on “Grand Unified Theories” in this *Review*), and many other models including supersymmetric and superstring inspired ones [424–427].

As discussed in Sec. 10.6, there is a 3.6% deviation in the asymmetry parameter  $A_b$ . Assuming that this is due to new physics affecting preferentially the third generation, we can perform a fit allowing additional  $Z \rightarrow b\bar{b}$  vertex corrections  $\rho_b$  and  $\kappa_b$  as in Eq. (10.53) (here defined to be due to new physics only with the SM contributions removed), as well as  $S$ ,  $T$ ,  $U$ , and the SM parameters, with the result,

$$\rho_b = 0.057 \pm 0.020 , \quad (10.100a)$$

$$\kappa_b = 0.183 \pm 0.067 , \quad (10.100b)$$

with an almost perfect correlation of 99% (because  $R_b$  is much better determined than  $A_b$ ). The central values of the oblique parameters are consistent with their SM values of zero (note, however, that  $S = -0.10 \pm 0.10$  is slightly outside its  $1\sigma$  range), and there is little change in the SM parameters, except that the value of  $\alpha_s(M_Z)$  is lower by 0.0009 compared to the SM fit. Given that an  $\mathcal{O}(20\%)$  correction to  $\kappa_b$  would be necessary, it would be difficult to account for the deviation in  $A_b$  by new physics that enters only at the level of radiative corrections. Thus, if it is due to new physics, it is most likely of tree-level type affecting preferentially the third generation. Examples include the decay of a scalar neutrino resonance [428], mixing of the  $b$  quark with heavy exotics [429], and a heavy  $Z'$  with family non-universal couplings [430, 431]. It is difficult, however, to simultaneously account for  $R_b$  without tuning, which has been measured on the  $Z$  peak and off-peak [432] at LEP 1.

There is no simple parametrization to describe the effects of every type of new physics on every possible observable. The  $S$ ,  $T$ , and  $U$  formalism describes many types of heavy physics

which affect only the gauge self-energies, and it can be applied to all precision observables. However, new physics which couples directly to ordinary fermions cannot be fully parametrized in this framework. Examples include heavy  $Z'$  bosons [376], mixing with exotic fermions [9, 433, 434], leptoquark exchange [294, 435, 436], supersymmetric models, strong EW dynamics [413], Little Higgs models [437, 438], and TeV-scale extra spatial dimensions [439–442] (for more details and references, see Section 85 on “Extra Dimensions” in this *Review*). These types of new physics can be parametrized in a model-independent way by using an effective field theory description [443–446]. Here the SM is extended by a set of higher-dimensional operators, denoted  $\mathcal{O}_i$ ,

$$\mathcal{L} = \mathcal{L}_{\text{SM}} + \sum_{d>4} \sum_i \frac{C_i}{\Lambda^{d-4}} \mathcal{O}_i , \quad (10.101)$$

where  $\Lambda$  is the characteristic scale of the new physics sector, which is assumed to satisfy  $\Lambda \gg v$ . For EW precision observables, the leading new operators enter at dimension  $d = 6$ . Note that  $S$  and  $T$  can be identified with two of these operators (or linear combinations thereof, depending on the chosen operator basis), while  $U$  corresponds to a dimension-8 operator [411, 447]. With current data on  $M_W$  and  $Z$  pole observables,  $\Lambda$  is constrained to be larger than  $\mathcal{O}(\text{TeV})$  if the Wilson coefficients  $C_i$  are of order unity [448–454].

Limits on new four-Fermi operators and on leptoquarks using LEP 2 and lower energy data are given in Refs. [294, 455–457], while constraints on various types of new physics are addressed in Refs. [9, 169, 319, 458, 459]. For a particularly well motivated and explored type of physics beyond the SM, see Section 87 on “ $Z'$ -Boson Searches” in this *Review*.

## 10.8 Alternative scenarios

For our evaluation of  $g_\mu - 2$  and  $\Delta\alpha_{\text{had}}^{(5)}(M_Z)$  we took the recent vacuum polarization constraints from CMD-3 [48] and LQCD into account. Both have the effect to move the SM prediction of  $g_\mu - 2$  closer to the new measurement result in Ref. [236], while reducing the indirect determination of  $M_H$  and slightly increasing the small tension with the direct LHC measurements [306, 307]. The discrepancies of CMD-3 and LQCD with some of the older data (especially KLOE) is presently not understood. Thus, it is illustrative to repeat the global fit by replacing  $\Delta\alpha_{\text{had}}^{(3)}(2 \text{ GeV}) = (60.30 \pm 0.43) \times 10^{-4}$  and  $a_\mu^{\text{had}, \text{VP}}(\alpha^2) = (65.44 \pm 0.25) \times 10^{-9}$  with the values that we used for the 2022 edition of this *Review*,  $\Delta\alpha_{\text{had}}^{(3)}(2 \text{ GeV}) = (58.84 \pm 0.51) \times 10^{-4}$  and  $a_\mu^{\text{had}, \text{VP}}(\alpha^2) = (64.49 \pm 0.33) \times 10^{-9}$ . As a result, the discrepancy between the SM prediction and the measurement of  $a_\mu$  would become  $5.1 \sigma$ , and Eq. (10.50) would change to

$$a_\mu^{\text{exp}} - a_\mu^{\text{theory}} = (2.08 \pm 0.41) \times 10^{-9} . \quad (10.102)$$

On the other hand, the result for the indirect determination of  $M_H$  in Eq. (10.80) would now read

$$M_H = 103_{-17}^{+18} \text{ GeV} . \quad (10.103)$$

The global fit reported in Sec. 10.6 excluded the recent  $M_W$  result by the CDF collaboration [289], because there is a roughly  $4 \sigma$  discrepancy with other measurements whose origin is currently not understood (Ref. [289] also contains the first high-precision measurement of  $M_Z$  at a hadron collider shown in Table 10.5, in perfect agreement with LEP). Here we study the effect of including this measurement as an additional constraint, using  $M_W = 80.432 \pm 0.016$  GeV (see Table 10.4), which is the result of the adjustment to the common PDF set CT18 [303] in Ref. [298]. The quality of the global fit deteriorates sharply with a  $\chi^2/\text{d.o.f.} = 70.1/48$  and a probability of a larger  $\chi^2$  of only 2%. The increase in  $\chi^2$  amounts to more than 20 for 1 additional degree of

freedom. Removing  $M_H$  from the LHC as a constraint gives a somewhat improved fit quality with a  $\chi^2/\text{d.o.f.} = 60.1/47$ , but with

$$M_H = 75^{+14}_{-12} \text{ GeV} , \quad (10.104)$$

driven to very low and excluded values. More acceptable is the  $\rho_0$  fit as in Eq. (10.87a) with a  $\chi^2/\text{d.o.f.} = 58.5/47$  (12%), and

$$\rho_0 = 1.00059 \pm 0.00016 , \quad (10.105)$$

corresponding to  $T = 0.08 \pm 0.02$ . Thus, if one views the discrepancies in the  $M_W$  measurements as statistical fluctuations, then ample parameter space would open up, allowing, *e.g.*, additional non-degenerate SU(2) doublets, as reviewed in Sec. 10.7. In the STU fit,

$$S = -0.04 \pm 0.10 , \quad (10.106a)$$

$$T = 0.01 \pm 0.12 , \quad (10.106b)$$

$$U = 0.05 \pm 0.09 , \quad (10.106c)$$

the effect is mostly moved to the  $U$  parameter when compared to Eqs. (10.98).  $S$ ,  $T$  and  $U$  are highly correlated and despite appearances the probability of all vanishing simultaneously is just 0.3%. Finally, Eq. (10.99) changes only moderately (see also the open black ellipse in Fig. 10.6),

$$S = -0.00 \pm 0.07 , \quad (10.107a)$$

$$T = 0.07 \pm 0.05 . \quad (10.107b)$$

Of course, more drastic changes would be observed with the constraint,  $M_W = 80.4335 \pm 9.4$  GeV from the original publication [289] with its much smaller quoted uncertainty. For related discussions of this issue, see Refs. [361, 460–463].

### Acknowledgments

It is a pleasure to thank Rodolfo Ferro-Hernández for discussions, for performing some of the calculations and checks, and for updating the plots. A.F. is supported in part by the National Science Foundation under grant no. PHY-2112829.

### References

- [1] S. Glashow, *Nucl. Phys.* **22**, 579 (1961).
- [2] S. Weinberg, *Phys. Rev. Lett.* **19**, 1264 (1967).
- [3] A. Salam, *Conf. Proc. C* **680519**, 367 (1968).
- [4] S. Glashow, J. Iliopoulos and L. Maiani, *Phys. Rev. D* **2**, 1285 (1970).
- [5] N. Cabibbo, *Phys. Rev. Lett.* **10**, 531 (1963).
- [6] M. Kobayashi and T. Maskawa, *Prog. Theor. Phys.* **49**, 652 (1973).
- [7] S. Descotes-Genon and P. Koppenburg, *Ann. Rev. Nucl. Part. Sci.* **67**, 97 (2017), [[arXiv:1702.08834](#)].
- [8] E. Commins and P. Bucksbaum, *Weak Interactions of Leptons and Quarks*, Cambridge Univ. Pr., Cambridge, USA (1983), ISBN 978-0-521-27370-1.
- [9] P. Langacker, editor, *Precision tests of the standard electroweak model*, volume 14, WSP, Singapore (1996).
- [10] P. Langacker, *The standard model and beyond*, CRC Pr., Boca Raton, USA (2010), ISBN 978-1-4200-7906-7.
- [11] T. Kinoshita, editor, *Quantum electrodynamics*, volume 7, WSP, Singapore (1990).

- [12] S. G. Karshenboim, *Phys. Rept.* **422**, 1 (2005), [[hep-ph/0509010](#)].
- [13] J. Erler and S. Su, *Prog. Part. Nucl. Phys.* **71**, 119 (2013), [[arXiv:1303.5522](#)].
- [14] I. Brivio *et al.* (2021), [[arXiv:2111.12515](#)].
- [15] D. Webber *et al.* (MuLan), *Phys. Rev. Lett.* **106**, 041803 (2011), [[arXiv:1010.0991](#)].
- [16] T. Kinoshita and A. Sirlin, *Phys. Rev.* **113**, 1652 (1959).
- [17] T. van Ritbergen and R. G. Stuart, *Nucl. Phys. B* **564**, 343 (2000), [[hep-ph/9904240](#)].
- [18] M. Steinhauser and T. Seidensticker, *Phys. Lett. B* **467**, 271 (1999), [[hep-ph/9909436](#)].
- [19] Y. Nir, *Phys. Lett. B* **221**, 184 (1989).
- [20] A. Pak and A. Czarnecki, *Phys. Rev. Lett.* **100**, 241807 (2008), [[arXiv:0803.0960](#)].
- [21] A. Ferroglio, G. Ossola and A. Sirlin, *Nucl. Phys. B* **560**, 23 (1999), [[hep-ph/9905442](#)].
- [22] M. Fael, K. Schönwald and M. Steinhauser, *Phys. Rev. D* **104**, 1, 016003 (2021), [[arXiv:2011.13654](#)].
- [23] M. Czakon, A. Czarnecki and M. Dowling, *Phys. Rev. D* **103**, L111301 (2021), [[arXiv:2104.05804](#)].
- [24] X. Fan *et al.*, *Phys. Rev. Lett.* **130**, 7, 071801 (2023), [[arXiv:2209.13084](#)].
- [25] T. Aoyama *et al.*, *Phys. Rev. Lett.* **109**, 111808 (2012), [[arXiv:1205.5370](#)].
- [26] T. Aoyama, T. Kinoshita and M. Nio, *Atoms* **7**, 1, 28 (2019).
- [27] S. Volkov (2024), [[arXiv:2404.00649](#)].
- [28] L. Morel *et al.*, *Nature* **588**, 7836, 61 (2020).
- [29] R. H. Parker *et al.*, *Science* **360**, 191 (2018), [[arXiv:1812.04130](#)].
- [30] G. Abbiendi *et al.* (OPAL), *Eur. Phys. J. C* **45**, 1 (2006), [[hep-ex/0505072](#)].
- [31] P. Achard *et al.* (L3), *Phys. Lett. B* **623**, 26 (2005), [[hep-ex/0507078](#)].
- [32] S. Fanchiotti, B. A. Kniehl and A. Sirlin, *Phys. Rev. D* **48**, 307 (1993), [[hep-ph/9212285](#)].
- [33] J. Erler, *Phys. Rev. D* **59**, 054008 (1999), [[hep-ph/9803453](#)].
- [34] J. Erler (1999), [[hep-ph/0005084](#)].
- [35] M. Steinhauser, *Phys. Lett. B* **429**, 158 (1998), [[hep-ph/9803313](#)].
- [36] C. Sturm, *Nucl. Phys. B* **874**, 698 (2013), [[arXiv:1305.0581](#)].
- [37] K. Chetyrkin, J. H. Kuhn and M. Steinhauser, *Nucl. Phys. B* **482**, 213 (1996), [[hep-ph/9606230](#)].
- [38] A. V. Nesterenko, *Strong interactions in spacelike and timelike domains: dispersive approach*, Elsevier (2016), ISBN 978-0-12-803448-4.
- [39] J. Erler and R. Ferro-Hernández, *JHEP* **03**, 196 (2018), [[arXiv:1712.09146](#)].
- [40] A. Blondel *et al.*, editors, *Theory for the FCC-ee: Report on the 11th FCC-ee Workshop Theory and Experiments*, volume 3/2020 of *CERN Yellow Reports: Monographs*, CERN, Geneva (2019), [[arXiv:1905.05078](#)].
- [41] M. Davier *et al.*, *Eur. Phys. J. C* **80**, 3, 241 (2020), [[arXiv:1908.00921](#)].
- [42] A. Keshavarzi, D. Nomura and T. Teubner, *Phys. Rev. D* **101**, 1, 014029 (2020), [[arXiv:1911.00367](#)].
- [43] M. Davier *et al.*, *Eur. Phys. J. C* **71**, 1515 (2011), [Erratum: *Eur.Phys.J.C* 72, 1874 (2012)], [[arXiv:1010.4180](#)].
- [44] K. Ackerstaff *et al.* (OPAL), *Eur. Phys. J. C* **7**, 571 (1999), [[hep-ex/9808019](#)].

- [45] S. Anderson *et al.* (CLEO), *Phys. Rev. D* **61**, 112002 (2000), [[hep-ex/9910046](#)].
- [46] S. Schael *et al.* (ALEPH), *Phys. Rept.* **421**, 191 (2005), [[hep-ex/0506072](#)].
- [47] M. Fujikawa *et al.* (Belle), *Phys. Rev. D* **78**, 072006 (2008), [[arXiv:0805.3773](#)].
- [48] F. V. Ignatov *et al.* (CMD-3) (2023), [[arXiv:2302.08834](#)].
- [49] M. Cè *et al.*, *JHEP* **08**, 220 (2022), [[arXiv:2203.08676](#)].
- [50] M. Davier *et al.* (2023), [[arXiv:2312.02053](#)].
- [51] B. Malaescu and M. Schott, *Eur. Phys. J. C* **81**, 1, 46 (2021), [[arXiv:2008.08107](#)].
- [52] S. Groote *et al.*, *Phys. Lett. B* **440**, 375 (1998), [[hep-ph/9802374](#)].
- [53] N. Krasnikov and R. Rodenberg, *Nuovo Cim. A* **111**, 217 (1998), [[hep-ph/9711367](#)].
- [54] J. H. Kuhn and M. Steinhauser, *Phys. Lett. B* **437**, 425 (1998), [[hep-ph/9802241](#)].
- [55] A. D. Martin, J. Outhwaite and M. Ryskin, *Phys. Lett. B* **492**, 69 (2000), [[hep-ph/0008078](#)].
- [56] J. de Troconiz and F. Yndurain, *Phys. Rev. D* **65**, 093002 (2002), [[hep-ph/0107318](#)].
- [57] H. Burkhardt and B. Pietrzyk, *Phys. Rev. D* **84**, 037502 (2011), [[arXiv:1106.2991](#)].
- [58] J. Erler, P. Masjuan and H. Spiesberger, *Eur. Phys. J. C* **77**, 2, 99 (2017), [[arXiv:1610.08531](#)].
- [59] V. Novikov *et al.*, *Phys. Rept.* **41**, 1 (1978).
- [60] J. Erler and M. Luo, *Phys. Lett. B* **558**, 125 (2003), [[hep-ph/0207114](#)].
- [61] J. Erler, P. Masjuan and H. Spiesberger, *Eur. Phys. J. C* **82**, 11, 1023 (2022), [[arXiv:2203.02348](#)].
- [62] T. Aaltonen *et al.* (CDF, DØ, Tevatron Electroweak Working Group) (2016), [[arXiv:1608.01881](#)].
- [63] A. Hayrapetyan *et al.* (ATLAS, CMS) (2023), [[arXiv:2402.08713](#)].
- [64] A. Tumasyan *et al.* (CMS), *Eur. Phys. J. C* **83**, 10, 963 (2023), [[arXiv:2302.01967](#)].
- [65] A. M. Sirunyan *et al.* (CMS), *Eur. Phys. J. C* **79**, 5, 368 (2019), [[arXiv:1812.10505](#)].
- [66] A. M. Sirunyan *et al.* (CMS), *Eur. Phys. J. C* **79**, 4, 313 (2019), [[arXiv:1812.10534](#)].
- [67] A. Tumasyan *et al.* (CMS), *JHEP* **12**, 161 (2021), [[arXiv:2108.10407](#)].
- [68] G. Aad *et al.* (ATLAS), *JHEP* **06**, 019 (2023), [[arXiv:2209.00583](#)].
- [69] Technical Report ATLAS-CONF-2023-058, CERN, Geneva (2022), URL <http://cds.cern.ch/record/2826701>.
- [70] J. Erler, *Eur. Phys. J. C* **75**, 9, 453 (2015), [[arXiv:1507.08210](#)].
- [71] A. H. Hoang, S. Plätzer and D. Samitz, *JHEP* **10**, 200 (2018), [[arXiv:1807.06617](#)].
- [72] J. Kieseler, K. Lipka and S.-O. Moch, *Phys. Rev. Lett.* **116**, 16, 162001 (2016), [[arXiv:1511.00841](#)].
- [73] B. Dehnadi *et al.*, *JHEP* **12**, 065 (2023), [[arXiv:2309.00547](#)].
- [74] M. Beneke *et al.*, *Phys. Lett. B* **775**, 63 (2017), [[arXiv:1605.03609](#)].
- [75] P. Marquard *et al.*, *Phys. Rev. Lett.* **114**, 14, 142002 (2015), [[arXiv:1502.01030](#)].
- [76] M. Beneke, *Phys. Rept.* **317**, 1 (1999), [[hep-ph/9807443](#)].
- [77] S. Catani *et al.*, *JHEP* **07**, 100 (2019), [[arXiv:1906.06535](#)].
- [78] S. Catani *et al.*, *Eur. Phys. J. C* **81**, 6, 491 (2021), [[arXiv:2102.03256](#)].
- [79] A. M. Sirunyan *et al.* (CMS), *Eur. Phys. J. C* **80**, 7, 658 (2020), [[arXiv:1904.05237](#)].
- [80] G. Aad *et al.* (ATLAS), *JHEP* **11**, 150 (2019), [[arXiv:1905.02302](#)].

- [81] A. Tumasyan *et al.* (CMS), JHEP **07**, 077 (2023), [arXiv:2207.02270].
- [82] G. Aad *et al.* (ATLAS, CMS), JHEP **07**, 213 (2023), [arXiv:2205.13830].
- [83] J. Erler and M. Schott, Prog. Part. Nucl. Phys. **106**, 68 (2019), [arXiv:1902.05142].
- [84] A. Sirlin, Phys. Rev. D **22**, 971 (1980).
- [85] W. J. Marciano and J. L. Rosner, Phys. Rev. Lett. **65**, 2963 (1990), [Erratum: Phys.Rev.Lett. 68, 898 (1992)].
- [86] G. Degrassi, S. Fanchiotti and A. Sirlin, Nucl. Phys. B **351**, 49 (1991).
- [87] A. Czarnecki and W. J. Marciano, Int. J. Mod. Phys. A **15**, 2365 (2000), [hep-ph/0003049].
- [88] J. Erler and M. J. Ramsey-Musolf, Phys. Rev. D **72**, 073003 (2005), [hep-ph/0409169].
- [89] K. Kumar *et al.*, Ann. Rev. Nucl. Part. Sci. **63**, 237 (2013), [arXiv:1302.6263].
- [90] G. Degrassi and A. Sirlin, Nucl. Phys. B **352**, 342 (1991).
- [91] P. Gambino and A. Sirlin, Phys. Rev. D **49**, 1160 (1994), [hep-ph/9309326].
- [92] W. Hollik, Fortsch. Phys. **38**, 165 (1990).
- [93] R. Barbieri *et al.*, Nucl. Phys. B **409**, 105 (1993).
- [94] J. Fleischer, O. Tarasov and F. Jegerlehner, Phys. Lett. B **319**, 249 (1993).
- [95] G. Degrassi, P. Gambino and A. Vicini, Phys. Lett. B **383**, 219 (1996), [hep-ph/9603374].
- [96] G. Degrassi, P. Gambino and A. Sirlin, Phys. Lett. B **394**, 188 (1997), [hep-ph/9611363].
- [97] A. Freitas *et al.*, Phys. Lett. B **495**, 338 (2000), [Erratum: Phys.Lett.B 570, 265 (2003)], [hep-ph/0007091].
- [98] M. Awramik and M. Czakon, Phys. Lett. B **568**, 48 (2003), [hep-ph/0305248].
- [99] A. Freitas *et al.*, Nucl. Phys. B **632**, 189 (2002), [Erratum: Nucl.Phys.B 666, 305–307 (2003)], [hep-ph/0202131].
- [100] M. Awramik and M. Czakon, Phys. Rev. Lett. **89**, 241801 (2002), [hep-ph/0208113].
- [101] A. Onishchenko and O. Veretin, Phys. Lett. B **551**, 111 (2003), [hep-ph/0209010].
- [102] G. Degrassi, P. Gambino and P. P. Giardino, JHEP **05**, 154 (2015), [arXiv:1411.7040].
- [103] M. Awramik *et al.*, Phys. Rev. D **69**, 053006 (2004), [hep-ph/0311148].
- [104] M. Awramik *et al.*, Phys. Rev. Lett. **93**, 201805 (2004), [hep-ph/0407317].
- [105] W. Hollik, U. Meier and S. Uccirati, Nucl. Phys. B **731**, 213 (2005), [hep-ph/0507158].
- [106] M. Awramik, M. Czakon and A. Freitas, Phys. Lett. B **642**, 563 (2006), [hep-ph/0605339].
- [107] W. Hollik, U. Meier and S. Uccirati, Nucl. Phys. B **765**, 154 (2007), [hep-ph/0610312].
- [108] M. Awramik *et al.*, Nucl. Phys. B **813**, 174 (2009), [arXiv:0811.1364].
- [109] I. Dubovyk *et al.*, Phys. Lett. B **762**, 184 (2016), [arXiv:1607.08375].
- [110] A. Freitas, Phys. Lett. B **730**, 50 (2014), [arXiv:1310.2256].
- [111] A. Freitas, JHEP **04**, 070 (2014), [arXiv:1401.2447].
- [112] I. Dubovyk *et al.*, Phys. Lett. B **783**, 86 (2018), [arXiv:1804.10236].
- [113] I. Dubovyk *et al.*, JHEP **08**, 113 (2019), [arXiv:1906.08815].
- [114] M. Awramik, M. Czakon and A. Freitas, JHEP **11**, 048 (2006), [hep-ph/0608099].
- [115] A. Djouadi and C. Verzegnassi, Phys. Lett. B **195**, 265 (1987).
- [116] A. Djouadi, Nuovo Cim. A **100**, 357 (1988).

- [117] K. Chetyrkin, J. H. Kuhn and M. Steinhauser, *Phys. Lett. B* **351**, 331 (1995), [[hep-ph/9502291](#)].
- [118] L. Avdeev *et al.*, *Phys. Lett. B* **336**, 560 (1994), [Erratum: *Phys.Lett.B* 349, 597–598 (1995)], [[hep-ph/9406363](#)].
- [119] Y. Schroder and M. Steinhauser, *Phys. Lett. B* **622**, 124 (2005), [[hep-ph/0504055](#)].
- [120] K. Chetyrkin *et al.*, *Phys. Rev. Lett.* **97**, 102003 (2006), [[hep-ph/0605201](#)].
- [121] R. Boughezal and M. Czakon, *Nucl. Phys. B* **755**, 221 (2006), [[hep-ph/0606232](#)].
- [122] B. A. Kniehl, J. H. Kuhn and R. Stuart, *Phys. Lett. B* **214**, 621 (1988).
- [123] B. A. Kniehl, *Nucl. Phys. B* **347**, 86 (1990).
- [124] F. Halzen and B. A. Kniehl, *Nucl. Phys. B* **353**, 567 (1991).
- [125] A. Djouadi and P. Gambino, *Phys. Rev. D* **49**, 3499 (1994), [Erratum: *Phys.Rev.D* 53, 4111 (1996)], [[hep-ph/9309298](#)].
- [126] A. Anselm, N. Dombey and E. Leader, *Phys. Lett. B* **312**, 232 (1993).
- [127] K. Chetyrkin, J. H. Kuhn and M. Steinhauser, *Phys. Rev. Lett.* **75**, 3394 (1995), [[hep-ph/9504413](#)].
- [128] J. van der Bij *et al.*, *Phys. Lett. B* **498**, 156 (2001), [[hep-ph/0011373](#)].
- [129] M. Faisst *et al.*, *Nucl. Phys. B* **665**, 649 (2003), [[hep-ph/0302275](#)].
- [130] L. Chen and A. Freitas, *JHEP* **07**, 210 (2020), [[arXiv:2002.05845](#)].
- [131] L. Chen and A. Freitas, *JHEP* **03**, 215 (2021), [[arXiv:2012.08605](#)].
- [132] R. Boughezal, J. Tausk and J. van der Bij, *Nucl. Phys. B* **725**, 3 (2005), [[hep-ph/0504092](#)].
- [133] A. Arbuzov *et al.*, *Comput. Phys. Commun.* **174**, 728 (2006), [[hep-ph/0507146](#)].
- [134] L. Chen and A. Freitas, *SciPost Phys. Codeb.* **2023**, 18 (2023), [[arXiv:2211.16272](#)].
- [135] J. Erler and M. J. Ramsey-Musolf, *Prog. Part. Nucl. Phys.* **54**, 351 (2005), [[hep-ph/0404291](#)].
- [136] J. Formaggio and G. Zeller, *Rev. Mod. Phys.* **84**, 1307 (2012), [[arXiv:1305.7513](#)].
- [137] J. Dorenbosch *et al.* (CHARM), *Z. Phys. C* **41**, 567 (1989), [Erratum: *Z.Phys.C* 51, 142 (1991)].
- [138] L. Ahrens *et al.*, *Phys. Rev. D* **41**, 3297 (1990).
- [139] P. Vilain *et al.* (CHARM-II), *Phys. Lett. B* **335**, 246 (1994).
- [140] R. Allen *et al.*, *Phys. Rev. D* **47**, 11 (1993).
- [141] L. Auerbach *et al.* (LSND), *Phys. Rev. D* **63**, 112001 (2001), [[hep-ex/0101039](#)].
- [142] M. Deniz *et al.* (TEXONO), *Phys. Rev. D* **81**, 072001 (2010), [[arXiv:0911.1597](#)].
- [143] J. M. Conrad, M. H. Shaevitz and T. Bolton, *Rev. Mod. Phys.* **70**, 1341 (1998), [[hep-ex/9707015](#)].
- [144] A. Blondel *et al.*, *Z. Phys. C* **45**, 361 (1990).
- [145] J. Allaby *et al.* (CHARM), *Z. Phys. C* **36**, 611 (1987).
- [146] K. S. McFarland *et al.* (CCFR, E744, E770), *Eur. Phys. J. C* **1**, 509 (1998), [[hep-ex/9701010](#)].
- [147] R. Barnett, *Phys. Rev. D* **14**, 70 (1976).
- [148] H. Georgi and H. Politzer, *Phys. Rev. D* **14**, 1829 (1976).
- [149] S. Rabinowitz *et al.*, *Phys. Rev. Lett.* **70**, 134 (1993).
- [150] E. Paschos and L. Wolfenstein, *Phys. Rev. D* **7**, 91 (1973).

- [151] G. Zeller *et al.* (NuTeV), *Phys. Rev. Lett.* **88**, 091802 (2002), [Erratum: *Phys. Rev. Lett.* 90, 239902 (2003)], [[hep-ex/0110059](#)].
- [152] D. Akimov *et al.* (COHERENT), *Science* **357**, 6356, 1123 (2017), [[arXiv:1708.01294](#)].
- [153] D. Akimov *et al.* (COHERENT), *Phys. Rev. Lett.* **126**, 1, 012002 (2021), [[arXiv:2003.10630](#)].
- [154] J. Erler *et al.*, *Ann. Rev. Nucl. Part. Sci.* **64**, 269 (2014), [[arXiv:1401.6199](#)].
- [155] C. Prescott *et al.*, *Phys. Lett. B* **84**, 524 (1979).
- [156] D. Wang *et al.* (PVDIS), *Nature* **506**, 7486, 67 (2014).
- [157] D. Wang *et al.*, *Phys. Rev. C* **91**, 4, 045506 (2015), [[arXiv:1411.3200](#)].
- [158] R. Hasty *et al.* (SAMPLE), *Science* **290**, 2117 (2000), [[arXiv:nucl-ex/0102001](#)].
- [159] E. Beise, M. Pitt and D. Spayde, *Prog. Part. Nucl. Phys.* **54**, 289 (2005), [[arXiv:nucl-ex/0412054](#)].
- [160] S.-L. Zhu *et al.*, *Phys. Rev. D* **62**, 033008 (2000), [[hep-ph/0002252](#)].
- [161] A. Argento *et al.*, *Phys. Lett. B* **120**, 245 (1983).
- [162] W. Heil *et al.*, *Nucl. Phys. B* **327**, 1 (1989).
- [163] P. Souder *et al.*, *Phys. Rev. Lett.* **65**, 694 (1990).
- [164] D. Armstrong and R. McKeown, *Ann. Rev. Nucl. Part. Sci.* **62**, 337 (2012), [[arXiv:1207.5238](#)].
- [165] E. Derman and W. J. Marciano, *Annals Phys.* **121**, 147 (1979).
- [166] P. Anthony *et al.* (SLAC E158), *Phys. Rev. Lett.* **95**, 081601 (2005), [[hep-ex/0504049](#)].
- [167] D. Andrović *et al.* (Qweak), *Nature* **557**, 7704, 207 (2018), [[arXiv:1905.08283](#)].
- [168] R. D. Carlini *et al.*, *Ann. Rev. Nucl. Part. Sci.* **69**, 191 (2019).
- [169] J. Erler, A. Kurylov and M. J. Ramsey-Musolf, *Phys. Rev. D* **68**, 016006 (2003), [[hep-ph/0302149](#)].
- [170] R. D. Young *et al.*, *Phys. Rev. Lett.* **99**, 122003 (2007), [[arXiv:0704.2618](#)].
- [171] A. Acha *et al.* (HAPPEX), *Phys. Rev. Lett.* **98**, 032301 (2007), [[arXiv:nucl-ex/0609002](#)].
- [172] M. Gorchtein and C. Horowitz, *Phys. Rev. Lett.* **102**, 091806 (2009), [[arXiv:0811.0614](#)].
- [173] M. Gorchtein, C. Horowitz and M. J. Ramsey-Musolf, *Phys. Rev. C* **84**, 015502 (2011), [[arXiv:1102.3910](#)].
- [174] N. Hall *et al.*, *Phys. Lett. B* **753**, 221 (2016), [[arXiv:1504.03973](#)].
- [175] J. Erler *et al.*, *Phys. Rev. D* **100**, 5, 053007 (2019), [[arXiv:1907.07928](#)].
- [176] M. Bouchiat and C. Bouchiat, *Phys. Lett. B* **48**, 111 (1974).
- [177] M. Safranova *et al.*, *Rev. Mod. Phys.* **90**, 2, 025008 (2018), [[arXiv:1710.01833](#)].
- [178] C. Wood *et al.*, *Science* **275**, 1759 (1997).
- [179] J. Guena, M. Lintz and M. Bouchiat, *Phys. Rev. A* **71**, 042108 (2005), [[arXiv:physics/0412017](#)].
- [180] N. Edwards *et al.*, *Phys. Rev. Lett.* **74**, 2654 (1995).
- [181] P. Vetter *et al.*, *Phys. Rev. Lett.* **74**, 2658 (1995).
- [182] D. Meekhof *et al.*, *Phys. Rev. Lett.* **71**, 3442 (1993).
- [183] M. Macpherson *et al.*, *Phys. Rev. Lett.* **67**, 20, 2784 (1991).
- [184] P. Blunden, W. Melnitchouk and A. Thomas, *Phys. Rev. Lett.* **109**, 262301 (2012), [[arXiv:1208.4310](#)].

- [185] S. Bennett and C. E. Wieman, *Phys. Rev. Lett.* **82**, 2484 (1999), [Erratum: Phys.Rev.Lett. 82, 4153 (1999), Erratum: Phys.Rev.Lett. 83, 889 (1999)], [[hep-ex/9903022](#)].
- [186] V. Dzuba and V. Flambaum., *Phys. Rev. A* **62**, 052101 (2000), [[arXiv:physics/0005038](#)].
- [187] V. Dzuba, V. Flambaum and O. Sushkov, *Phys. Rev. A* **56**, 4357 (1997), [[hep-ph/9709251](#)].
- [188] D. Cho *et al.*, *Phys. Rev. A* **55**, 1007 (1997).
- [189] H. B. Tran Tan, D. Xiao and A. Derevianko, *Phys. Rev. A* **108**, 2, 022808 (2023), [[arXiv:2306.09573](#)].
- [190] A. A. Vasilyev *et al.*, *Phys. Rev. A* **66**, 020101 (2002).
- [191] V. Dzuba, V. Flambaum and J. Ginges, *Phys. Rev. D* **66**, 076013 (2002), [[hep-ph/0204134](#)].
- [192] J. Ginges and V. Flambaum, *Phys. Rept.* **397**, 63 (2004), [[arXiv:physics/0309054](#)].
- [193] A. Derevianko and S. G. Porsev, *Eur. Phys. J. A* **32**, 4, 517 (2007), [[hep-ph/0608178](#)].
- [194] B. Roberts, V. Dzuba and V. Flambaum, *Ann. Rev. Nucl. Part. Sci.* **65**, 63 (2015), [[arXiv:1412.6644](#)].
- [195] A. Derevianko, *Phys. Rev. Lett.* **85**, 1618 (2000), [[hep-ph/0005274](#)].
- [196] W. Johnson, I. Bednyakov and G. Soff, *Phys. Rev. Lett.* **87**, 233001 (2001), [Erratum: Phys.Rev.Lett. 88, 079903 (2002)], [[hep-ph/0110262](#)].
- [197] M. Kuchiev and V. Flambaum, *Phys. Rev. Lett.* **89**, 283002 (2002), [[hep-ph/0206124](#)].
- [198] A. Milstein, O. Sushkov and I. Terekhov, *Phys. Rev. Lett.* **89**, 283003 (2002), [[hep-ph/0208227](#)].
- [199] S. Porsev, K. Beloy and A. Derevianko, *Phys. Rev. Lett.* **102**, 181601 (2009), [[arXiv:0902.0335](#)].
- [200] V. Dzuba *et al.*, *Phys. Rev. Lett.* **109**, 203003 (2012), [[arXiv:1207.5864](#)].
- [201] C. Bouchiat and C. Piketty, *Phys. Lett. B* **128**, 73 (1983).
- [202] I. Zel'dovich, *J. Exp. Theor. Phys.* **6**, 1184 (1958).
- [203] V. Flambaum and D. Murray, *Phys. Rev. C* **56**, 1641 (1997), [[arXiv:nucl-th/9703050](#)].
- [204] W. Haxton and C. E. Wieman, *Ann. Rev. Nucl. Part. Sci.* **51**, 261 (2001), [[arXiv:nucl-th/0104026](#)].
- [205] V. Dzuba *et al.*, *J. Phys. B* **20**, 3297 (1987).
- [206] J. L. Rosner, *Phys. Rev. D* **53**, 2724 (1996), [[hep-ph/9507375](#)].
- [207] D. Antypas *et al.*, *Nature Phys.* **15**, 2, 120 (2019), [[arXiv:1804.05747](#)].
- [208] M. Ramsey-Musolf, *Phys. Rev. C* **60**, 015501 (1999), [[hep-ph/9903264](#)].
- [209] S. Pollock, E. Fortson and L. Wilets, *Phys. Rev. C* **46**, 2587 (1992), [[arXiv:nucl-th/9211004](#)].
- [210] B. Chen and P. Vogel, *Phys. Rev. C* **48**, 1392 (1993), [[arXiv:nucl-th/9303003](#)].
- [211] C. Horowitz *et al.*, *Phys. Rev. C* **63**, 025501 (2001), [[arXiv:nucl-th/9912038](#)].
- [212] D. Adhikari *et al.* (PREX), *Phys. Rev. Lett.* **126**, 17, 172502 (2021), [[arXiv:2102.10767](#)].
- [213] D. Adhikari *et al.* (CREX), *Phys. Rev. Lett.* **129**, 4, 042501 (2022), [[arXiv:2205.11593](#)].
- [214] H. Davoudiasl, H.-S. Lee and W. J. Marciano, *Phys. Rev. D* **86**, 095009 (2012), [[arXiv:1208.2973](#)].
- [215] E. Braaten, S. Narison and A. Pich, *Nucl. Phys. B* **373**, 581 (1992).
- [216] A. Pich, *Prog. Part. Nucl. Phys.* **75**, 41 (2014), [[arXiv:1310.7922](#)].
- [217] M. Davier *et al.*, *Eur. Phys. J. C* **74**, 3, 2803 (2014), [[arXiv:1312.1501](#)].

- [218] K. Chetyrkin, A. Kataev and F. Tkachov, *Phys. Lett. B* **85**, 277 (1979).
- [219] M. Dine and J. Sapirstein, *Phys. Rev. Lett.* **43**, 668 (1979).
- [220] S. Gorishnii, A. Kataev and S. Larin, *Phys. Lett. B* **259**, 144 (1991).
- [221] L. R. Surguladze and M. A. Samuel, *Phys. Rev. Lett.* **66**, 560 (1991), [Erratum: *Phys. Rev. Lett.* **66**, 2416 (1991)].
- [222] P. Baikov, K. Chetyrkin and J. H. Kuhn, *Phys. Rev. Lett.* **101**, 012002 (2008), [[arXiv:0801.1821](#)].
- [223] F. Le Diberder and A. Pich, *Phys. Lett. B* **286**, 147 (1992).
- [224] M. Beneke and M. Jamin, *JHEP* **09**, 044 (2008), [[arXiv:0806.3156](#)].
- [225] A. H. Hoang and C. Regner, *Phys. Rev. D* **105**, 9, 096023 (2022), [[arXiv:2008.00578](#)].
- [226] M. Golterman, K. Maltman and S. Peris, *Phys. Rev. D* **108**, 1, 014007 (2023), [[arXiv:2305.10386](#)].
- [227] M. A. Benitez-Rathgeb *et al.*, *JHEP* **09**, 223 (2022), [[arXiv:2207.01116](#)].
- [228] M. Beneke and H. Takaora, in “16th International Symposium on Radiative Corrections: Applications of Quantum Field Theory to Phenomenology,” (2023), [[arXiv:2309.10853](#)].
- [229] E. Braaten and C.-S. Li, *Phys. Rev. D* **42**, 3888 (1990).
- [230] W. Marciano and A. Sirlin, *Phys. Rev. Lett.* **61**, 1815 (1988).
- [231] J. Erler, *Rev. Mex. Fis.* **50**, 200 (2004), [[hep-ph/0211345](#)].
- [232] D. Boito *et al.*, *Phys. Rev. D* **85**, 093015 (2012), [[arXiv:1203.3146](#)].
- [233] D. Boito *et al.*, *Phys. Rev. D* **91**, 3, 034003 (2015), [[arXiv:1410.3528](#)].
- [234] J. Erler (2011), [[arXiv:1102.5520](#)].
- [235] G. Bennett *et al.* (Muon g-2), *Phys. Rev. Lett.* **92**, 161802 (2004), [[hep-ex/0401008](#)].
- [236] D. P. Aguillard *et al.* (Muon g-2), *Phys. Rev. Lett.* **131**, 16, 161802 (2023), [[arXiv:2308.06230](#)].
- [237] T. Aoyama *et al.*, *PTEP* **2012**, 01A107 (2012).
- [238] P. Baikov, A. Maier and P. Marquard, *Nucl. Phys. B* **877**, 647 (2013), [[arXiv:1307.6105](#)].
- [239] S. Laporta, *Phys. Lett. B* **772**, 232 (2017), [[arXiv:1704.06996](#)].
- [240] G. Li, R. Mendel and M. A. Samuel, *Phys. Rev. D* **47**, 1723 (1993).
- [241] S. Laporta and E. Remiddi, *Phys. Lett. B* **301**, 440 (1993).
- [242] S. Laporta and E. Remiddi, *Phys. Lett. B* **379**, 283 (1996), [[hep-ph/9602417](#)].
- [243] A. Czarnecki and M. Skrzypek, *Phys. Lett. B* **449**, 354 (1999), [[hep-ph/9812394](#)].
- [244] J. Erler and M. Luo, *Phys. Rev. Lett.* **87**, 071804 (2001), [[hep-ph/0101010](#)].
- [245] S. J. Brodsky and J. D. Sullivan, *Phys. Rev.* **156**, 1644 (1967).
- [246] T. Burnett and M. Levine, *Phys. Lett. B* **24**, 467 (1967).
- [247] R. Jackiw and S. Weinberg, *Phys. Rev. D* **5**, 2396 (1972).
- [248] I. Bars and M. Yoshimura, *Phys. Rev. D* **6**, 374 (1972).
- [249] K. Fujikawa, B. Lee and A. Sanda, *Phys. Rev. D* **6**, 2923 (1972).
- [250] W. A. Bardeen, R. Gastmans and B. Lautrup, *Nucl. Phys. B* **46**, 319 (1972).
- [251] T. Kukhto *et al.*, *Nucl. Phys. B* **371**, 567 (1992).
- [252] S. Peris, M. Perrottet and E. de Rafael, *Phys. Lett. B* **355**, 523 (1995), [[hep-ph/9505405](#)].

- [253] A. Czarnecki, B. Krause and W. J. Marciano, Phys. Rev. D **52**, 2619 (1995), [hep-ph/9506256].
- [254] A. Czarnecki, B. Krause and W. J. Marciano, Phys. Rev. Lett. **76**, 3267 (1996), [hep-ph/9512369].
- [255] C. Gnendiger, D. Stöckinger and H. Stöckinger-Kim, Phys. Rev. D **88**, 053005 (2013), [arXiv:1306.5546].
- [256] G. Degrassi and G. Giudice, Phys. Rev. D **58**, 053007 (1998), [hep-ph/9803384].
- [257] A. Czarnecki, W. J. Marciano and A. Vainshtein, Phys. Rev. D **67**, 073006 (2003), [Erratum: Phys. Rev. D **73**, 119901 (2006)], [hep-ph/0212229].
- [258] F. Jegerlehner, EPJ Web Conf. **166**, 00022 (2018), [arXiv:1705.00263].
- [259] M. Hoferichter, B.-L. Hoid and B. Kubis, JHEP **08**, 137 (2019), [arXiv:1907.01556].
- [260] P. D. Kennedy, J. Erler and H. Spiesberger (2021), [arXiv:2111.13016].
- [261] T. Aoyama *et al.*, Phys. Rept. **887**, 1 (2020), [arXiv:2006.04822].
- [262] S. Borsanyi *et al.*, Nature **593**, 7857, 51 (2021), [arXiv:2002.12347].
- [263] A. Anastasi *et al.* (KLOE-2), JHEP **03**, 173 (2018), [arXiv:1711.03085].
- [264] M. Davier *et al.*, Phys. Rev. D **109**, 7, 076019 (2024), [arXiv:2308.04221].
- [265] G. Benton *et al.*, Phys. Rev. D **109**, 3, 036010 (2024), [arXiv:2311.09523].
- [266] C. Lehner and A. S. Meyer, Phys. Rev. D **101**, 074515 (2020), [arXiv:2003.04177].
- [267] G. Wang *et al.* (chiQCD), Phys. Rev. D **107**, 3, 034513 (2023), [arXiv:2204.01280].
- [268] C. Aubin *et al.*, Phys. Rev. D **106**, 5, 054503 (2022), [arXiv:2204.12256].
- [269] M. Cè *et al.*, Phys. Rev. D **106**, 11, 114502 (2022), [arXiv:2206.06582].
- [270] C. Alexandrou *et al.* (Extended Twisted Mass), Phys. Rev. D **107**, 7, 074506 (2023), [arXiv:2206.15084].
- [271] T. Blum *et al.* (RBC, UKQCD), Phys. Rev. D **108**, 5, 054507 (2023), [arXiv:2301.08696].
- [272] A. Bazavov *et al.* (Fermilab Lattice, HPQCD, MILC), Phys. Rev. D **107**, 11, 114514 (2023), [arXiv:2301.08274].
- [273] B. Krause, Phys. Lett. B **390**, 392 (1997), [hep-ph/9607259].
- [274] A. Kurz *et al.*, Phys. Lett. B **734**, 144 (2014), [arXiv:1403.6400].
- [275] K. Melnikov and A. Vainshtein, Phys. Rev. D **70**, 113006 (2004), [hep-ph/0312226].
- [276] J. Erler and G. Toledo Sanchez, Phys. Rev. Lett. **97**, 161801 (2006), [hep-ph/0605052].
- [277] J. Prades, E. de Rafael and A. Vainshtein **20**, 303 (2009), [arXiv:0901.0306].
- [278] M. Knecht and A. Nyffeler, Phys. Rev. D **65**, 073034 (2002), [hep-ph/0111058].
- [279] I. Danilkin, C. F. Redmer and M. Vanderhaeghen, Prog. Part. Nucl. Phys. **107**, 20 (2019), [arXiv:1901.10346].
- [280] P. Masjuan and P. Roig, in “20th International Conference on Hadron Spectroscopy and Structure,” (2024), [arXiv:2401.05666].
- [281] E.-H. Chao *et al.*, Eur. Phys. J. C **81**, 7, 651 (2021), [arXiv:2104.02632].
- [282] E.-H. Chao *et al.*, Eur. Phys. J. C **82**, 8, 664 (2022), [arXiv:2204.08844].
- [283] T. Blum *et al.* (2023), [arXiv:2304.04423].
- [284] G. Colangelo *et al.*, Phys. Lett. B **735**, 90 (2014), [arXiv:1403.7512].
- [285] J. L. Lopez, D. V. Nanopoulos and X. Wang, Phys. Rev. D **49**, 366 (1994), [hep-ph/9308336].

- [286] G. Passarino and M. Veltman, *Nucl. Phys. B* **160**, 151 (1979).
- [287] W. Hollik and G. Duckeck, Springer Tracts Mod. Phys. **162**, 1 (2000).
- [288] S. Schael *et al.* (ALEPH, DELPHI, L3, OPAL, SLD, LEP Electroweak Working Group, SLD Electroweak Group, SLD Heavy Flavour Group), *Phys. Rept.* **427**, 257 (2006), [[hep-ex/0509008](#)].
- [289] T. Aaltonen *et al.* (CDF), *Science* **376**, 6589, 170 (2022).
- [290] B. Lynn and R. Stuart, *Nucl. Phys. B* **253**, 216 (1985).
- [291] S. L. Wu, *Phys. Rept.* **107**, 59 (1984).
- [292] R. Marshall, *Z. Phys. C* **43**, 607 (1989).
- [293] D. de Florian *et al.* (LHC Higgs Cross Section Working Group) (2016), [[arXiv:1610.07922](#)].
- [294] S. Schael *et al.* (ALEPH, DELPHI, L3, OPAL, LEP Electroweak), *Phys. Rept.* **532**, 119 (2013), [[arXiv:1302.3415](#)].
- [295] G. Aad *et al.* (ATLAS) (2024), [[arXiv:2403.15085](#)].
- [296] R. Aaij *et al.* (LHCb), *JHEP* **01**, 036 (2022), [[arXiv:2109.01113](#)].
- [297] V. M. Abazov *et al.* (D0), *Phys. Rev. Lett.* **108**, 151804 (2012), [[arXiv:1203.0293](#)].
- [298] S. Amoroso *et al.* (LHC-TeV MW Working Group) (2023), [[arXiv:2308.09417](#)].
- [299] Technical Report TEVEWWG/WZ 2010/01, FERMILAB, Batavia (2010), [[arXiv:1003.2826](#)], URL <https://www-d0.fnal.gov/Run2Physics/WWW/results/prelim/EW/E34>.
- [300] A. Tumasyan *et al.* (CMS), *Phys. Rev. D* **105**, 7, 072008 (2022), [[arXiv:2201.07861](#)].
- [301] T. A. Aaltonen *et al.* (CDF, DØ), *Phys. Rev. D* **88**, 5, 052018 (2013), [[arXiv:1307.7627](#)].
- [302] M. Aaboud *et al.* (ATLAS), *Eur. Phys. J. C* **78**, 2, 110 (2018), [Erratum: *Eur.Phys.J.C* 78, 898 (2018)], [[arXiv:1701.07240](#)].
- [303] T.-J. Hou *et al.* (2019), [[arXiv:1908.11394](#)].
- [304] G. Aad *et al.* (ATLAS), *Phys. Lett. B* **716**, 1 (2012), [[arXiv:1207.7214](#)].
- [305] S. Chatrchyan *et al.* (CMS), *Phys. Lett. B* **716**, 30 (2012), [[arXiv:1207.7235](#)].
- [306] G. Aad *et al.* (ATLAS), *Phys. Rev. Lett.* **131**, 25, 251802 (2023), [[arXiv:2308.04775](#)].
- [307] Technical Report CMS-PAS-HIG-21-019, CERN, Geneva (2023), URL <http://cds.cern.ch/record/2871702>.
- [308] G. Aad *et al.* (ATLAS), *Phys. Lett. B* **846**, 138223 (2023), [[arXiv:2304.01532](#)].
- [309] T. A. Aaltonen *et al.* (CDF, DØ), *Phys. Rev. D* **97**, 11, 112007 (2018), [[arXiv:1801.06283](#)].
- [310] G. Aad *et al.* (ATLAS), *JHEP* **09**, 049 (2015), [[arXiv:1503.03709](#)].
- [311] Technical Report ATLAS-CONF-2018-037, CERN, Geneva (2018), URL <https://cds.cern.ch/record/2630340>.
- [312] A. M. Sirunyan *et al.* (CMS), *Eur. Phys. J. C* **78**, 9, 701 (2018), [[arXiv:1806.00863](#)].
- [313] Technical Report CMS-PAS-SMP-22-010, CERN, Geneva (2024), URL <http://cds.cern.ch/record/2893842>.
- [314] R. Aaij *et al.* (LHCb), *JHEP* **11**, 190 (2015), [[arXiv:1509.07645](#)].
- [315] K. Abe *et al.* (SLD), *Phys. Rev. Lett.* **84**, 5945 (2000), [[hep-ex/0004026](#)].
- [316] K. Abe *et al.* (SLD), *Phys. Rev. Lett.* **86**, 1162 (2001), [[hep-ex/0010015](#)].
- [317] A. Hayrapetyan *et al.* (CMS), *JHEP* **01**, 101 (2024), [[arXiv:2309.12408](#)].
- [318] D. Kennedy *et al.*, *Nucl. Phys. B* **321**, 83 (1989).

- [319] S. Riemann, *Rept. Prog. Phys.* **73**, 126201 (2010).
- [320] K. Abe *et al.* (SLD), *Phys. Rev. Lett.* **85**, 5059 (2000), [[hep-ex/0006019](#)].
- [321] K. Abe *et al.* (SLD), *Phys. Rev. Lett.* **78**, 17 (1997), [[hep-ex/9609019](#)].
- [322] M. Aaboud *et al.* (ATLAS), *Eur. Phys. J. C* **77**, 6, 367 (2017), [[arXiv:1612.03016](#)].
- [323] W. Bernreuther *et al.*, *JHEP* **01**, 053 (2017), [[arXiv:1611.07942](#)].
- [324] S. Catani and M. H. Seymour, *JHEP* **07**, 023 (1999), [[hep-ph/9905424](#)].
- [325] A. Djouadi, J. H. Kuhn and P. Zerwas, *Z. Phys. C* **46**, 411 (1990).
- [326] T. A. Aaltonen *et al.* (CDF), *Phys. Rev. D* **93**, 11, 112016 (2016), [Addendum: *Phys. Rev. D* 95, 119901 (2017)], [[arXiv:1605.02719](#)].
- [327] V. M. Abazov *et al.* (DØ), *Phys. Rev. Lett.* **120**, 24, 241802 (2018), [[arXiv:1710.03951](#)].
- [328] V. Abazov *et al.* (DØ), *Phys. Rev. D* **84**, 012007 (2011), [[arXiv:1104.4590](#)].
- [329] D. Acosta *et al.* (CDF), *Phys. Rev. D* **71**, 052002 (2005), [[hep-ex/0411059](#)].
- [330] V. Andreev *et al.* (H1), *Eur. Phys. J. C* **78**, 9, 777 (2018), [[arXiv:1806.01176](#)].
- [331] H. Abramowicz *et al.* (ZEUS), *Phys. Rev. D* **93**, 9, 092002 (2016), [[arXiv:1603.09628](#)].
- [332] P. Janot and S. Jadach, *Phys. Lett. B* **803**, 135319 (2020), [[arXiv:1912.02067](#)].
- [333] D. Albert *et al.*, *Nucl. Phys. B* **166**, 460 (1980).
- [334] K. Chetyrkin, J. H. Kuhn and A. Kwiatkowski, *Phys. Rept.* **277**, 189 (1996), [[hep-ph/9503396](#)].
- [335] B. A. Kniehl and J. H. Kuhn, *Nucl. Phys. B* **329**, 547 (1990).
- [336] K. Chetyrkin and A. Kwiatkowski, *Phys. Lett. B* **319**, 307 (1993), [[hep-ph/9310229](#)].
- [337] S. Larin, T. van Ritbergen and J. Vermaseren, *Phys. Lett. B* **320**, 159 (1994), [[hep-ph/9310378](#)].
- [338] K. Chetyrkin and O. Tarasov, *Phys. Lett. B* **327**, 114 (1994), [[hep-ph/9312323](#)].
- [339] P. Baikov *et al.*, *Phys. Rev. Lett.* **108**, 222003 (2012), [[arXiv:1201.5804](#)].
- [340] A. Kataev, *Phys. Lett. B* **287**, 209 (1992).
- [341] B. W. Lynn and R. G. Stuart, *Phys. Lett. B* **252**, 676 (1990).
- [342] J. Bernabeu, A. Pich and A. Santamaria, *Nucl. Phys. B* **363**, 326 (1991).
- [343] A. Czarnecki and J. H. Kuhn, *Phys. Rev. Lett.* **77**, 3955 (1996), [[hep-ph/9608366](#)].
- [344] R. Harlander, T. Seidensticker and M. Steinhauser, *Phys. Lett. B* **426**, 125 (1998), [[hep-ph/9712228](#)].
- [345] J. Fleischer *et al.*, *Phys. Lett. B* **459**, 625 (1999), [[hep-ph/9904256](#)].
- [346] P. A. Grassi, B. A. Kniehl and A. Sirlin, *Phys. Rev. Lett.* **86**, 389 (2001), [[hep-th/0005149](#)].
- [347] A. Akhundov, D. Bardin and T. Riemann, *Nucl. Phys. B* **276**, 1 (1986).
- [348] F. Jegerlehner, *Z. Phys. C* **32**, 425 (1986), [Erratum: *Z. Phys. C* 38, 519 (1988)].
- [349] W. Beenakker and W. Hollik, *Z. Phys. C* **40**, 141 (1988).
- [350] D. Bardin *et al.*, *Z. Phys. C* **44**, 493 (1989).
- [351] A. Borrelli *et al.*, *Nucl. Phys. B* **333**, 357 (1990).
- [352] A. Denner and T. Sack, *Z. Phys. C* **46**, 653 (1990).
- [353] A. Denner, *Fortsch. Phys.* **41**, 307 (1993), [[arXiv:0709.1075](#)].
- [354] G. Aad *et al.* (ATLAS), *Nature Phys.* **17**, 7, 813 (2021), [[arXiv:2007.14040](#)].

- [355] U. Amaldi *et al.*, *Phys. Rev. D* **36**, 1385 (1987).
- [356] G. Costa *et al.*, *Nucl. Phys. B* **297**, 244 (1988).
- [357] P. Langacker and M. Luo, *Phys. Rev. D* **44**, 817 (1991).
- [358] J. Erler and P. Langacker, *Phys. Rev. D* **52**, 441 (1995), [[hep-ph/9411203](#)].
- [359] J. Haller *et al.*, *Eur. Phys. J. C* **78**, 8, 675 (2018), [[arXiv:1803.01853](#)].
- [360] J. de Blas *et al.*, *Phys. Rev. D* **106**, 3, 033003 (2022), [[arXiv:2112.07274](#)].
- [361] J. de Blas *et al.*, *Phys. Rev. Lett.* **129**, 27, 271801 (2022), [[arXiv:2204.04204](#)].
- [362] A. Crivellin *et al.*, *Phys. Rev. Lett.* **125**, 9, 091801 (2020), [[arXiv:2003.04886](#)].
- [363] A. Keshavarzi *et al.*, *Phys. Rev. D* **102**, 3, 033002 (2020), [[arXiv:2006.12666](#)].
- [364] M. Aaboud *et al.* (ATLAS), *Phys. Lett. B* **784**, 345 (2018), [[arXiv:1806.00242](#)].
- [365] A. M. Sirunyan *et al.* (CMS), *Phys. Lett. B* **805**, 135425 (2020), [[arXiv:2002.06398](#)].
- [366] A. Tumasyan *et al.* (CMS) (2022), [[arXiv:2202.06923](#)].
- [367] B. Abi *et al.* (Muon g-2), *Phys. Rev. Lett.* **126**, 14, 141801 (2021), [[arXiv:2104.03281](#)].
- [368] F. James and M. Roos, *Comput. Phys. Commun.* **10**, 343 (1975).
- [369] G. Aad *et al.* (ATLAS) (2023), [[arXiv:2309.12986](#)].
- [370] V. Abazov *et al.* (DØ), *Phys. Rev. D* **80**, 111107 (2009), [[arXiv:0911.2710](#)].
- [371] J. Bagger, K. T. Matchev and D. Pierce, *Phys. Lett. B* **348**, 443 (1995), [[hep-ph/9501277](#)].
- [372] P. Langacker and N. Polonsky, *Phys. Rev. D* **52**, 3081 (1995), [[hep-ph/9503214](#)].
- [373] M. Veltman, *Nucl. Phys. B* **123**, 89 (1977).
- [374] M. S. Chanowitz, M. Furman and I. Hinchliffe, *Phys. Lett. B* **78**, 285 (1978).
- [375] J. van der Bij and F. Hoogeveen, *Nucl. Phys. B* **283**, 477 (1987).
- [376] P. Langacker and M. Luo, *Phys. Rev. D* **45**, 278 (1992).
- [377] A. Denner, R. Guth and J. H. Kuhn, *Phys. Lett. B* **240**, 438 (1990).
- [378] W. Grimus *et al.*, *J. Phys. G* **35**, 075001 (2008), [[arXiv:0711.4022](#)].
- [379] H. E. Haber and D. O’Neil, *Phys. Rev. D* **83**, 055017 (2011), [[arXiv:1011.6188](#)].
- [380] S. Bertolini and A. Sirlin, *Phys. Lett. B* **257**, 179 (1991).
- [381] M. Golden and L. Randall, *Nucl. Phys. B* **361**, 3 (1991).
- [382] B. Holdom and J. Terning, *Phys. Lett. B* **247**, 88 (1990).
- [383] M. E. Peskin and T. Takeuchi, *Phys. Rev. Lett.* **65**, 964 (1990).
- [384] K. Hagiwara *et al.*, *Z. Phys. C* **64**, 559 (1994), [Erratum: Z.Phys.C 68, 352 (1995)], [[hep-ph/9409380](#)].
- [385] M. E. Peskin and T. Takeuchi, *Phys. Rev. D* **46**, 381 (1992).
- [386] I. Maksymyk, C. Burgess and D. London, *Phys. Rev. D* **50**, 529 (1994), [[hep-ph/9306267](#)].
- [387] R. Barbieri *et al.*, *Nucl. Phys. B* **703**, 127 (2004), [[hep-ph/0405040](#)].
- [388] M. Farina *et al.*, *Phys. Lett. B* **772**, 210 (2017), [[arXiv:1609.08157](#)].
- [389] G. Altarelli and R. Barbieri, *Phys. Lett. B* **253**, 161 (1991).
- [390] D. Kennedy and P. Langacker, *Phys. Rev. D* **44**, 1591 (1991).
- [391] L. Randall and R. Sundrum, *Phys. Rev. Lett.* **83**, 3370 (1999), [[hep-ph/9905221](#)].
- [392] M. Carena *et al.*, *Nucl. Phys. B* **759**, 202 (2006), [[hep-ph/0607106](#)].

- [393] R. Contino, in “Theoretical Advanced Study Institute in Elementary Particle Physics: Physics of the Large and the Small,” 235–306 (2011), [[arXiv:1005.4269](#)].
- [394] D. D. Dietrich, F. Sannino and K. Tuominen, *Phys. Rev. D* **72**, 055001 (2005), [[hep-ph/0505059](#)].
- [395] M. T. Frandsen and M. Rosenlyst, *JHEP* **03**, 222 (2023), [[arXiv:2207.01465](#)].
- [396] E. Gates and J. Terning, *Phys. Rev. Lett.* **67**, 1840 (1991).
- [397] H. Georgi, *Nucl. Phys. B* **363**, 301 (1991).
- [398] M. J. Dugan and L. Randall, *Phys. Lett. B* **264**, 154 (1991).
- [399] H. E. Haber and G. L. Kane, *Phys. Rept.* **117**, 75 (1985).
- [400] A. Djouadi, *Phys. Rept.* **459**, 1 (2008), [[hep-ph/0503173](#)].
- [401] R. Barbieri *et al.*, *Nucl. Phys. B* **341**, 309 (1990).
- [402] R. Barbieri, M. Frigeni and F. Caravaglios, *Phys. Lett. B* **279**, 169 (1992).
- [403] J. Erler and D. M. Pierce, *Nucl. Phys. B* **526**, 53 (1998), [[hep-ph/9801238](#)].
- [404] G.-C. Cho and K. Hagiwara, *Nucl. Phys. B* **574**, 623 (2000), [[hep-ph/9912260](#)].
- [405] G. Altarelli *et al.*, *JHEP* **06**, 018 (2001), [[hep-ph/0106029](#)].
- [406] S. Heinemeyer, W. Hollik and G. Weiglein, *Phys. Rept.* **425**, 265 (2006), [[hep-ph/0412214](#)].
- [407] S. P. Martin, K. Tobe and J. D. Wells, *Phys. Rev. D* **71**, 073014 (2005), [[hep-ph/0412424](#)].
- [408] M. Ramsey-Musolf and S. Su, *Phys. Rept.* **456**, 1 (2008), [[hep-ph/0612057](#)].
- [409] S. Heinemeyer *et al.*, *JHEP* **04**, 039 (2008), [[arXiv:0710.2972](#)].
- [410] O. Buchmueller *et al.*, *Eur. Phys. J. C* **72**, 2020 (2012), [[arXiv:1112.3564](#)].
- [411] B. Grinstein and M. B. Wise, *Phys. Lett. B* **265**, 326 (1991).
- [412] A. Pich, I. Rosell and J. Sanz-Cillero, *JHEP* **01**, 157 (2014), [[arXiv:1310.3121](#)].
- [413] C. T. Hill and E. H. Simmons, *Phys. Rept.* **381**, 235 (2003), [Erratum: *Phys.Rept.* 390, 553–554 (2004)], [[hep-ph/0203079](#)].
- [414] G. Panico and A. Wulzer, *The Composite Nambu-Goldstone Higgs*, volume 913, Springer (2016), [[arXiv:1506.01961](#)].
- [415] J. A. Cabrer, G. von Gersdorff and M. Quiros, *JHEP* **05**, 083 (2011), [[arXiv:1103.1388](#)].
- [416] J. Erler and P. Langacker, *Phys. Rev. Lett.* **105**, 031801 (2010), [[arXiv:1003.3211](#)].
- [417] J. Gunion, D. W. McKay and H. Pois, *Phys. Rev. D* **53**, 1616 (1996), [[hep-ph/9507323](#)].
- [418] A. Lenz, *Adv. High Energy Phys.* **2013**, 910275 (2013).
- [419] S. Chatrchyan *et al.* (CMS), *Phys. Rev. D* **86**, 112003 (2012), [[arXiv:1209.1062](#)].
- [420] A. Djouadi and A. Lenz, *Phys. Lett. B* **715**, 310 (2012), [[arXiv:1204.1252](#)].
- [421] O. Eberhardt *et al.*, *Phys. Rev. Lett.* **109**, 241802 (2012), [[arXiv:1209.1101](#)].
- [422] J. Maalampi and M. Roos, *Phys. Rept.* **186**, 53 (1990).
- [423] P. Langacker, *Phys. Rept.* **72**, 185 (1981).
- [424] J. L. Hewett and T. G. Rizzo, *Phys. Rept.* **183**, 193 (1989).
- [425] J. Kang, P. Langacker and B. D. Nelson, *Phys. Rev. D* **77**, 035003 (2008), [[arXiv:0708.2701](#)].
- [426] S. P. Martin, *Phys. Rev. D* **81**, 035004 (2010), [[arXiv:0910.2732](#)].
- [427] P. W. Graham *et al.*, *Phys. Rev. D* **81**, 055016 (2010), [[arXiv:0910.3020](#)].
- [428] J. Erler, J. L. Feng and N. Polonsky, *Phys. Rev. Lett.* **78**, 3063 (1997), [[hep-ph/9612397](#)].

- [429] D. Choudhury, T. M. Tait and C. Wagner, *Phys. Rev. D* **65**, 053002 (2002), [[hep-ph/0109097](#)].
- [430] J. Erler and P. Langacker, *Phys. Rev. Lett.* **84**, 212 (2000), [[hep-ph/9910315](#)].
- [431] P. Langacker and M. Plumacher, *Phys. Rev. D* **62**, 013006 (2000), [[hep-ph/0001204](#)].
- [432] P. Abreu *et al.* (DELPHI), *Eur. Phys. J. C* **10**, 415 (1999).
- [433] P. Langacker and D. London, *Phys. Rev. D* **38**, 886 (1988).
- [434] F. del Aguila, J. de Blas and M. Perez-Victoria, *Phys. Rev. D* **78**, 013010 (2008), [[arXiv:0803.4008](#)].
- [435] M. Chemtob, *Prog. Part. Nucl. Phys.* **54**, 71 (2005), [[hep-ph/0406029](#)].
- [436] R. Barbier *et al.*, *Phys. Rept.* **420**, 1 (2005), [[hep-ph/0406039](#)].
- [437] T. Han, H. E. Logan and L.-T. Wang, *JHEP* **01**, 099 (2006), [[hep-ph/0506313](#)].
- [438] M. Perelstein, *Prog. Part. Nucl. Phys.* **58**, 247 (2007), [[hep-ph/0512128](#)].
- [439] I. Antoniadis, in “Supergravity, Superstrings and M-Theory,” (2001), [[hep-th/0102202](#)].
- [440] M. Carena *et al.*, *Phys. Rev. D* **68**, 035010 (2003), [[hep-ph/0305188](#)].
- [441] K. Agashe *et al.*, *JHEP* **08**, 050 (2003), [[hep-ph/0308036](#)].
- [442] I. Gogoladze and C. Macesanu, *Phys. Rev. D* **74**, 093012 (2006), [[hep-ph/0605207](#)].
- [443] S. Weinberg, *Phys. Rev. Lett.* **43**, 1566 (1979).
- [444] W. Buchmuller and D. Wyler, *Nucl. Phys. B* **268**, 621 (1986).
- [445] B. Grzadkowski *et al.*, *JHEP* **10**, 085 (2010), [[arXiv:1008.4884](#)].
- [446] R. Contino *et al.*, *JHEP* **07**, 035 (2013), [[arXiv:1303.3876](#)].
- [447] K. Hagiwara *et al.*, *Phys. Rev. D* **48**, 2182 (1993).
- [448] A. Pomarol and F. Riva, *JHEP* **01**, 151 (2014), [[arXiv:1308.2803](#)].
- [449] J. Ellis, V. Sanz and T. You, *JHEP* **03**, 157 (2015), [[arXiv:1410.7703](#)].
- [450] A. Efrati, A. Falkowski and Y. Soreq, *JHEP* **07**, 018 (2015), [[arXiv:1503.07872](#)].
- [451] J. de Blas *et al.*, *PoS EPS-HEP2017*, 467 (2017), [[arXiv:1710.05402](#)].
- [452] E. da Silva Almeida *et al.*, *Phys. Rev. D* **99**, 3, 033001 (2019), [[arXiv:1812.01009](#)].
- [453] S. Dawson and P. P. Giardino, *Phys. Rev. D* **101**, 1, 013001 (2020), [[arXiv:1909.02000](#)].
- [454] T. Corbett *et al.*, *Phys. Rev. D* **107**, 11, 115013 (2023), [[arXiv:2304.03305](#)].
- [455] G.-C. Cho, K. Hagiwara and S. Matsumoto, *Eur. Phys. J. C* **5**, 155 (1998), [[hep-ph/9707334](#)].
- [456] K. Cheung, *Phys. Lett. B* **517**, 167 (2001), [[hep-ph/0106251](#)].
- [457] Z. Han and W. Skiba, *Phys. Rev. D* **71**, 075009 (2005), [[hep-ph/0412166](#)].
- [458] P. Langacker, M. Luo and A. K. Mann, *Rev. Mod. Phys.* **64**, 87 (1992).
- [459] P. Langacker, *Rev. Mod. Phys.* **81**, 1199 (2009), [[arXiv:0801.1345](#)].
- [460] P. Asadi *et al.*, *Phys. Rev. D* **108**, 5, 055026 (2023), [[arXiv:2204.05283](#)].
- [461] E. Bagnaschi *et al.*, *JHEP* **08**, 308 (2022), [[arXiv:2204.05260](#)].
- [462] J. Gu *et al.*, *Chin. Phys. C* **46**, 12, 123107 (2022), [[arXiv:2204.05296](#)].
- [463] A. Paul and M. Valli, *Phys. Rev. D* **106**, 1, 013008 (2022), [[arXiv:2204.05267](#)].